AD-A106 117 GRUMMAN AEROSPACE CORP BETHPAGE NY F/G 13/1
STUDY OF FIBER OPTICS TO ENHANCE AN ENVIRONMENTAL LIGHTING LABO--ETC(U)
AUG 81 J CONNELLY F33615-79-C-3629
UNCLASSIFIED AFWAL-TR-81-3098 NL

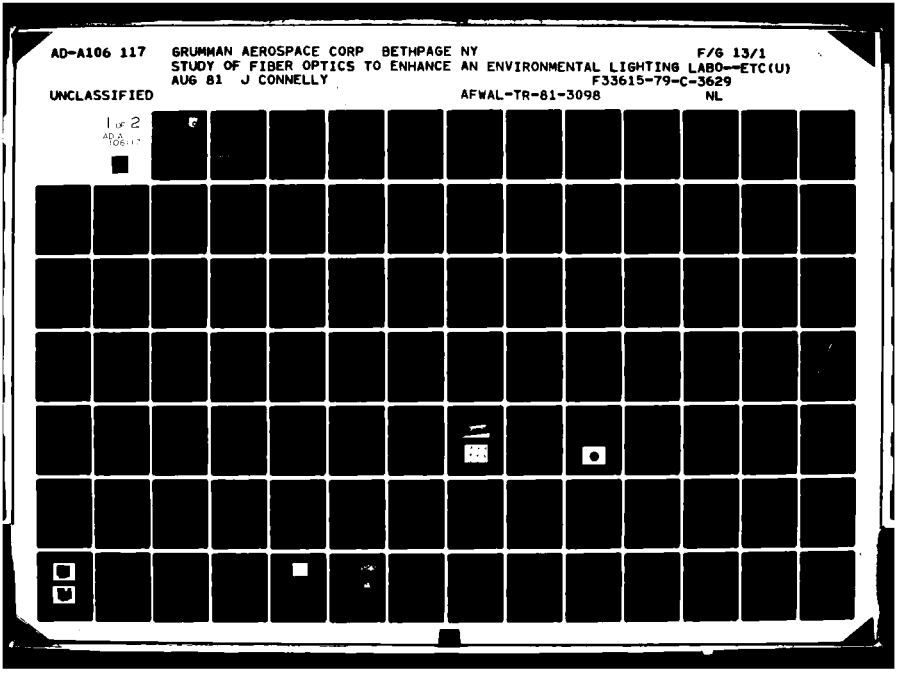

(14) AFWAL-TR-81-3098 (17)

(6) STUDY OF FIBER OPTICS TO ENHANCE AN ENVIRONMENTAL LIGHTING LABORATORY

Grumman Aerospace Corporation
Bethpage, New York 11714

(11) Aug 81 (12) 154

(9) Final Report, Nov 79 — Mar 81

(10) J. Donnelly (15) 33615-79-C-3121

Approved for public release; distribution unlimited

(16) 2403 (17) 04

FLIGHT DYNAMICS LABORATORY
AIR FORCE WRIGHT AERONAUTICAL LABORATORIES
AIR FORCE SYSTEMS COMMAND
WRIGHT-PATTERSON AIR FORCE BASE, OHIO 45433

NOTICE

When Government drawings, specifications, or other data are used for any purpose other than in connection with a definitely related Government procurement operation, the United States Government thereby incurs no responsibility nor any obligation whatsoever; and the fact that the government may have formulated, furnished, or in any way supplied the said drawings, specifications, or other data, is not to be regarded by implication or otherwise as in any manner licensing the holder or any other person or corporation, or conveying any rights or permission to manufacture, use, or sell any patented invention that may in any way be related thereto.

This report has been reviewed by the Office of Public Affairs (ASD/PA) and is releasable to the National Technical Information Service (NTIS). At NTIS, it will be available to the general public, including foreign nations.

This technical report has been reviewed and is approved for publication.

James A. Uphaus Jr.
James A. Uphaus, Jr.
Electronic Systems Engineer

Charles R Goss Jr.
Charles R. Goss, Jr. Lt Col, USAF
Chief, Crew Sys Development Br

FOR THE COMMANDER

Robert C. Ettinger, Col, USAF
Chief, Flight Control Division

"If your address has changed, if you wish to be removed from our mailing list, or if the addressee is no longer employed by your organization, please notify AFWAL/FIGR, W-PAFB, OH 45433 to help us maintain a current mailing list."

Copies of this report should not be returned unless return is required by security considerations, contractual obligations, or notice on a specific document.

UNCLASSIFIED

SECURITY CLASSIFICATION OF THIS PAGE *(When Data Entered)*

REPORT DOCUMENTATION PAGE	READ INSTRUCTIONS BEFORE COMPLETING FORM
1. REPORT NUMBER: AFWAL-TR-81-3098	2. GOVT ACCESSION NO.: AD A106117
3. RECIPIENT'S CATALOG NUMBER	
4. TITLE *(and Subtitle)*: STUDY OF FIBER OPTICS TO ENHANCE AN ENVIRONMENTAL LIGHTING LABORATORY	5. TYPE OF REPORT & PERIOD COVERED: Final Technical Report Nov 1979 - Mar 1981
	6. PERFORMING ORG. REPORT NUMBER
7. AUTHOR(s): J. Connelly	8. CONTRACT OR GRANT NUMBER(s): F33615-79-C-3629
9. PERFORMING ORGANIZATION NAME AND ADDRESS: Grumman Aerospace Corporation, Bethpage NY 11714	10. PROGRAM ELEMENT, PROJECT, TASK AREA & WORK UNIT NUMBERS: Project 2403; Task 240304; Work Unit 24030421
11. CONTROLLING OFFICE NAME AND ADDRESS: Flight Dynamics Laboratory (AFWAL/FIGR), AF Wright Aeronautical Laboratories, AFSC, Wright-Patterson AFB OH 45433	12. REPORT DATE: August 1981
	13. NUMBER OF PAGES: 154
14. MONITORING AGENCY NAME & ADDRESS *(if different from Controlling Office)*	15. SECURITY CLASS. *(of this report)*: Unclassified
	15a. DECLASSIFICATION/DOWNGRADING SCHEDULE: N/A

16. DISTRIBUTION STATEMENT *(of this Report)*

Approved for Public Release; Distribution Unlimited

17. DISTRIBUTION STATEMENT *(of the abstract entered in Block 20, if different from Report)*

18. SUPPLEMENTARY NOTES

19. KEY WORDS *(Continue on reverse side if necessary and identify by block number)*

Fiber Optics
Lighting Simulation Facility
High/Low Ambient Illumination Simulation
Translucent Spherical Lighting Enclosure
Opaque Ellipsoidal Lighting Enclosure

20. ABSTRACT *(Continue on reverse side if necessary and identify by block number)*

This report documents the results of an investigation to determine how fiber optic materials can be utilized to substantially increase the simulation capabilities of an Environmental Lighting Laboratory. This Laboratory must provide the capability to dynamically simulate the ambient environmental illumination conditions encountered in day, night and high threat/high risk aircraft missions. Three cockpit lighting simulator concepts were studied. Two of these concepts utilized a spherical lighting enclosure with a visual scene being projected at the inner surface via a remote projection input surface; fiber optics carry the

DD FORM 1 JAN 73 1473 EDITION OF 1 NOV 65 IS OBSOLETE

UNCLASSIFIED

SECURITY CLASSIFICATION OF THIS PAGE *(When Data Entered)*

image from input surface to output surface. In one concept, the pilot views a back-projected image on a translucent spherical screen via a spherical output surface with imbedded fiber optics. In the other concept, the pilot views the spherical fiber optic output surface directly. Both concepts were considered possible to implement; each concept having appropriate cost vs. performance tradeoffs. No useful solution was found using the third concept, a fiber optic input to a mirrored ellipsoidal enclosure. It was found that the spherical enclosure concept with an internal translucent projection screen offers the best combination of illumination level and resolution; however, the cost of implementing this concept is substantial.

FOREWORD

This final report describes the engineering effort performed by Grumman Aerospace Corporation, Bethpage, New York 11714 and its subcontractor, Galileo Electro-Optics Corporation, Sturbridge, Massachusetts 01518, to determine how fiber optic materials can be utilized to increase substantially the simulation capabilities of an environmental lighting laboratory. This work was sponsored by the U.S. Air Force Flight Dynamics Laboratory, Wright-Patterson Air Force Base, Ohio, under Contract Number F33615-79-C-3629.

Mr. J. A. Uphaus was the Air Force Project Engineer during the term of the work reported herein.

Mr. J. Connelly, the Project Engineer for Grumman Aerospace Corporation, and Mr. David Ruppel performed the work. They wish to thank Messrs. Rodney J. Anderson and Richard L. Kirk of Galileo Electro-Optics for their contributions.

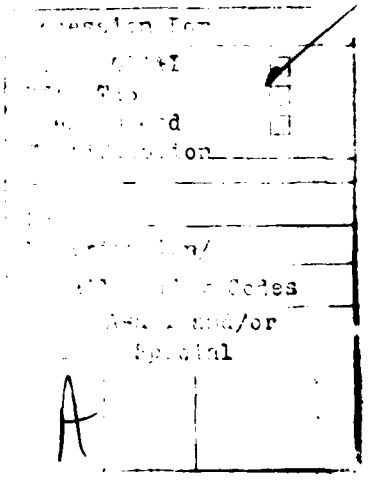

CONTENTS

CONTENTS (Cont)

ILLUSTRATIONS

ILLUSTRATIONS (Cont)

ILLUSTRATIONS (Cont)

TABLES

SYMBOLS

A_F	Area of Fiber Core
A_W	Area of Illuminated Pattern on CSDF Wall
A_{IN}	Illuminated Area on Input Surface
A_C	Area of Cockpit to be Illuminated
B_W	Luminance of the Translucent Wall
C_C	Diameter of the Fiber Core Divided by the Overall Diameter
CSDF	Crew System Design Facility
D	Perceived Diameter of Pixel Spot
E	Overall Diameter of Clad Fiber
E_1	Illumination of Input Shaping Filter
E_2	Illumination of Rear Surface of Translucent Screen
E_{SI}	Illumination of Solar Intensity Desired at the CSDF Cockpit
E_{hp}	Illumination on a Hypothetical Plane
G_W	Gain of the Translucent Wall
K_1	The watts of flux delivered by the lamp source divided by the watts of flux emerging from the fiber
K_2	The relative illumination at a point of interest at an angle from the axis of a radiating cone of light divided by .5.
M	Linear Magnification
N	Number of Fibers used for Solar Simulation

SYMBOLS (Cont)

NA	Numerical Aperture
P_i	Fraction of Input Surface Area Occupied by Fiber Cores
P_o	Fraction of Output Surface Area Occupied by Fiber Cores
R	Radius
T_λ	Spectral Transmission
T_w	Transmission through Translucent Wall
W_T	Total Lumens Delivered by the Lamp System
Z	Signal amplitude
a	Distance between fiber centers
b	Distance between fiber centers normal to a
d	Diameter of fiber core
h	Spacing between center of nested fibers in a triangular arrangement
m	Interpixel modulation
n_w	Index of refraction of the translucent wall material
s	Projection distance from fiber to screen
t	Thickness of projection screen
δ	Angle whose sine is the numerical aperture
ρ	Specular reflectivity
ρ_1	Reflectivity of fiber optic input surface
ρ_2	Reflectivity of fiber optic output surface
ρ_3	Reflectivity of rear surface of the translucent screen
ϕ	Solid angle in steradians

SECTION I

INTRODUCTION AND SUMMARY

BACKGROUND

In the early 1960s, cockpit simulators had been developed to a point where aircraft dynamics and flight control response could be realistically duplicated. Up to that time, however, little had been attempted in developing realistic out-the-window visual displays. The first attempts to overcome this deficiency met with limited success and some of the compromises exist to this day.

The visual displays that evolved used a wide range of techniques and devices. Closed circuit television both monochrome and color, model boards, computer-generated inputs, and transparency projections, among others, were used. None of these, however, addressed the problem of operation in a highly illuminated environment, but were all designed to be used at low ambient light levels, usually in darkened areas. With the increased use of electronic displays and the complexity of future aircraft systems, the effect of ambient lighting on crew efficiency has become a major design consideration. It is therefore desirable to have a facility available which can simulate the external illumination levels for man-machine evaluation under controlled conditions. Fiber optics have several characteristics that may make such a simulation feasible.

OBJECTIVES

The objective of this study was to determine the electro-optical characteristics of fiber optic materials that can be used to increase the simulation capabilities of an environmental lighting laboratory, to determine those characteristics of fiber optics which permit the projection of intensely illuminated moving airborne and ground targets, and to investigate the rapid movement of intense solar images that can be positioned to simulate 360° aircraft rolls, loops, etc.

RESULTS AND SUMMARY

The study developed the relationships between the desired performance of a fiber optic Crew System Design Facility (CSDF) and the physical features required to achieve it. Three systems were studied. Two systems were considered possible to build, one in which the pilot views a spherical screen and the image is back-projected by the fiber optics and another where the fiber optics are viewed directly. No useful solution was found using the third concept, a fiber optic input to a mirrored ellipsoidal enclosure.

A 3-inch by 3-inch fiber optic test specimen was fabricated to permit the demonstration and measurement of the performance parameters for comparison with the predicted results. A simple cost model was used to predict CSDF fabrication costs versus optical performance.

The study established the possibility of building a CSDF that could impose the desired illumination levels, with image quality comparable to present state of the art large-dome simulators. The cost is considerable and may not be justified for a system with marginal image quality. The physical requirements and the predicted cost to improve the image quality were investigated. While it is possible to provide both the desired illumination and image quality, the cost is substantial.

SECTION II

CREW SYSTEM DESIGN FACILITY REQUIREMENTS

The ability of fiber optic faceplates to transfer images with good resolution is well known. This suggests the possibility of transferring images in a Crew Systems Design Facility (CSDF) that would be acceptable to the subjects. To some degree, the physical size of the fibers and the fiber-to-fiber spacing could be modified for the viewing conditions in a CSDF. The extent of the change and the other requirements that the fibers must satisfy will depend on the CSDF configuration.

GENERAL CSDF REQUIREMENTS

A satisfactory solution of the CSDF design problem must simultaneously satisfy the following requirements:

Resolution - The image presented to the pilot should be sufficiently sharp so that his eye is the limit of resolution in those areas of the simulator where normal visual acuity is necessary. Resolution may be decreased in peripheral areas of the simulator.

Image Fidelity - The sky, terrain and target images should have the correct luminosity and color. Targets should be presentable with positive and negative contrast.

Solar Illumination - The solar illumination should have the correct apparent intensity and color. The angular subtense and collimation of the simulated solar disc should be small enough to provide realistic shadowing in the cockpit, believable size when the pilot looks close to it, and confine the illumination to the cockpit to minimize contrast-reducing reflections from the walls.

Physical Size - The apparent image location should be sufficiently far from the subject to allow his eyes to accommodate for infinity. In a bright environment, the resting eye has a depth of field from approximately six

meters to infinity. In addition, the apparent distance to the image surface over the entire CSDF should vary uniformly and as little as possible.

CRITICAL ISSUES FOR FIBER OPTICS

There are essentially two critical issues that will determine the suitability of fiber optics in a CSDF. The first is the ability to simulate sunlight and the second is the cost. If the sun can be simulated, then the other requirements for resolution, uniformity, size, etc., will combine to drive the cost. The fiber material, and therefore its relative cost, will be dictated by the solar simulation requirement. Naturally, some of the parameters will be involved in both issues.

In both issues, the parameters are profoundly influenced by the Fiber Optic Crew System Design Facility (FOCSDF) configuration. The study sought to add configurations beyond those cited in the Statement of Work (SOW), but only one additional configuration with any merit was defined.

STUDY PLAN

The study plan is illustrated in Figure 1. It began with an analytic phase that traded off existing fiber optic performance data, CSDF requirements, and feasible CSDF configurations. Guided by the analysis, the critical technical parameters were identified, a verification test series was planned, and a test article was fabricated. The results of the tests were compared with the initial parametric analysis. The study conclusions were determined by the feed back test results and the analytical CSDF performance projections.

CANDIDATE CSDF CONFIGURATIONS

The first configuration contained in the SOW is illustrated in Figure 2. It is a crew station situated in the center of a "sphere". The wall seen from the crew station is a translucent screen material. Images are rear-projected on the screen by the fiber optics which carry the image information from the input projection surface. The size of the individual image spot depends on the distance between the screen and the fiber optic. This configuration permits resolution changes in different areas of the dome by varying the pitch between fibers and the corresponding fiber-to-screen distance. Offsetting this advantage, the translucent screen complicates the solar simulation.

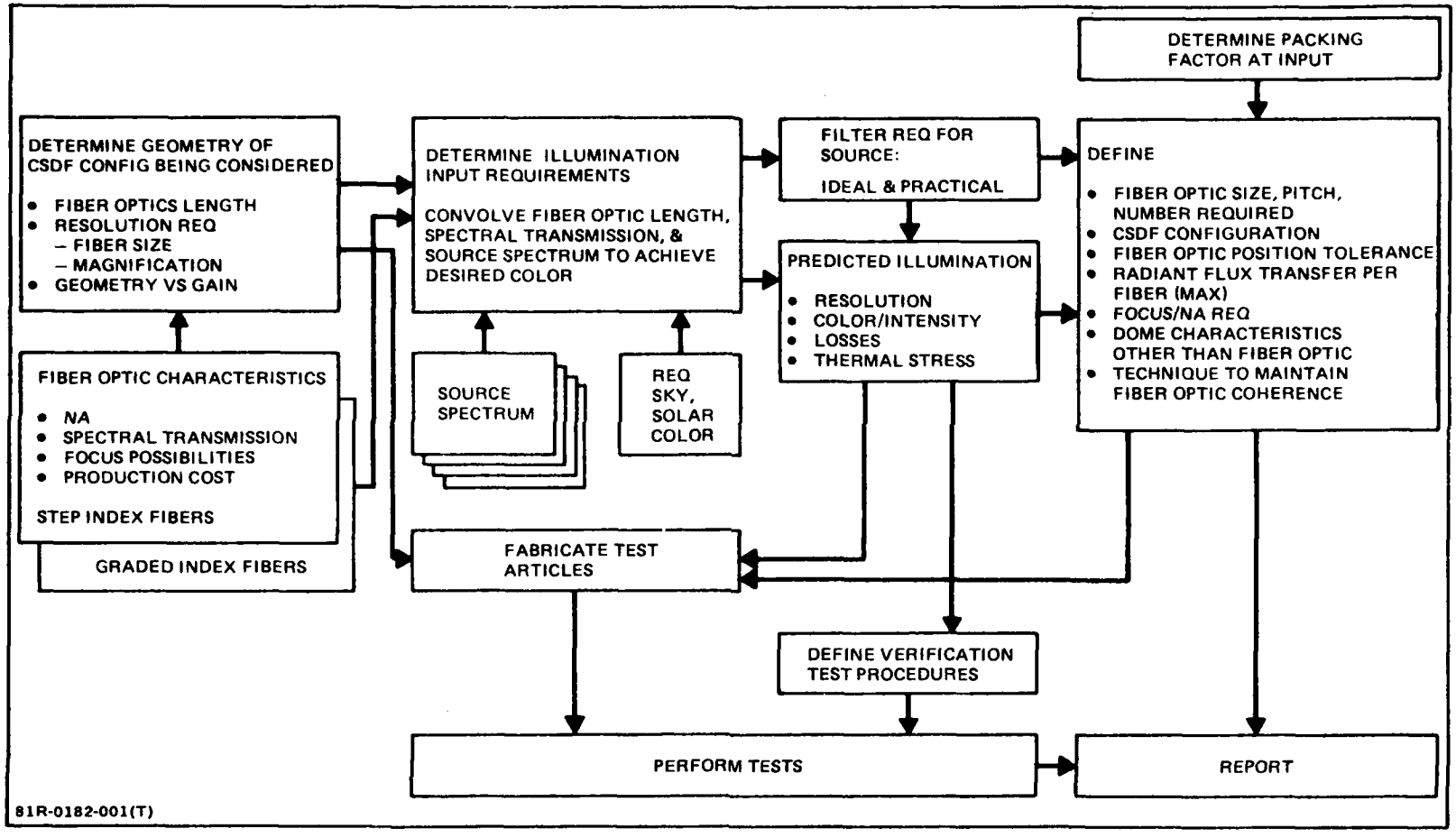

Figure 1 Study Plan

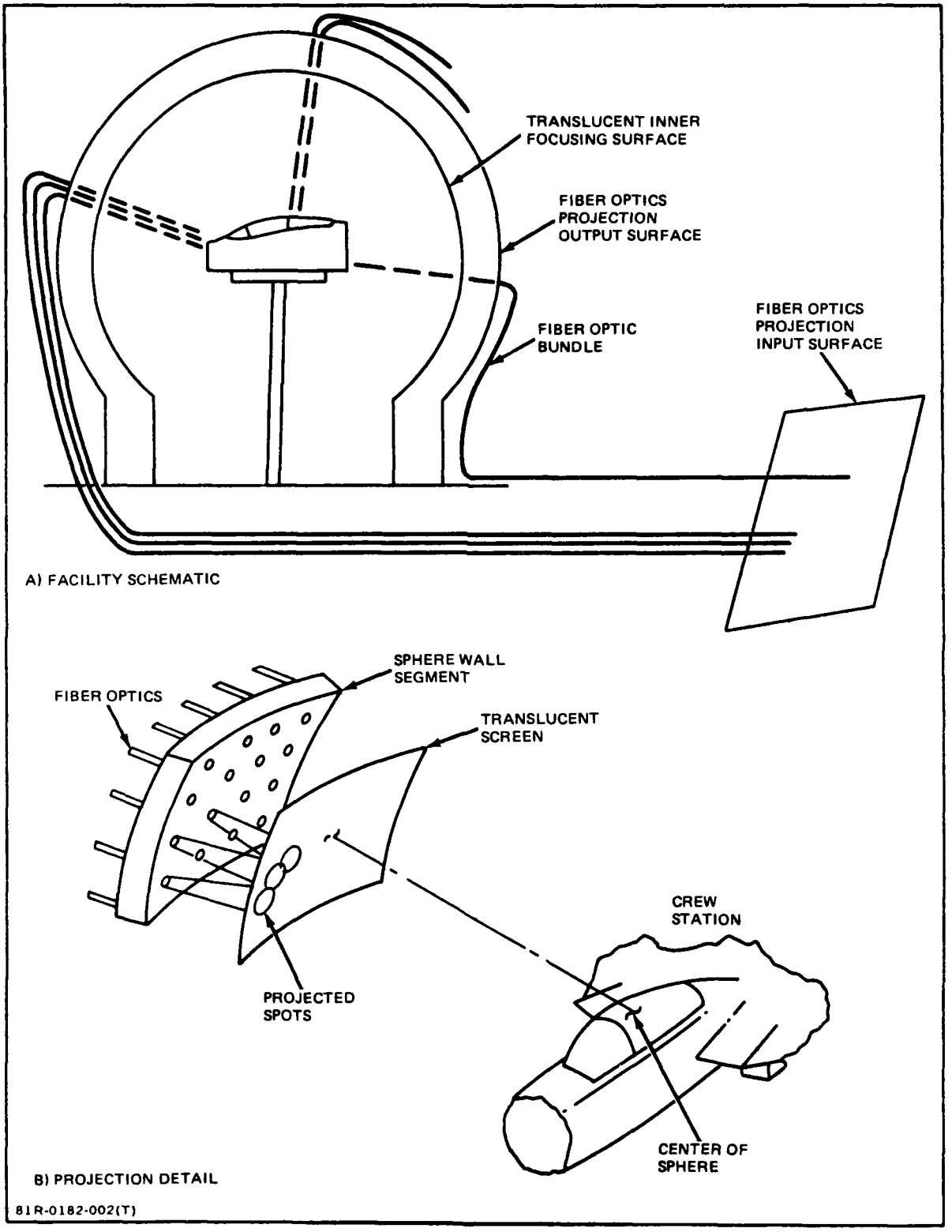

Figure 2 Translucent Spherical Enclosure

A variant of the first configuration is illustrated in Figure 3 where the fiber optic ends in the sphere wall are viewed directly. This is equivalent to a screen at zero distance from the wall, which avoids the screen mounting problem entirely. It reduces the problem of solar simulation but complicates the provision of variable resolution, with its attendant economy in fiber optics.

The third configuration is illustrated in Figure 4. It consists of a crew station located at one foci of an ellipsoid with a fiber optic projection surface at the other. The input to the fiber optic surface comes from an external projection surface in a manner similar to the other configurations. In this scheme, the viewer sees an image of the input surface relected off the mirrored inner surface of the ellipsoid. The viewer is expected to see an enlarged view of the input surface, in correct orientation, regardless of the direction in which he is looking. It is apparent that, if this configuration and either of the others had the same resolution, as seen by the user, they would each have the same number of fibers. In this case, the small size of the input surface would drive the fiber size to the smallest possible diameters. This would complicate the solar simulation. Because of the differences between this configuration and the others, it will be analyzed separately.

BASELINE DIMENSIONS

A number of parameters can have at least one dimension fixed as a result of previous studies or anticipated values. This includes the minimum internal radius of the CSDF dome and the size of the cockpit area to be illuminated. The length of the fiber optics between the CSDF and the input screen has a minimum practical length that must be estimated.

The minimum distance from the observer to the image is assumed to be 6.1 meters in order to permit the user's eyes to be accommodated to a distant object. Lesser distances are acceptable for simulators that operate at lower levels of illumination. However, a lesser radius in a full-brightness simulation would introduce experimental errors in behavioral data.

It is inadvisable to subject the fibers to sharp bends or other stress raising conditions between the dome wall and the image input surface. A substantial fiber length must be provided to accommodate all the unknowns associated with

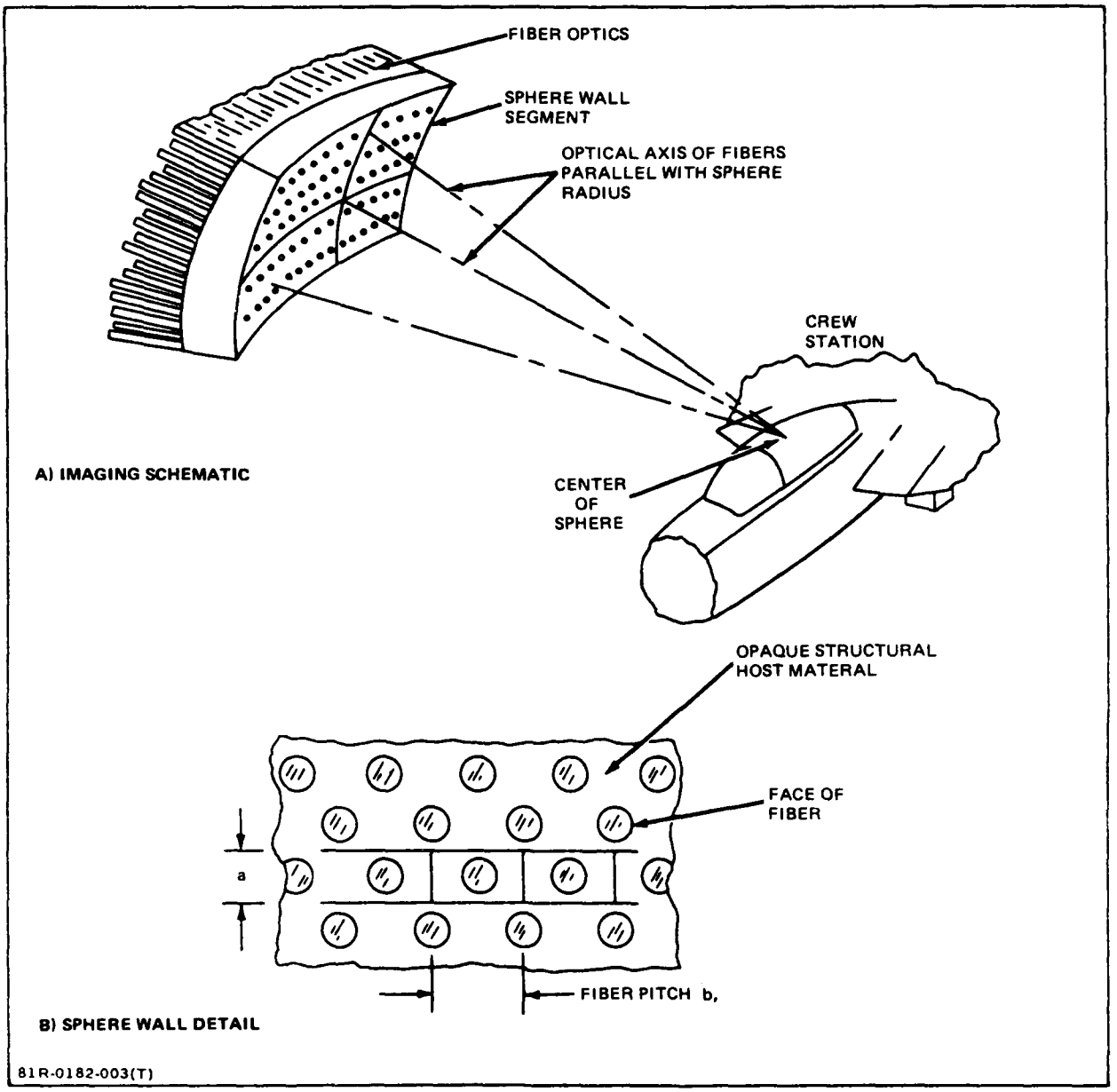

Figure 3 CSDF Based on Direct View of Fiber Optic Wall Segments

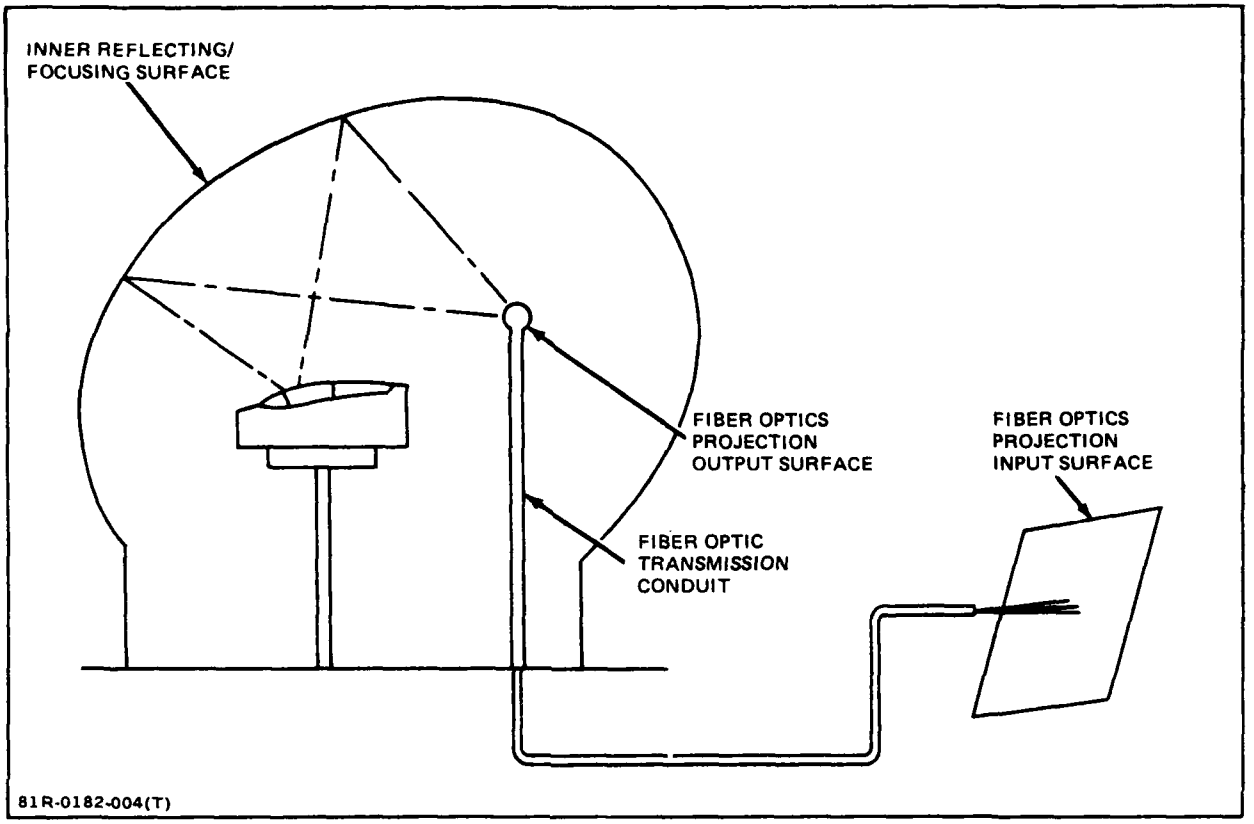

Figure 4 Opaque Ellipsoidal Enclosure

the cable runs. Accordingly, fiber optic lengths up to 100 meters were studied.

The cockpit area that must be serviced in the CSDF is essentially contained in a 3.5-meter diameter. This will be sufficient for side-by-side or tandem seating arrangements. This results in a requirement to provide solar simulation in a solid angle of 0.26 steradians.

SECTION III

CSDF PERFORMANCE PREDICTION

SOLAR SIMULATION

Solar simulation is physically the most demanding requirement in all CSDF configurations. There are more similarities than differences in the physical satisfaction of this requirement for each CSDF configuration. The analysis was performed for the Translucent Dome configuration and the predicted results were modified for the other configurations.

Procedure

The major system losses or inputs are identified in Figure 5 for the translucent dome configuration. The flux arriving at the cockpit (E_{SI}) must be essentially correct in spectrum and intensity. It is subjected to the following losses or gains:

1. A loss in the spectral correcting filter due to the color correcting function of the filter.
2. A loss on the input surface due to the packing efficiency.
3. A reflection loss from the input fiber optic surface (ρ_1).
4. Absorption in the fiber optic as a function of length and propagating wave length.
5. A reflection from the exit face of the fiber optic (ρ_2).
6. A reflection from the outer surface of the translucent wall (ρ_3).
7. A loss due to scattering and absorption in the translucent wall.
8. A possible gain factor due to the treatment of the inner surface of the translucent wall.

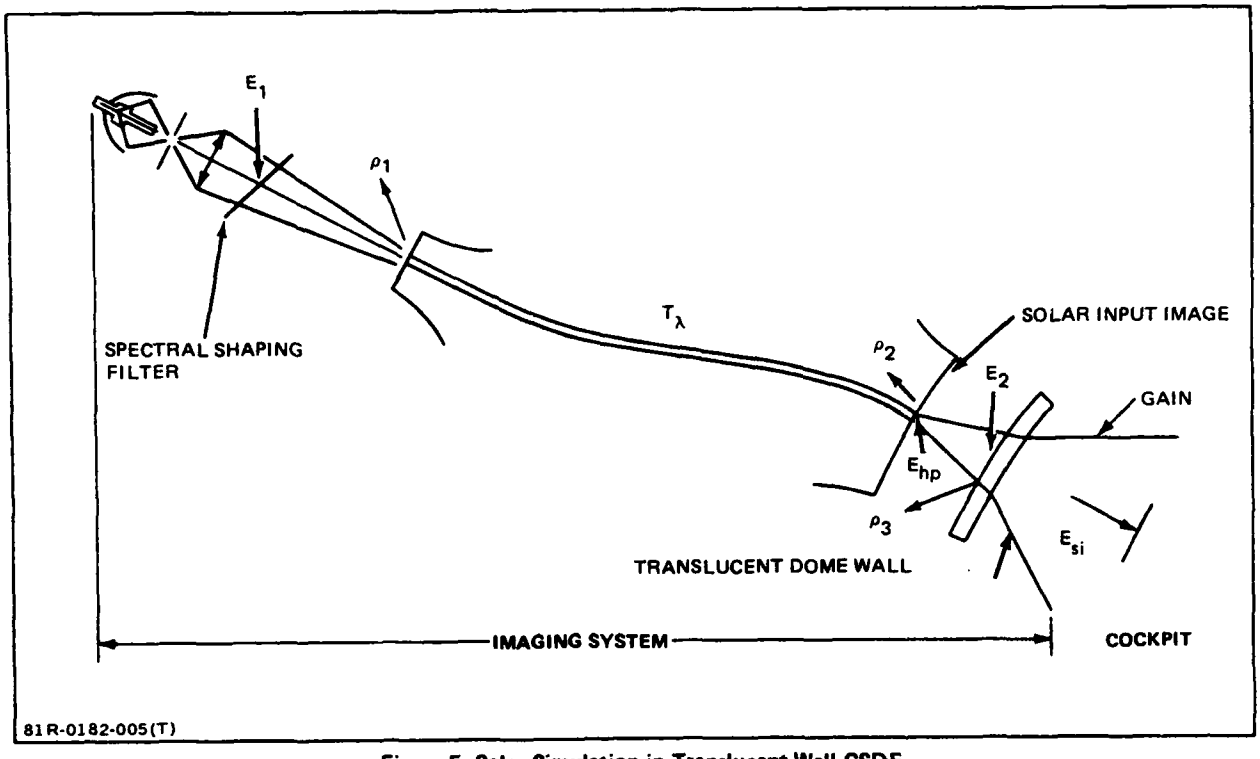

Figure 5 Solar Simulation in Translucent-Wall CSDF

For the alternate configuration where the ends of the fiber optics are viewed directly, the changes to the system losses are:

- Factors 6, 7, and 8 do not apply
- The mismatch between the area to be illuminated and the exiting intensity pattern of the fiber optics must be accounted for.

For the ellipsoidal configuration, the factors include all those for the direct view CSDF plus the following:

- A specular reflection must be added
- The magnification factor between the input surface and the viewed image must be accounted for.

If the fiber optic portion of the CSDF transmitted energy equally at all visual wavelengths, the illumination analysis could be performed entirely in watts. It is well known, however, that this is not the case. A spectral filter in the solar simulator reshapes the input spectrum to compensate for the spectral attenuation in the fibers. Therefore, a correction factor must be applied to account

for the expected loss. The unneeded energy extracted by the spectral filter can be assumed to be reflected out of the system. Therefore, the solar simulation requirement will be analyzed by:

- Determining the flux that must be transmitted through the system in watts, assuming an acceptable spectral distribution at the center of the CSDF.
- Determining the ratio of flux into the fibers to flux out of the fibers, to provide an acceptable spectral distribution.
- Defining the characteristics of a spectral filter and its effect on the input to output flux ratio.
- Determining the resulting flux density on the input face of the fibers, the quality of the simulation and the requirements for the solar illumination source using all of the above factors.

Solar Simulation Power for Translucent-Wall CSDF

The direct solar illumination at high altitude is approximately 0.125 watts per square centimeter, of which 40 percent is between 400 and 700 nanometers. (These limits were chosen because the relative values on the Standard Visibility Curve are 4×10^{-4} and 4×10^{-3} respectively). Consequently, an acceptable solar simulation would provide 5×10^{-2} watts cm^{-2} at the cockpit as long as the relative spectral distribution of the solar spectrum is achieved. This irradiation is also roughly equivalent to an illuminance of 12.4 lumens cm^{-2}.

In Figure 6, the solar illumination at the cockpit, E_{SI} (lumen cm^{-2}), is shown arriving from a radiating area of the CSDF translucent wall. The spot on the wall subtends ϕ steradians from the cockpit and has a luminance of B_W (lumens cm^{-2} $ster^{-1}$). Therefore:

$$E_{SI} = B_W \phi \quad \text{lumen cm}^{-2} \tag{1}$$

The luminance of the wall, B_W, is produced by illumination E_2 coming from the fibers and can be expressed as:

$$B_W = \frac{E_2 (1-\rho_3) T_W G_W}{\pi} \qquad \text{lumen cm}^{-2} \text{ ster}^{-1} \tag{2}$$

where ρ_3 is the reflectivity of the translucent wall's outer surface, T_W is the

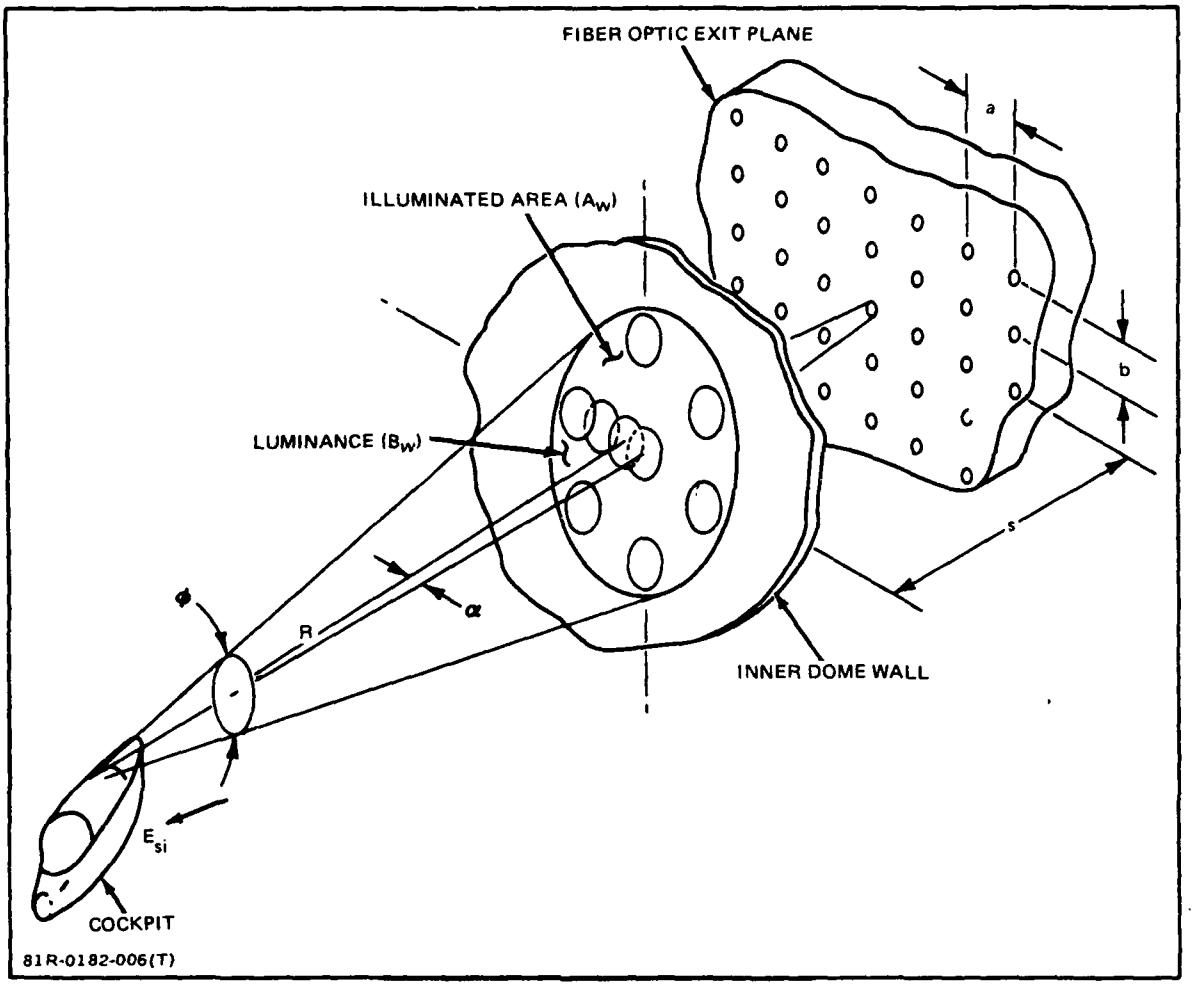

Figure 6 Translucent-Wall CSDF Geometry

effective transmittance of the wall, accounting for absorption, scatter and reflection from the inner surface, and G_W is a gain factor for the surface of the translucent wall. It is defined as the ratio of illumination arriving at the cockpit from a given wall surface to the illumination that would arrive if the flux distribution was lambertian. Therefore, the illumination, E_2, that must be delivered by the fibers to the wall surface is given by:

$$E_2 = \frac{\pi E_{SI}}{(1-\rho_3)\, T_W\, G_W\, \phi} \qquad \text{lumen cm}^{-2} \qquad (3)$$

To determine the total illumination that must be delivered by the light source, additional factors must be considered:

- The surface reflection ρ_1 and ρ_2 at each end of the fiber

- The transmission loss in the fiber
- The loss at the spectral shaping filter
- The packing coefficient in the input and output faces of the fiber.

A lumped constant, K_1 will be defined as the ratio of flux delivered by the lamp source to flux out of the fibers. It will take into account the reflection losses ρ_1 and ρ_2, the spectral transmission losses in the fibers and the flux rejected from the lamp output by the spectral shaping filter. The flux (E_2) irradiating the translucent wall will have an acceptable spectral distribution and K_1 times as much flux must be delivered by the lamp system to achieve it.

The output packing coefficient (P_o) is considered to be the fraction of the output surface area that is occupied by the flux carrying core of fibers. P_o is defined as:

$$P_o = \frac{A_F}{ab} \tag{4}$$

where A_F is the area of the flux-carrying core of an individual fiber and a and b are the distances between fibers, as illustrated in Figure 7.

If we make the assumption that all the flux is being emitted by one loss-free fiber, then E_{hp}, the illumination of a fictitious surface an insignificant distance from the output face of the fiber, is greater than E_2 by the ratio of the illuminated area of the wall A_W to the area of the core of the fiber A_F. Therefore:

$$F_{hp} = \frac{\pi E_{SI} A_W}{(1-\rho_3) T_W G_W \phi A_F} \qquad \text{lumens cm}^{-2} \tag{5}$$

However, there will be many fibers contributing to the illumination on the wall. The number of fibers used for solar simulation, N, is:

$$N = \frac{A_W}{ab} \tag{6}$$

The average illumination on the fictitious surface can be determined by dividing E_{hp} by the number of fibers used, N. Substituting Equation 4 into 5 and dividing by equation 6 yields:

$$E_{hp} = \frac{\pi E_{SI}}{(1-\rho_3) T_W G_W \phi P_o} \qquad \text{lumens cm}^{-2} \tag{7}$$

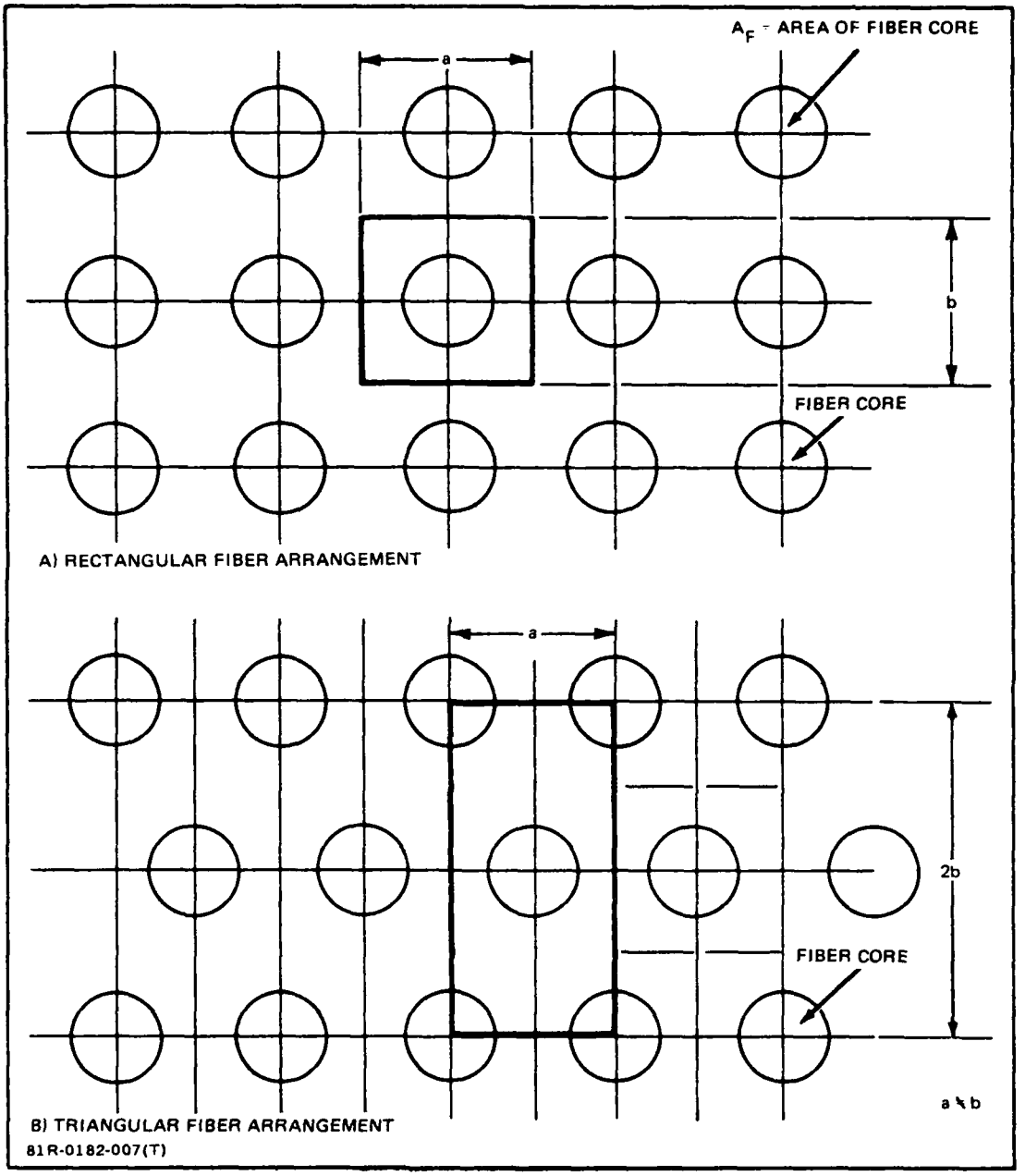

Figure 7 Output Packing Coefficient Fiber Geometry

The illumination must be increased to compensate for the fiber absorption and reflection losses. A spectral compensation factor, K_1, was previously described that included the losses between the illuminator and the input face of the fibers. Therefore, the input luminance that must be produced by the lamp system, E_l, is K_l times E_{hp}:

$$E_1 = \frac{\pi E_{SI} K_1}{(1-\rho_3) T_W G_W \phi P_o} \quad \text{lumens cm}^{-2} \tag{8}$$

The total illumination delivered by the lamp, W_T, can be expressed as the product of:

$$W_T = E_1 A_{IN} \quad \text{lumens} \tag{9}$$

where A_{IN} is the illuminated area on the fiber optic input surface. The input packing coefficient P_i is defined for the input surface similar to equation 4 for P_o. Then:

$$\frac{A_{IN}}{A_W} = \frac{P_o}{P_i} \tag{10}$$

If the fiber-to-fiber spacing of the input and output surfaces were the same, the total lumens required from the lamp would be E_l times A_W. However, if the fiber-to-fiber spacing of the input surface were less than for the output surface, the lamp requirement would become E_l times the smaller area. Expressing the input packing fraction as P_i, then the total lumens from the lamp system, W_T, is:

$$W_T = E_1 A_W \frac{P_o}{P_i} \quad \text{lumens} \tag{11}$$

In Equation 8, E_l is expressed as a function of ϕ, the angular subtense of the simulated sun in the CSDF. If ϕ is allowed to be larger than the real solar subtense, then the associated value of E_l can be reduced. If the angular subtense ϕ is replaced by A_W/R^2, where R is the radius of the CSDF, then Equation 11 can be reordered to read:

$$W_T = \frac{\pi E_{SI} K_1 R^2}{(1-\rho_3) T_W G_W P_i} \quad \text{lumens} \tag{12}$$

The total lumens required from the lamp system in order to illuminate the CSDF cockpit area with 12.4 lumens cm^2 is illustrated in Figure 8. Screen reflection ρ_3 is assumed to be .04 and the product of screen transmission, T_W, and screen gain, G_W, is a parameter. In the case illustrated, a spectral compensation factor of 6.0 and an input fiber packing efficiency of .5 requires 17.5 megalumens if the screen transmission gain product is 10, or 35 megalumens if the gain is 5.

The distribution of flux in the CSDF cockpit area can be expected to be a maximum along the CSDF radius and to decrease laterally. The value of the $G_W T_W$ term should be determined at the lateral distance established by the crew member location.

In a cockpit with a maximum lateral dimension of 3.5 meters, the distance between crew members and their critical displays could be as much as 2.5 meters. From the edge of the illuminated area, the viewer would be 16 degrees off-axis. At the expected maximum pilot spacing of 2.5 meters, they would be 11.6 degrees off-axis. The effect of this lateral spacing on the usable $T_W G_W$ product is illustrated in Figure 9 for a selection of commercial rear-projection screen materials. The screen gain used in Figure 9 is equivalent to the $T_W G_W$ product term used in Equation 12. A reasonable value for $T_W G_W$ appears to be 10 for a single cockpit, 5 for the probable separation of a tandem cockpit, and 3 at the 3.5 meter limit.

Sky Simulation for Translucent-Wall CSDF

In addition to solar simulation, a substantial sky brightness is required over a portion of the CSDF. This can be simulated on the translucent wall (B_W) in lumens cm^{-2} ster $^{-1}$ by illumination E_2 where:

$$E_2 = \frac{\pi B_W}{(1-\rho_3)\ T_W\ G_W} \quad \text{lumens cm}^{-2} \tag{13}$$

If the wall area subtended by one steradian (R^2) was illuminated by one fiber with a core area A_F, the illumination on the fictitious surface E_{hp} would be increased by the ratio of R^2/A_F. Since N fibers will be used and the input illumination will be reduced by N, Equation 13 becomes:

$$E_{hp} = \frac{\pi B_W\ ab\ R^2}{(1-\rho_3)\ T_W\ G_W\ A_F\ A_W} \quad \text{lumens cm}^{-2} \tag{14}$$

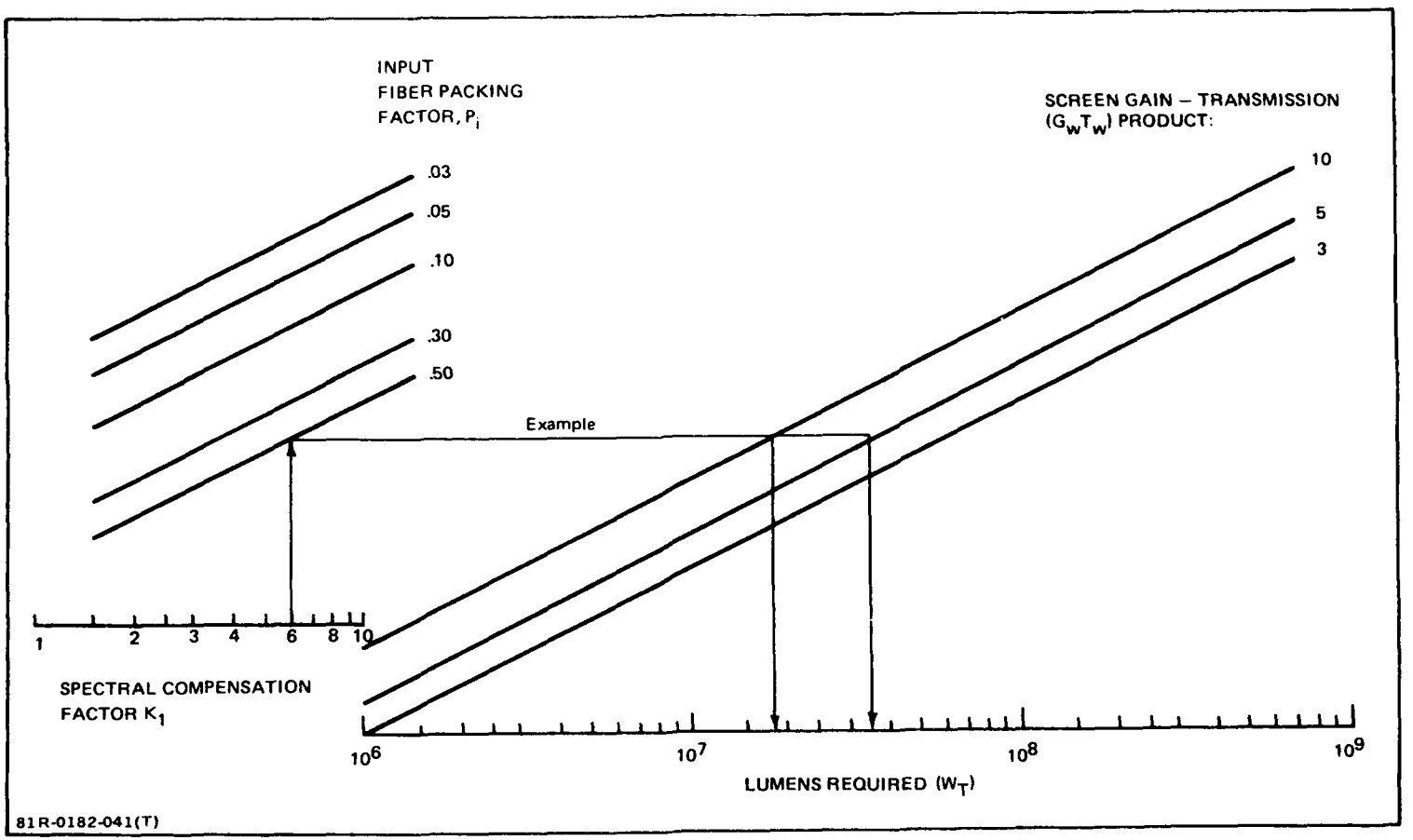

Figure 8 Solar Simulation Lumens Required for Translucent - Wall CSDF vs Input Fiber Packing Factor, Spectral Compensation Factor and Screen Gain – Transmission Product

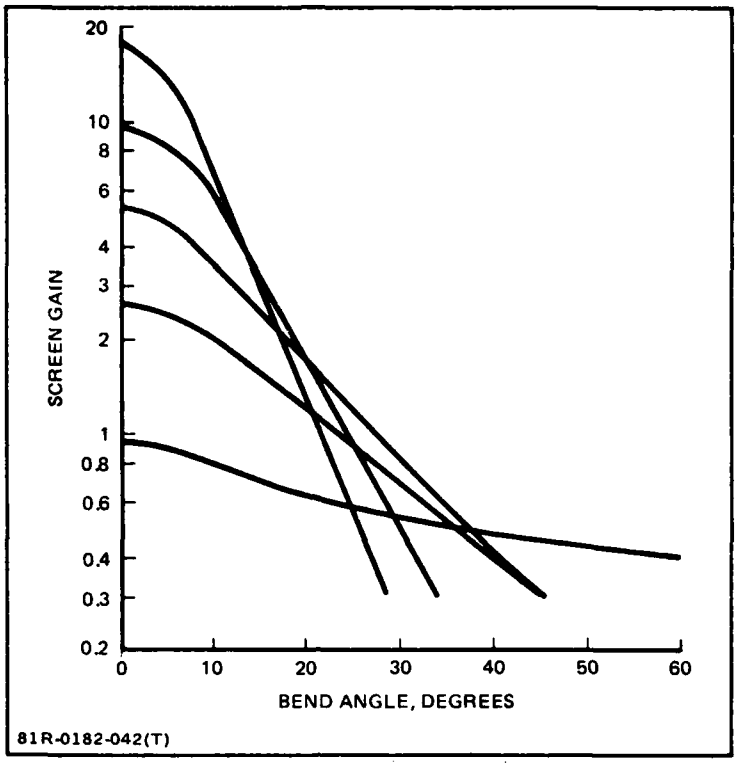

Figure 9 Typical Diffusion Characteristics of Several Commercial Rear-Projection Screens

Using the relationship between ab and A_F from Equation 4 and the relationship between the input area illuminated, A_{in}, and the wall area, A_W from Equation 10, Equation 14 becomes:

$$E_{hp} = \frac{\pi B_W R^2}{(1-\rho_3) T_W G_W P_i A_{in}} \quad \text{lumens cm}^{-2} \tag{15}$$

Correcting for the spectral loss in the fibers:

$$E_1 = K_1 E_{hp} \quad \text{lumens cm}^{-2} \tag{16}$$

and the total lumens required (W_T) is:

$$W_T = E_1 A_{in} \quad \text{lumens} \tag{17}$$

Therefore:

$$W_T = \frac{\pi B_W K_1 R^2}{(1-\rho_3) T_W G_W P_i} \quad \text{lumens} \tag{18}$$

Solar Simulation Power for Direct-View CSDF

In the CSDF configuration, where the ends of the fibers are viewed directly, the expression for solar simulation power does not use the factors ρ_3, T_W, and screen gain factor G_W. However, the numerical aperture of the fiber now affects the illumination at the CSDF cockpit.

If a hypothetical plane is assumed to exist an infinitesimal distance beyond the exit face of a lossless fiber, the illumination on that plane is related to the illumination at the cockpit by the ratio of the flux-carrying area of fiber, A_F, and the projected area at the cockpit, A_C. Letting E_{SI} be the desired illumination at the cockpit and E_{hp} be the illumination produced on the hypothetical plane by the single fiber, then:

$$E_{hp} = E_{SI} \frac{A_C}{A_F} \qquad \text{lumens cm}^{-2} \qquad (19)$$

The solar illumination will come from many fibers in an area on the wall of the CSDF (A_W) that subtends ϕ steradians at the distance R. The number of fibers in ϕ steradians is:

$$\text{Number of fibers} = \frac{R^2 \phi}{ab} \qquad (20)$$

The illumination on the hypothetical plane can be reduced by the number of fibers being used. Therefore E_{hp} can become:

$$E_{hp} = \frac{E_{SI} A_C}{R^2 \phi P_o} \qquad \text{lumens cm}^{-2} \qquad (21)$$

In the direct-view CSDF, the illumination pattern depends on the numerical aperture (NA) of the fiber. The area of an illuminated plane R meters from the fiber is:

$$A_C = \pi R^2 \, \text{Tan}^2 (\sin^{-1} \text{NA}) \qquad \text{cm}^2 \qquad (22)$$

The input illumination level, E_1 is:

$$E_1 = K_1 E_{hp} \qquad \text{lumens cm}^{-2} \qquad (23)$$

Substituting Equation 22 for A_C assumes that the illumination is uniformly distributed, which it is not. The flux distribution is maximum in the center of

the radiating pattern, decreasing with angle to the edge of the cone. Therefore, on the axis of the radiating cone, the illumination will exceed the average and, beyond an angle that is a function of each NA, the illumination will be less than average. To account for this variation, a factor K_2 is used. K_2 is defined as the relative illumination at the point of interest from the fiber being considered, divided by 0.5. For example, on axis, where the relative illumination value is 1.0, the value of K_2 is 2.0. If the cockpit is centered where the relative illumination is 0.4, then K_2 is 0.8. Using this convention, it follows that the NA is defined by the angle when the illumination is 50% of the on-axis value.

Combining Equations 21, 22 and 23 and using the factor K_2 yields:

$$E_1 = \frac{\pi E_{SI} K_1 \tan^2 (\sin^{-1} NA)}{\phi P_o K_2} \quad \text{lumens cm}^{-2} \tag{24}$$

It follows that the total luminance required at the input face is:

$$W_T = \frac{\pi E_{SI} K_1 R^2 \tan^2 (\sin^{-1} NA)}{P_i K_2} \quad \text{lumens} \tag{25}$$

There is a tradeoff between NA and K_2 to minimize W_T.

Using a solar illumination value of 12.4 lumens per square centimeter and a NA of 0.275, the relationship between the input packing coefficient (P_i) and the spectral compensation factor K_1 is illustrated in Figure 10. The cockpit is assumed to be at the point in the distribution pattern where $K_2 = 0.5$.

Solar Simulation Power for Ellipsoidal CSDF

In the ellipsoidal concept the viewer is expected to see an image of an input ball structure reflected off the wall. Without considering whether the image is real, virtual or even possible, the scale factor must be correct. If that can be achieved, the ellipsoidal wall magnifies the individual pixels in the input ball to essentially the same angles they represent in the direct-view CSDF. Consequently, the luminance requirements are virtually the same except that terms must be added for the specular wall reflections and the linear magnifications. Letting ρ_s represent the specular wall reflection and M the linear magnification, Equation 24 can be modified to read:

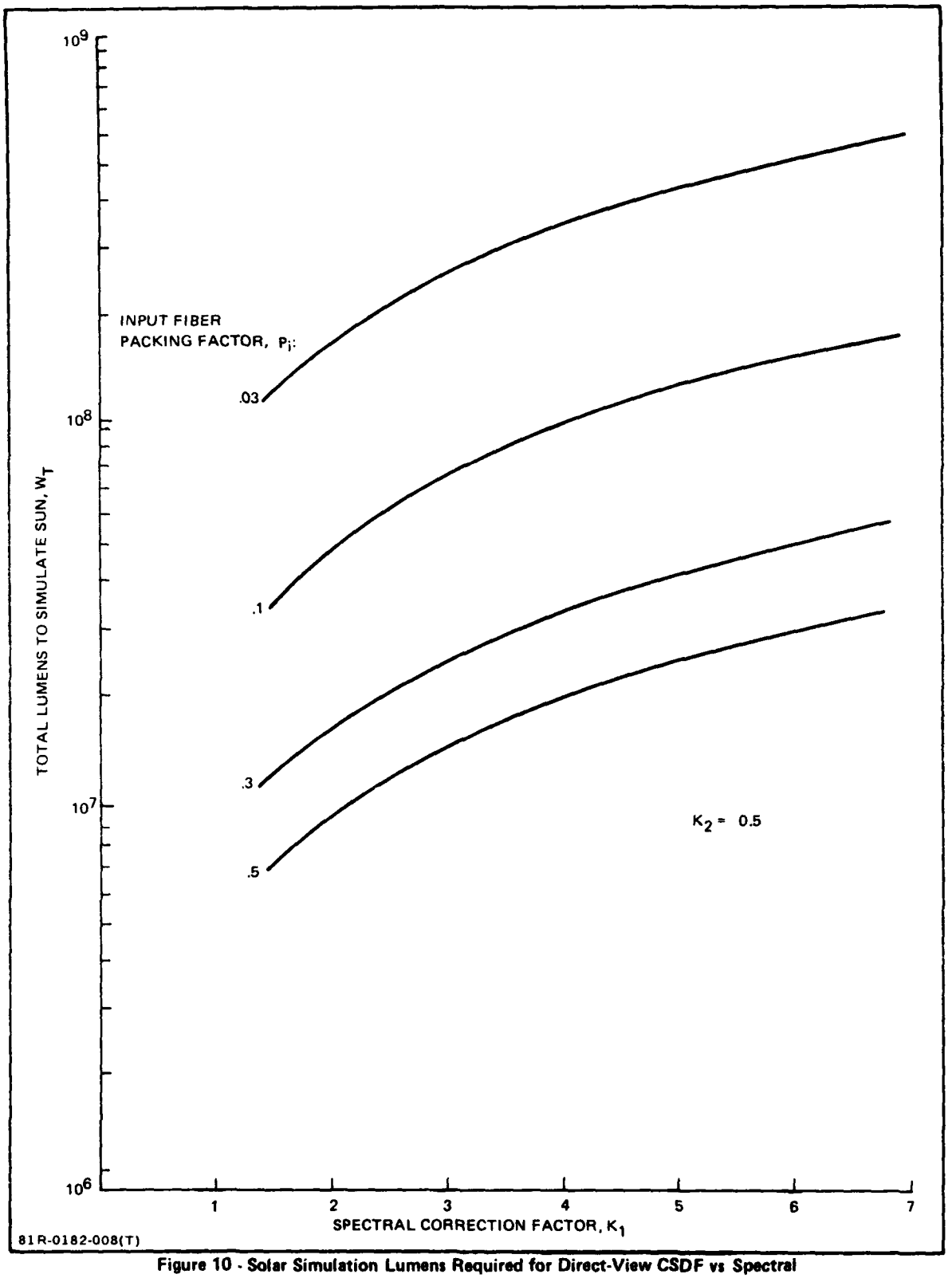

Figure 10 - Solar Simulation Lumens Required for Direct-View CSDF vs Spectral Correction Factor and Fiber Packing Factor

$$E_1 = \frac{\pi E_{SI} K_1 \tan^2 (\sin^{-1} NA) M^2}{\phi P_o K_2 \rho_s} \quad \text{lumens cm}^{-2} \qquad (26)$$

The input solar image must be M^2 times as bright as the input for the direct-view CSDF. While the flux density on each fiber is increased by the factor M^2, the area of the input image is reduced by M^2. Therefore, the total luminance required on the input face is:

$$W_T = \frac{\pi E_{SI} K_1 \tan^2 (\sin^{-1} NA)}{P_i K_2 \rho_s} \quad \text{lumens} \qquad (27)$$

A number of the individual terms will have different values for the ellipsoidal configuration. The value of M must be substantially greater than 1.0, however its value would depend on the results of a ray trace. The spectral compensation factor, K_1, can be substantially reduced because the fiber length required to go from the CSDF to the input surface facility is much less than the direct-view or translucent-wall CSDFs.

Illumination Pattern

The illumination pattern generated by the fibers on the translucent wall of the CSDF will have a modulation similar to the inter-raster modulation seen in television. It is caused by the individual illumination pattern, the thickness of the translucent wall, the separation between fibers and the distance from the fibers to the translucent wall.

The illumination pattern from a typical fiber is illustrated in Figure 11. The projection distance(s) is the distance between the fiber and the screen. In the figure, the intensity is directly related to the angle from the center of the pattern. In the CSDF, the size of the spot visible from the cockpit depends on the projection distance and the thickness of the translucent wall. This geometry is illustrated in Figure 12. The perceived diameter, D, of the spot is given by:

$$D = 2 s \tan \delta + 2t \tan \delta' \qquad (28)$$

The refracted angle δ' is related to δ by:

$$\sin \delta' = \frac{\text{Sin } \delta}{n_w} \qquad (29)$$

where n_w is the index of refraction of the translucent screen.

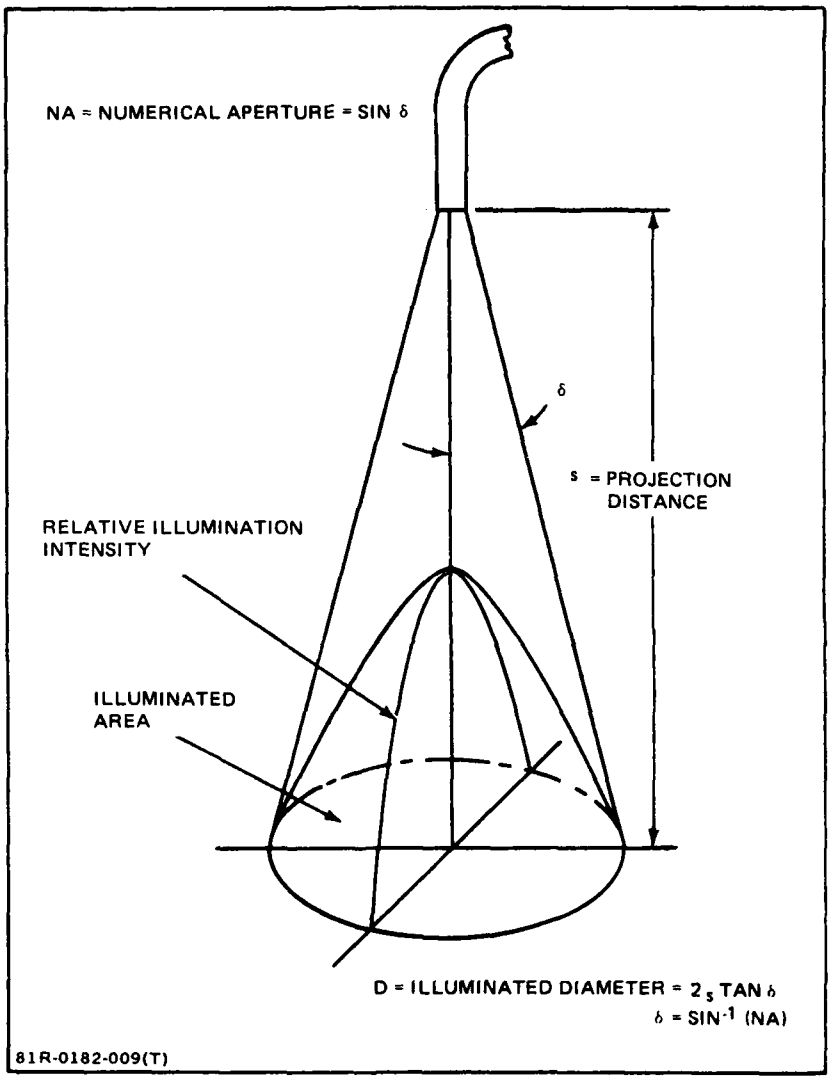

Figure 11 Illuminated Area vs Fiber Optic Numerical Aperture

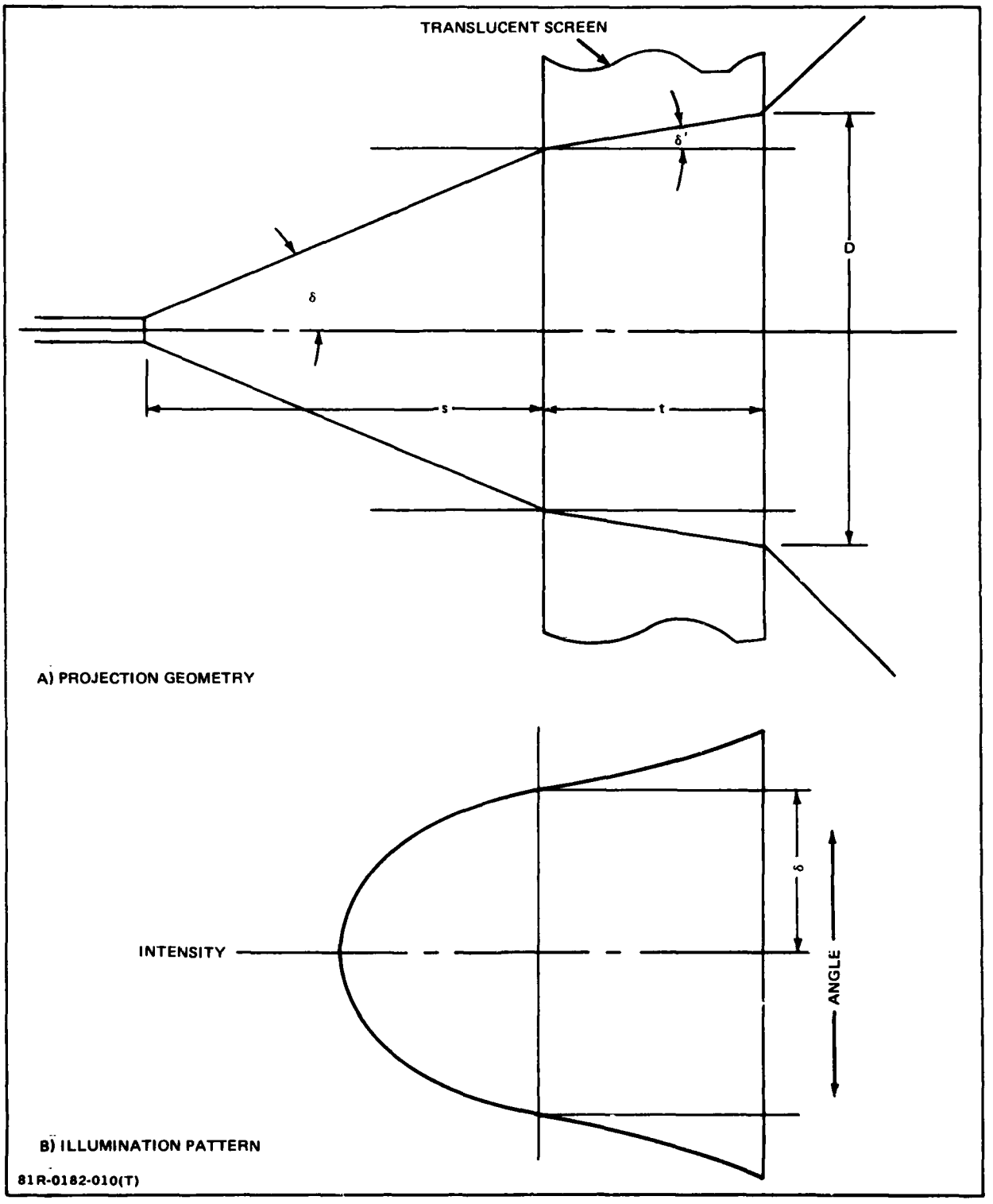

Figure 12 Translucent-Wall CSDF Fiber Optic Illumination

The depth of modulation between spots intended to portray a uniformly luminous surface is illustrated in Figure 13. The unintended modulation m is shown for two spacings between the fiber. In addition to this modulation, there is modulation on the bias between adjacent rows and columns of fibers. If the value of (m) is greater than .02 to .05 per cent of Z, it will be apparent to the observer. The shape of the illumination patterns will be modified by scattering in the translucent panel. This can be expected to reduce resolution and reduce the depth of undesired modulation.

Resolution

The size of the dot patterns will be related to the apparent resolution displayed in the CSDF. If α is the angle subtended by the height of a row of dots from the cockpit, it can be expressed as:

$$\tan \alpha = \frac{D}{R} = \frac{2s \tan \delta + 2t \tan \delta'}{R} \qquad (30)$$

The relationship between NA, s, t, and the angle subtended to the observer is illustrated in Figure 14 for resolution, α , of 1 to 4 minutes of arc. The figure

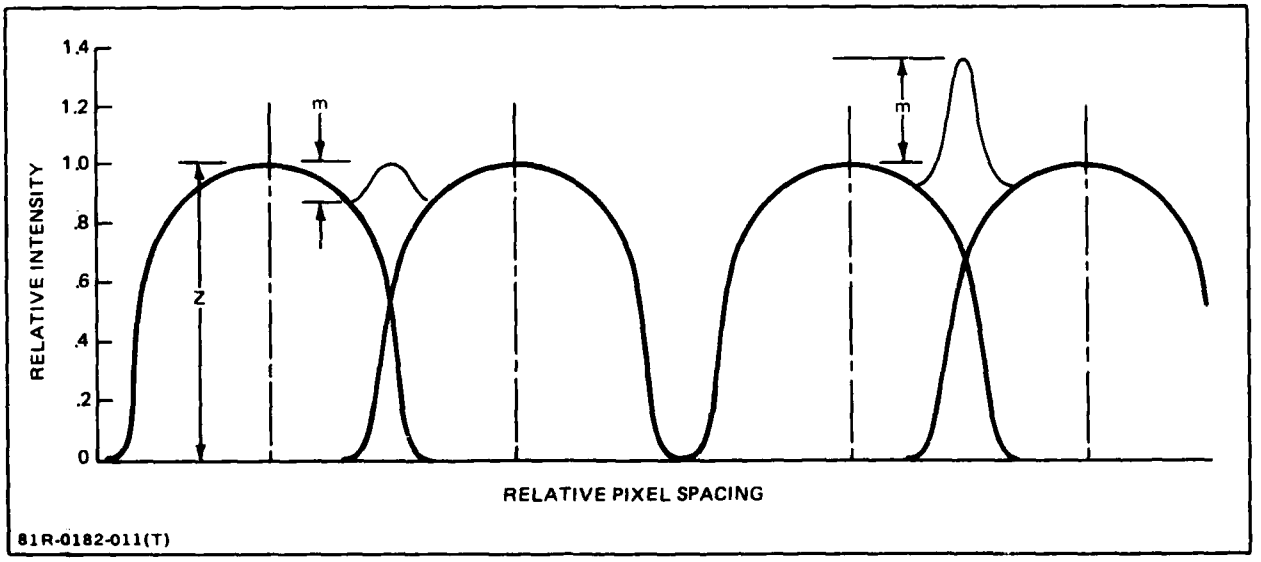

Figure 13 - Spot Luminance Distribution on Translucent Wall

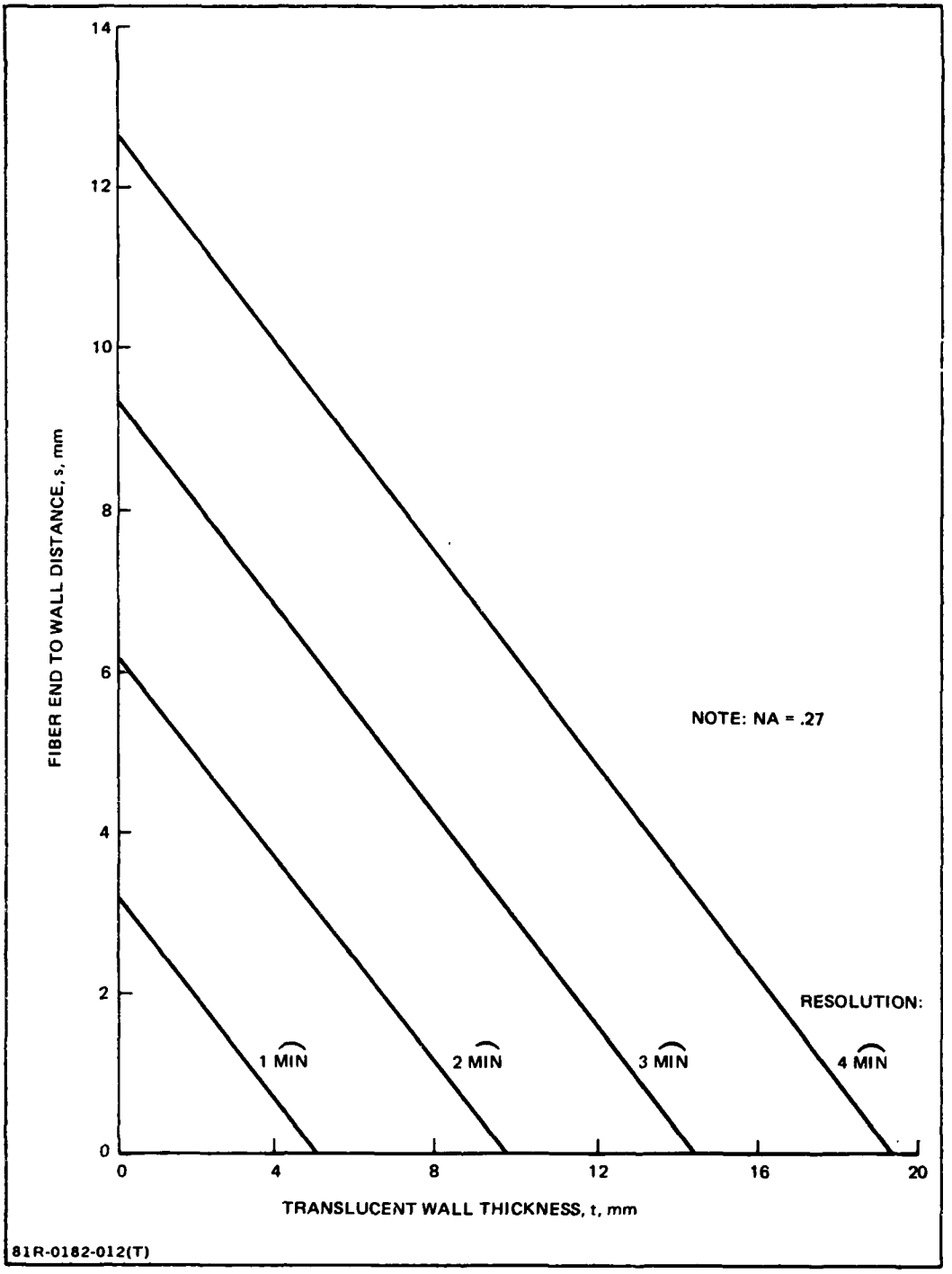

Figure 14 Effect of Resolution Requirement on Allowable Wall Thickness and Fiber-to-Wall Spacing

illustrates a design problem. If the observer's eye is the limit of resolution, the wall must be relatively thin. Even if the exit surface of the fibers are in contact with the wall, it must be no thicker than 5 mm or the value of ϕ must be reduced. For relatively thin sections, the fiber optic structure would support the translucent wall. However, if the displayed resolution is varied in different areas of the CSDF, then a transition region exists as well as a probable change in the wall support procedure.

The relative geometry can be changed by varying the numerical aperture. Figure 15 illustrates the effect of varying the NA from .27 to .10. If this option is used to satisfy construction requirements, it will complicate the design of the input illumination system and the smaller numerical apertures must be attainable for the length of fiber needed.

Numerical Aperture vs Fiber Length

Any particular fiber optic will exhibit an apparent change of NA with fiber length. A fiber used in a face plate may have a particular NA. However, that same fiber material drawn to a long length will exhibit a reduced NA because the rays, which would be at the edge of the emerging cone, would be attenuated to a greater degree. To avoid needless losses, the input numerical aperture should be no greater than that which the length of fiber will support. Too small a numerical aperture, or a collimated input, will cause the emerging cone of light to be dark in the center unless the fiber length is sufficiently long to stimulate all possible propagation modes. These effects may be illustrated by comparison of the input NA and exiting NA measured for 10- and 100-meter lengths of Galite 5020, as shown in Table 1.

Table 1 Output and Input NA vs Fiber Length

	OUTPUT NA	
INPUT NA	10-METER FIBER	100-METER FIBER
.10	.225	.206
.25	.268	.23[illegible]
.40	.257	.237

81R-0182-014(T)

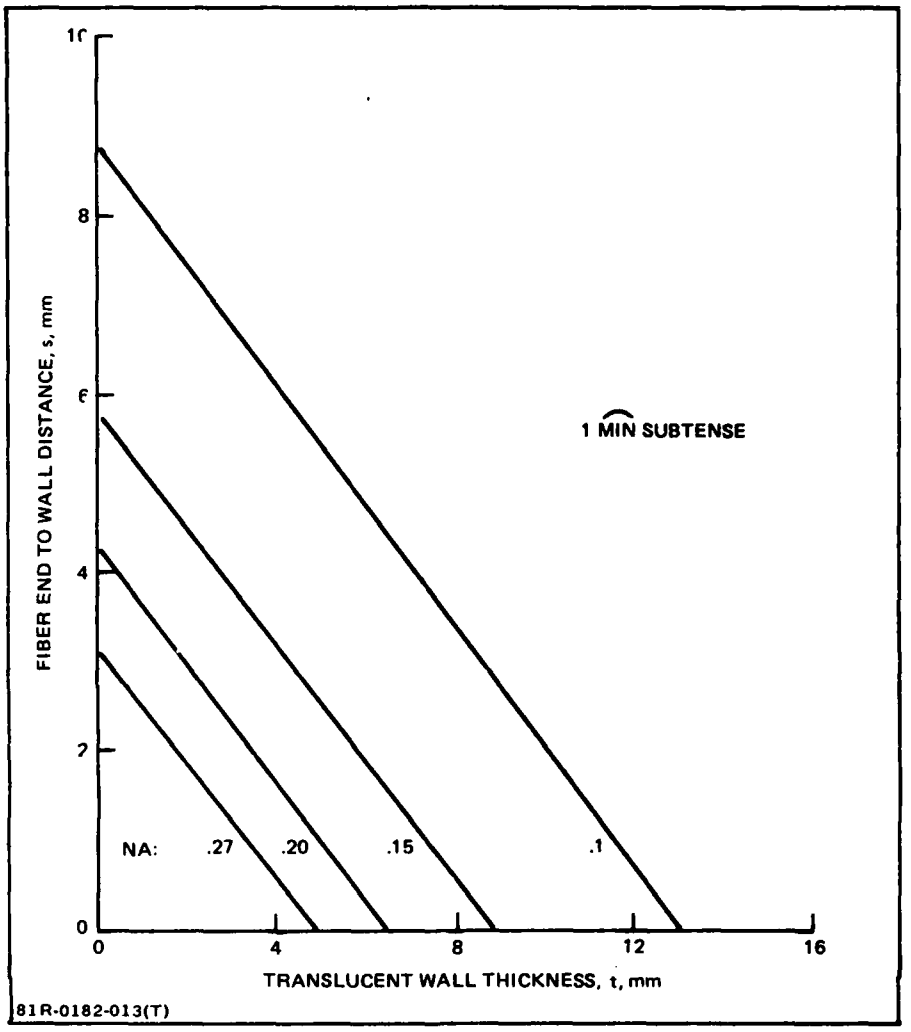

Figure 15 Effect of Numerical Aperture on Wall Thickness and Fiber-to-Wall Spacing

Input Packing Efficiency

There is a possible choice of output fiber-to-fiber spacing, depending on the final CSDF resolution requirements. However, on the input surface, any spaces between the fibers will waste illumination and contribute to thermal problems. Consequently, the input fibers must maintain image coherence and be in contact with one another.

There are three packing arrangements generally used: rectangular, triangular and hexagonal. The hexagonal has application in endoscopes and face plates, but is inappropriate for CSDF fabrication. The square or triangular can be used. The fiber arrangements are illustrated in Figure 16 a and b.

The packing efficiency (P_i) is defined as the ratio of the area of the core to the total area required to accommodate the fiber.

Rectangular Packing Factor

In the rectangular arrangement, d is the core diameter and E represents both the diameter over the clad and the spacing between fibers in both dimensions. Therefore:

$$P_i = \frac{\pi d^2}{4 E^2} \tag{31}$$

The relative area of core and cladding is not as convenient for fiber design as the diameter of the core and the overall diameter. Defining a core/clad diameter ratio (C_c) as d/E, the expression for P_i becomes:

$$P_i = \frac{\pi}{4} (C_c)^2 \tag{32}$$

Triangular Packing Factor

The packing geometry in Figure 16 shows h as the core center-to-center spacing normal to E. A rectangle is highlighted with an area 2Eh. This rectangle can be repeated through the pattern without leaving gaps. It can be seen to contain the equivalent of two core areas. Therefore, Eh is the total area required to accommodate one fiber. Consequently:

$$P_i = \frac{\pi d^2}{4 Eh} \tag{33}$$

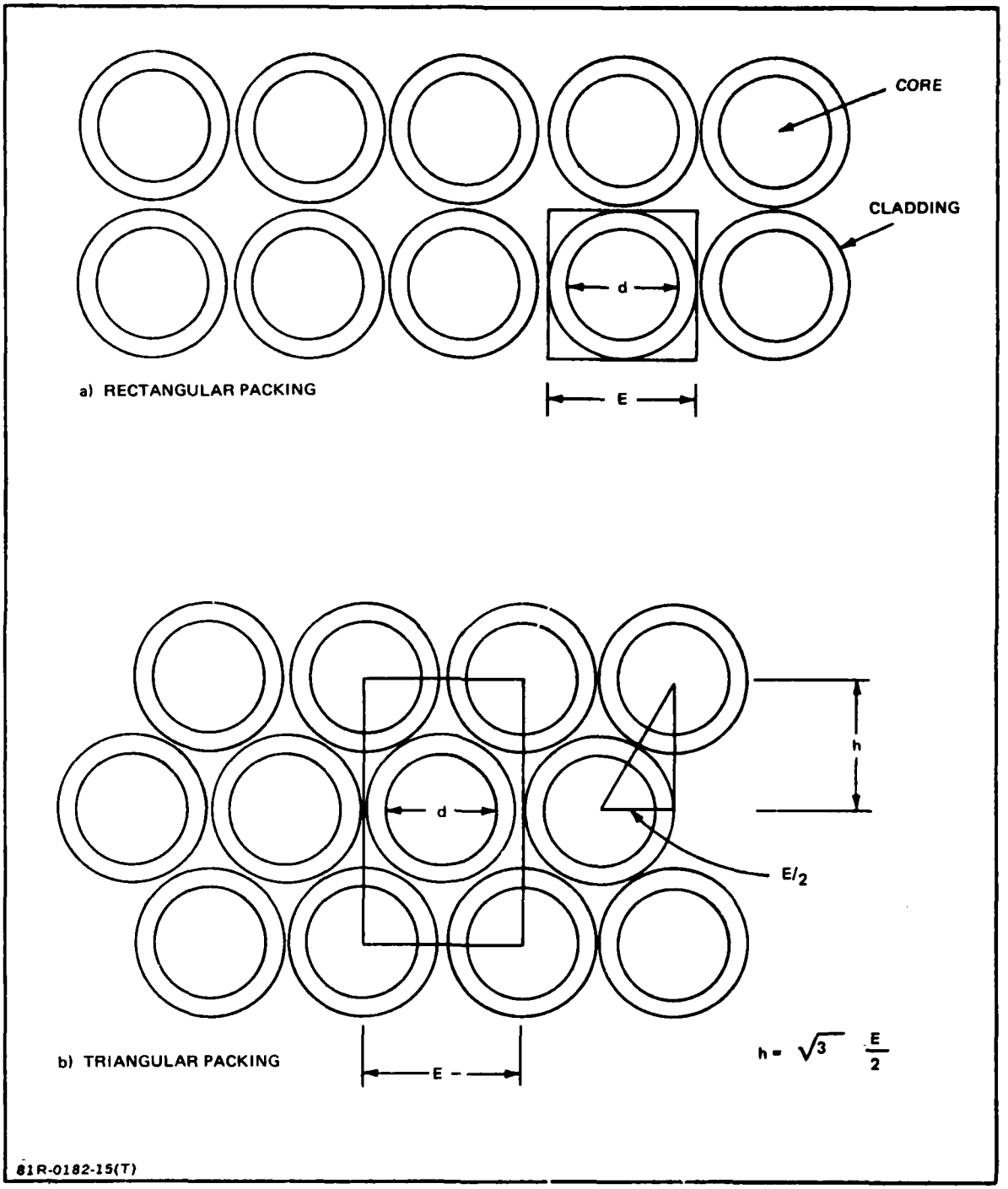

Figure 16 - Input Fiber Packing Arrangements

Since the centers of three fibers define an equilateral triangle, the elevation h is equal to:

$$h = \frac{\sqrt{3}\,E}{2} \tag{34}$$

Combining Equations 33 and 34 and the definition of C_c yields:

$$P_i = \frac{\pi}{2\sqrt{3}} (C_c)^2 \tag{35}$$

The relationship between P_i and C_c is illustrated in Figure 17.

Compensation for Spectral Losses

It is well known that if white light is launched into a long fiber, it will emerge as red because the fiber absorbs shorter wave lengths to a greater degree than longer wave lengths. Consequently, if the emerging illumination is to appear as sunlight in the CSDF, then two factors must be introduced. One is the use of a light source that is as rich in blue as possible. The second is to distort the entering spectral distribution of the flux with a filter assembly that makes the emerging spectral distribution acceptably similar to sunlight.

Assuming the spectral similarity is achieved, the spectral compensatiion factor, K_1, is defined as:

$$K_1 = \frac{\int_{\lambda_1}^{\lambda_2} J_{\lambda_{LAMP}}\, d\lambda}{(1-\rho_1)\,(1-\rho_2)\int_{\lambda_1}^{\lambda_2} J_{\lambda_{LAMP}}\, T_{\lambda_{FIBER}}\, T_{\lambda_{FILTER}}\, d\lambda} \tag{36}$$

The reflectance losses ρ_1 and ρ_2 are not measured when T_λ is measured for the fiber. The reflection coefficients ρ_1 and ρ_2 may be taken as .04 across the visible spectrum with little loss of accuracy.

The spectral attenuation of Galite 5020 is illustrated in Figure 18. It expresses the attenuation in db per kilometer vs wave length measured on 20 long specimens. The average values are connected by a solid line and the range of measured values by the broken lines. The absolute limit imposed by Rayleigh scattering is also shown for comparison.

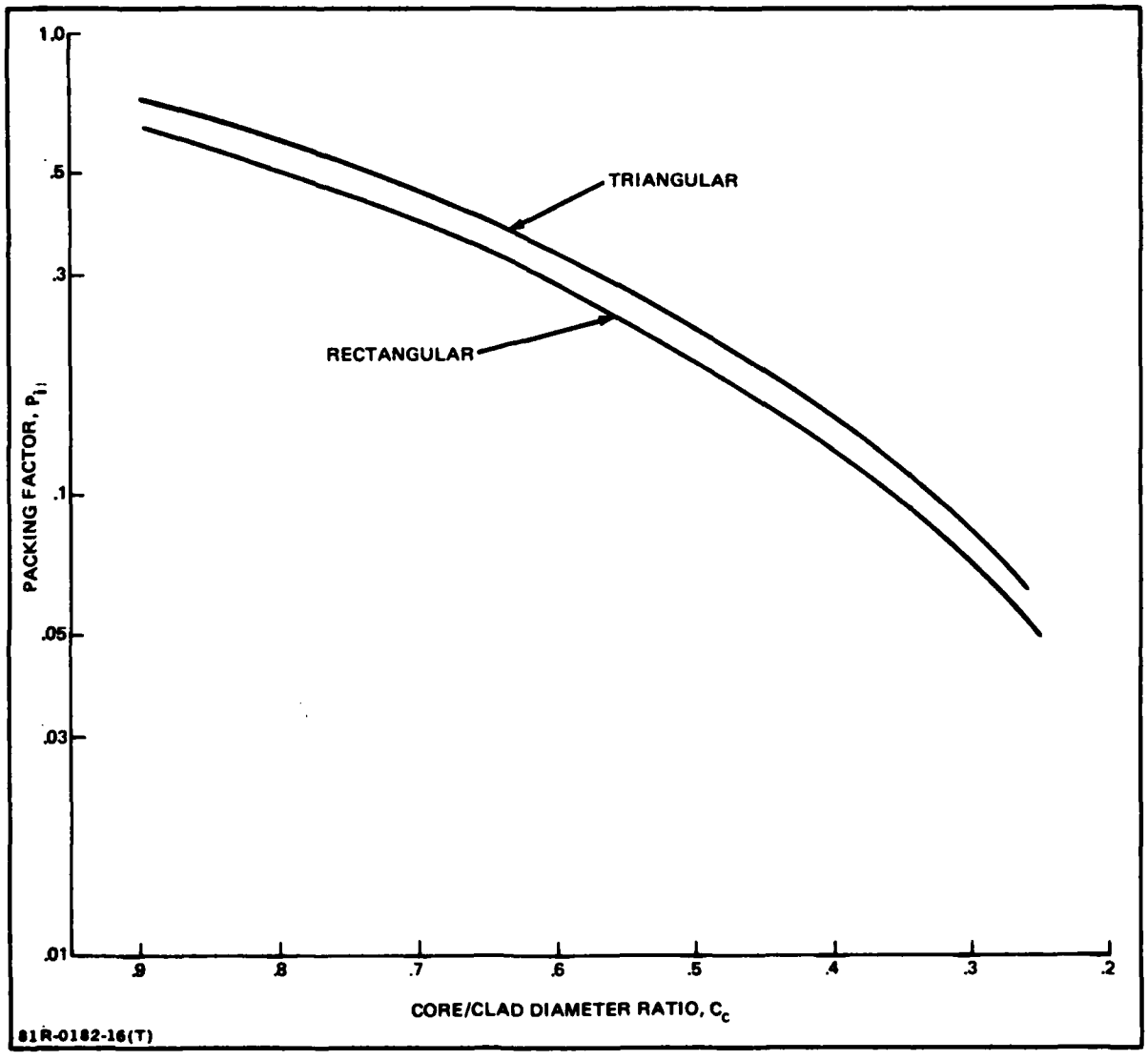

Figure 17 - Input Packing Factors

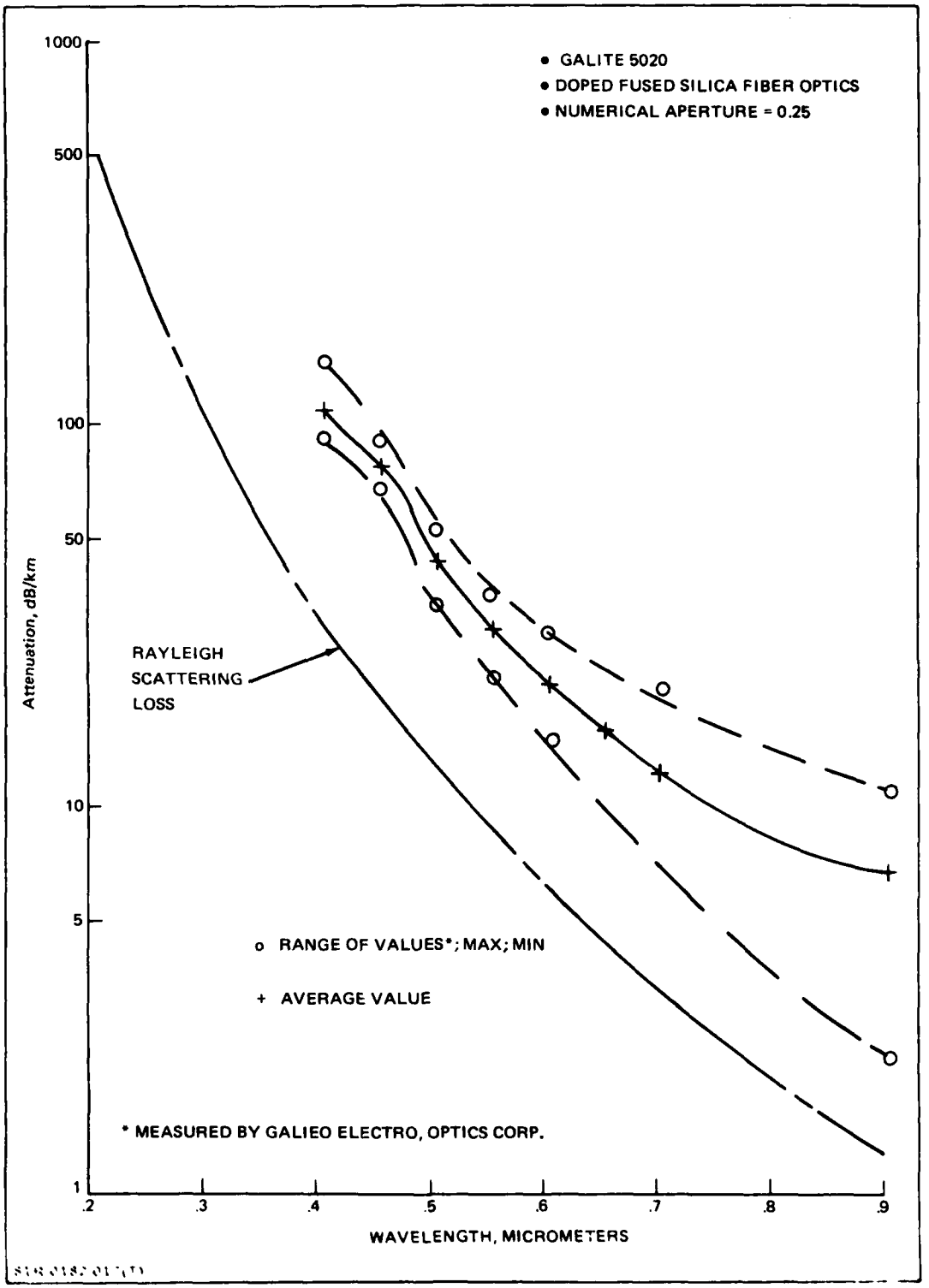

Figure 18 - Spectral Attenuation vs Wavelength

The figure illustrates the excellent performance of Galite 5020. Its attenuation approaches an average value of 7 db per kilometer for the longer (communications) wave length. It characteristically shows higher attenuation at the shorter wave lengths, approaching 100 db per kilometer for blue light. The increasing absolute limit (Rayleigh loss) confirms the difficulty associated with realistic simulation of sunlight. The term $T_{\lambda\ \text{fiber}}$ is the spectral transmission of the fiber and, therefore, the reciprocal of the attenuation shown in Figure 18.

The relative spectral content of sunlight, Xenon and HMI lamps is illustrated in Figure 19. The wavelength for normalization of the respective lamp spectrum was shifted to separate the curves for legibility. Both sources are rich in blue relative to red. Xenon is used commercially for illumination of stadiums, shopping malls, etc., and HMI for television studio lighting. The Xenon lamps are available with outputs up to 1.6×10^6 lumens (30kw), and commercial HMIs produce 4.1×10^5 lumens (4kw). The HMI have greater relative blue content than Xenon, and are more than twice as efficient as Xenon. However, they are prone to exhibit flicker unless the power supply system is efficiently designed. For purposes of comparison, both lamp spectrums were used to evaluate K_1.

The procedure for evaluating K_1 is illustrated in Figure 20 using the Xenon spectrum. The integrated lamp emission in the visual region is shown as the hatched area (A) under the Xenon spectrum in the standard visible range .47 to .67 microns. The lower curve is the relative spectrum that emerges from 100-meter fibers using the average fiber attenuation. The calculation was performed at .01 micron intervals and the emerging relative intensities did not match the relative solar intensity also shown in the figure.

An ideal filter was assumed to be available to reshape the after-transmission spectrum to match the solar spectrum. The cross hatched area (B) represents the usable portion of the total lamp flux (A). The ratio of A/B represents the value of K_1 with an ideal spectral shaping filter. The comparison of Xenon and HMI lamps for 100 meters of fiber showed a K_1 of 6.8 for Xenon and 6.2 for HMI. The HMI lamp system must produce more than 6.2 times as much flux as the CSDF needs to correct for spectral losses in the fibers. The Xenon is somewhat more demanding at 6.8 times, but would probably be a better choice because of its greater output. Relative values of K_1 for fiber lengths other than 100 meters is illustrated in Figure 21 using the Xenon source.

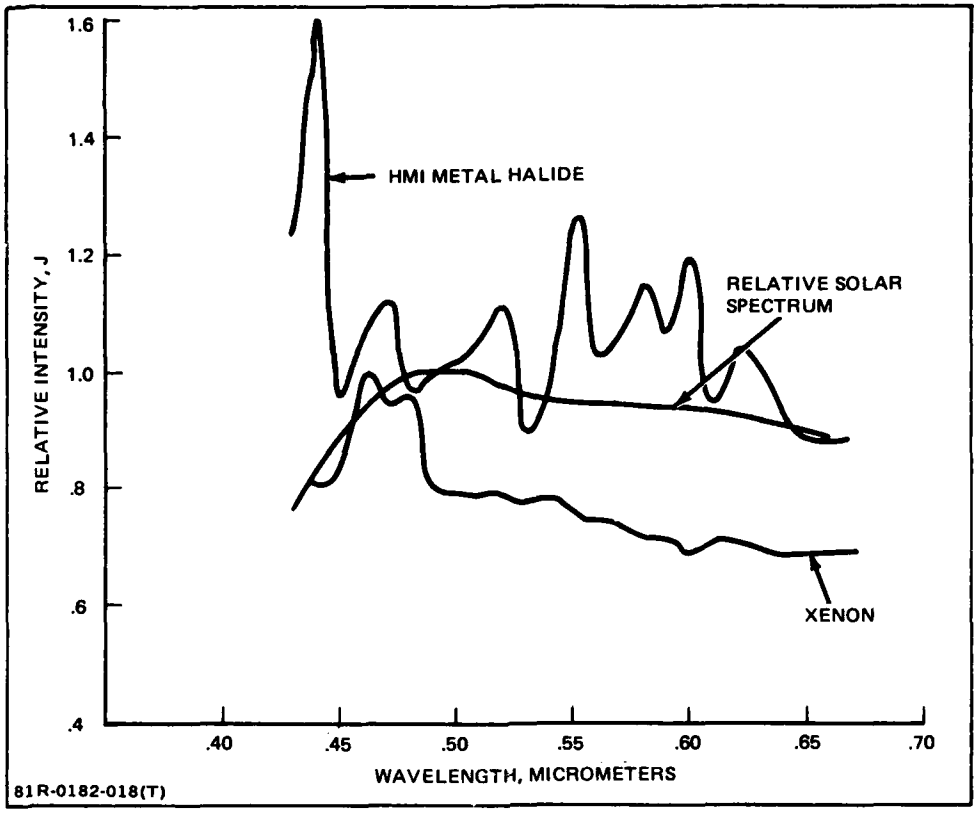

Figure 19 Relative Spectral Emittance of Sun, HMI and Xenon Lamps

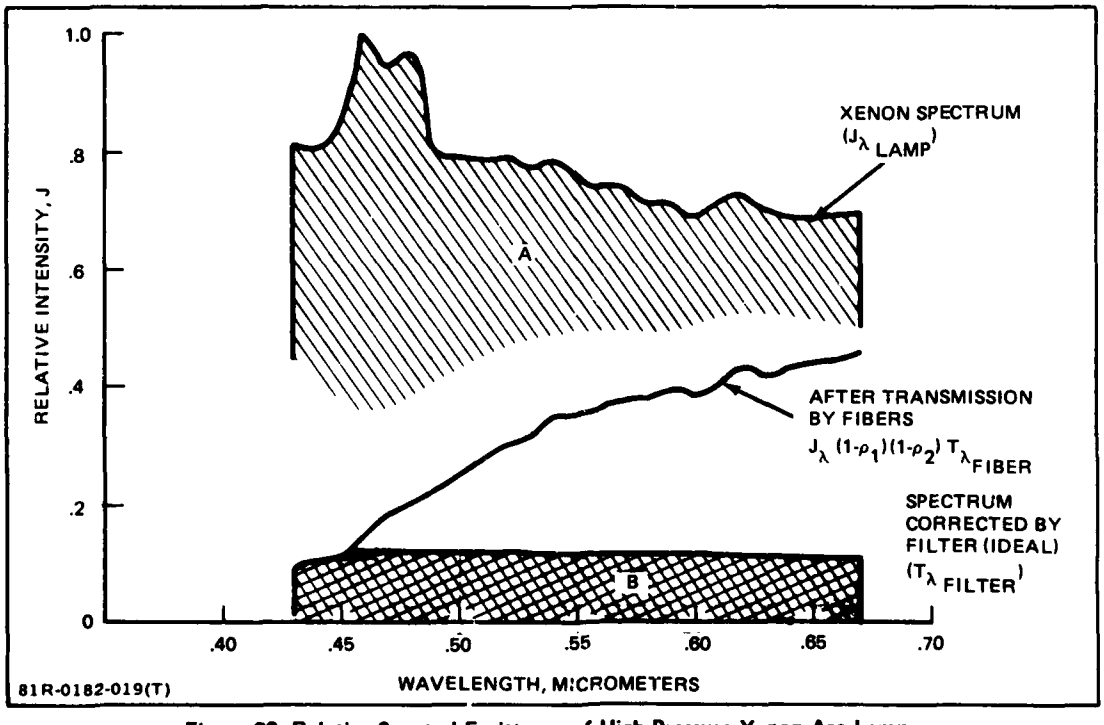

Figure 20 Relative Spectral Emittance of High Pressure Xenon Arc Lamp

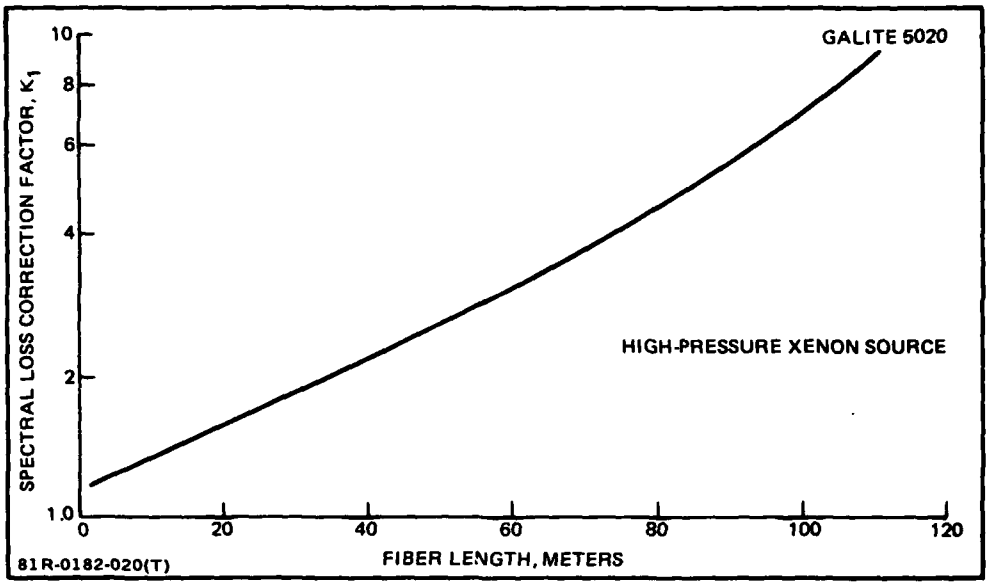

Figure 21 - Spectral Loss Correction Factor (K_1) vs Fiber Length

The desired characteristic of the spectral shaping filter is illustrated in Figure 22 for a 100 meter fiber, considering Xenon and HMI lamps. The ideal filter transmittance is shown in Figure 23 for a Xenon source as a function of fiber length.

ELLIPSOIDAL CSDF IMAGE FORMATION

An ellipsoidal dome with a small fiber optic input assembly located near one foci and the CSDF cockpit near the other was included in the statement of work as a possible solution (ref Figure 4). The property of a theoretical ellipsoidal mirror, where a point at one foci is imaged at the other, is the basic principle which suggests this approach. To be feasible the concept must:

- Provide an image of acceptable quality, magnification and orientation
- Provide an image surface which is continuous, complete and at least 6.1 meters from the CSDF cockpit.

In this concept, the ellipsoidal wall has a high quality "mirror" finish and acts as a reflecting lens. The image it produces will appear differently to observers depending on their position with respect to the foci. This is illustrated in Figure 24a. A simple concave spherical reflector is shown forming a real inverted image at point C. A spherical surface is used in the illustration because its properties are well known and the principle it demonstrates is applicable to all con-

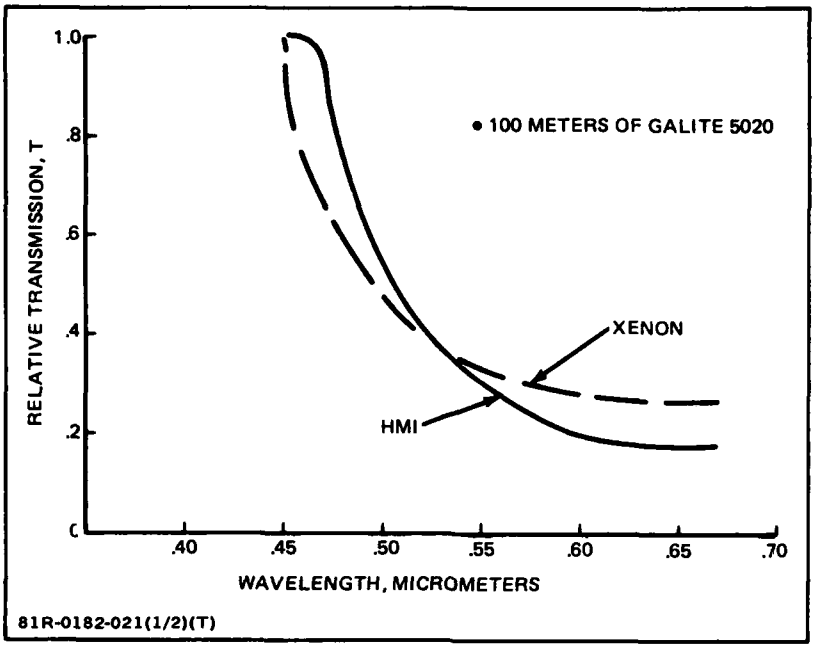

Figure 22 Ideal Spectral Correction Filters for Xenon and HMI Lamps

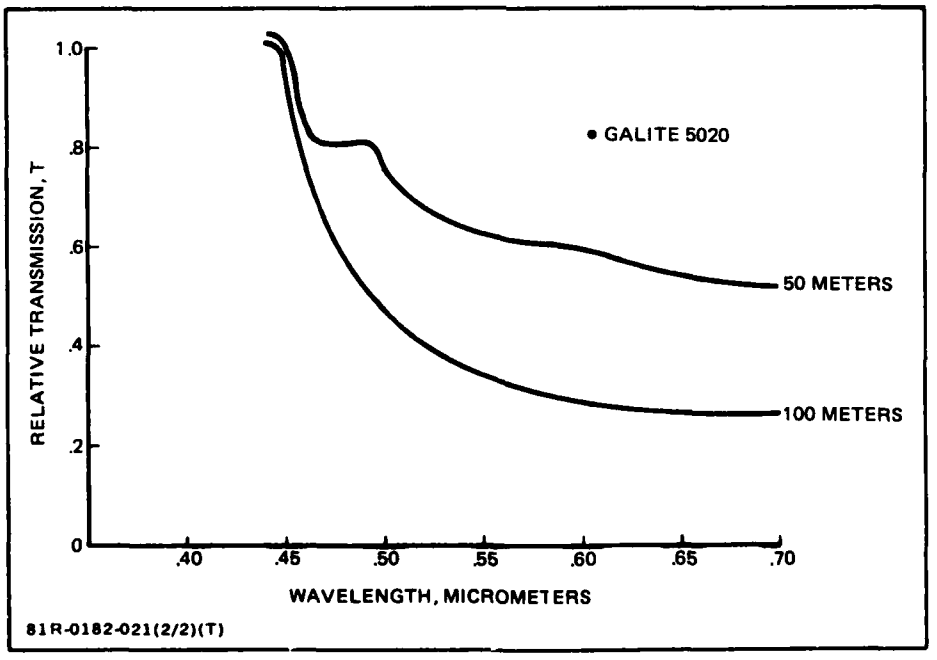

Figure 23 Ideal Spectral Correction Filter for Xenon Source vs Fiber Length

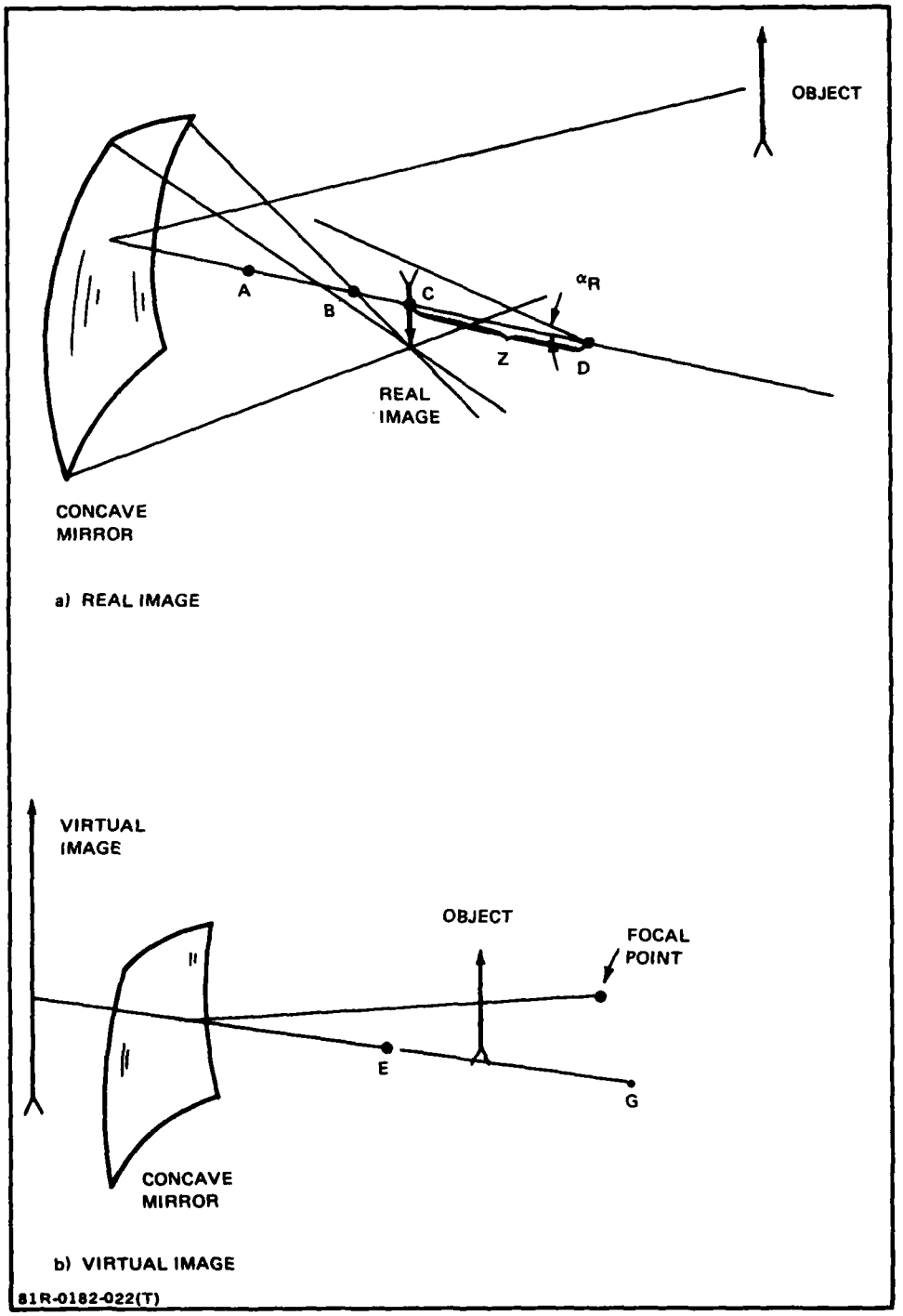

Figure 24 Mirror Imaging

cave reflecting surfaces. If the viewer is at point D, the real inverted image will be seen positioned z units of distance from the viewer. If the viewer is at C no image will be seen. The entire mirror will assume a luminance related to the average luminance of the portion of the image intercepted by the pupil of the observer's eye. Viewed from points A or B, the image will be virtual and erect. However, it will also be distorted and highly aberrated.

In Figure 24b, an image is illustrated where the object is inside the focal point, letting the mirror act as a simple magnifier. The image is enlarged and virtual and, if viewed from points E or G, the magnification change is moderate. However, the image will be distorted.

Ellipsoidal elements are frequently used as secondary relay elements in high-quality astronomical telescopes that operate over very small fields. The image quality is satisfactory because the input and output images are confined to the foci and the fields of view are small to control aberrations.

An ellipsoidal CSDF whose resolution performance was equal to a translucent-walled CSDF would have an equal number of input fibers. An estimate of the distance from the focus that the fiber bundle would have to be placed can be determined as follows. If each fiber is intended to subtend 1 minute of arc, there would be 11.82×10^6 fibers per steradian in the CSDF. If triangular packing with a 50 micron core and 60 micron diameter fiber is used, the fiber ends would cover a surface area of 0.23 m^2 to input 1 hemisphere. The diameter of the input bundle would be 0.54 meters. If the output end of the fibers were made to form the surface of a hemisphere (projection output surface), it would have a diameter of 0.66 meters assuming no allowance for properly forming the surface. Therefore, the fibers would be at least 0.33 meters from the focus of the ellipsoid if the projection output surface were symmetrically located.

In the search for a solution, a complete ray trace analysis of the ellipsoidal concept could be extremely time consuming and expensive. To analyze this concept efficiently, it was decided to trace the image surface on one plane through the ellipsoid. If an acceptable solution could be found for this plane, it would be valid for all other planes rotated around the major axis. Following this, the analysis could be extended to a real cockpit case by moving the observer's position and the inputs out of the plane. An acceptable solution is one where the previously defined image quality criteria are met out of the single plane.

A computer program was written that permitted the ellipticity of the CSDF plane, its general size, and the size of the input fiber optic surface to be varied. Numerous trials were run without finding a satisfactory single-plane solution. An illustration of the typical image location in the meridinal plane is contained in Figure 25. Two image points, A and B, are used for illustration. The broken lines represent the center of the emerging cone of light from each fiber. The extent of the light cone is shown by hash marks for point A and cross hatches for point B.

It has been established that an image will be formed at one focus if the input surface is made very small and it is positioned at the other focus. However, this image will be too small; to be useful, the image would have to be virtual. This is illustrated in Figure 25 for image points A and B. The central rays from fibers at points A or B (rays 2 and 5) pass through the second focus because they are defined as coming from the first focus. All other rays from fibers at A or B (rays 1, 3, 4, 6), when projected back toward focus #1, miss the focus. After reflection from the elliptical surface, they will have a corresponding variation in position near focus #2. The net effect is illustrated for observers at two cockpit positions, F and R. The observer's eye will intercept energy from points A and B separated by the angles between the heavy lines. The angular separation of the points is substantially different for both observers. If this was allowed in a simulator, objects seen by separated observers would be a different size and would appear in different locations. This could also be apparent to an observer if he moved his head.

A series of investigations were conducted to achieve consistent image quality. They all produced unsatisfactory results for a variety of reasons. Figure 26 illustrates a major consideration that becomes important if imaging could become acceptable. The front cockpit is shown with 110° of vertical field of view. A dashed line is shown to represent a line along which the emitting fibers could be located. The exact location of the line and the mapping of the emitting fibers along the line has not been determined. The restricted fields of view and shadowing, however, can be seen. The forward field of view, extending from -15 degrees to +95 degrees, is shown in the figure. To map the detectors properly, the emitting line of fibers must be located where the lines of sight 5, 6 and 7 have not crossed over. When this requirement is satisfied, the pilot can see the emitting surface directly at a line of sight of +115 degrees. The useful field of view is

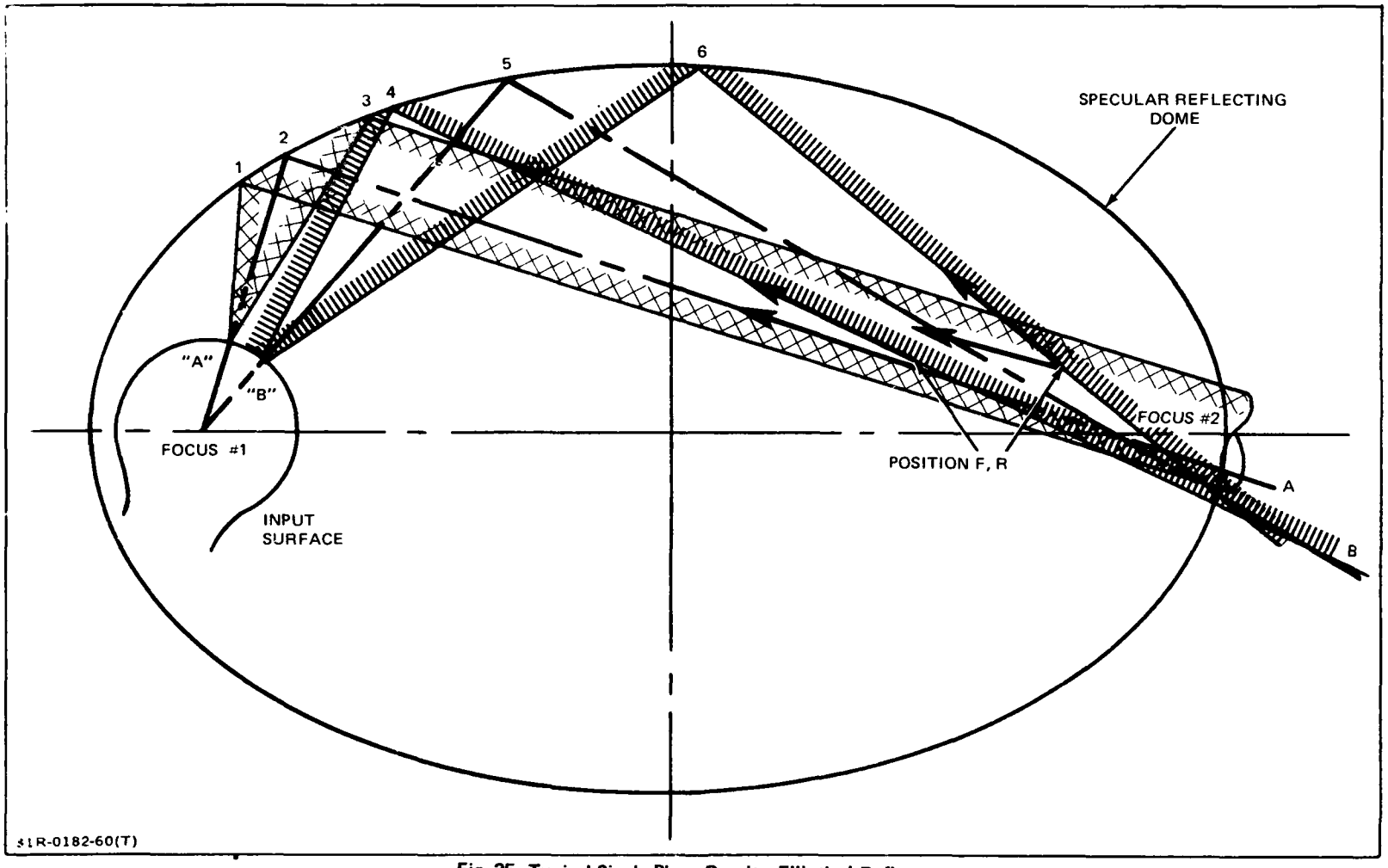

Fig. 25 Typical Single-Plane Results, Elliptical Reflector

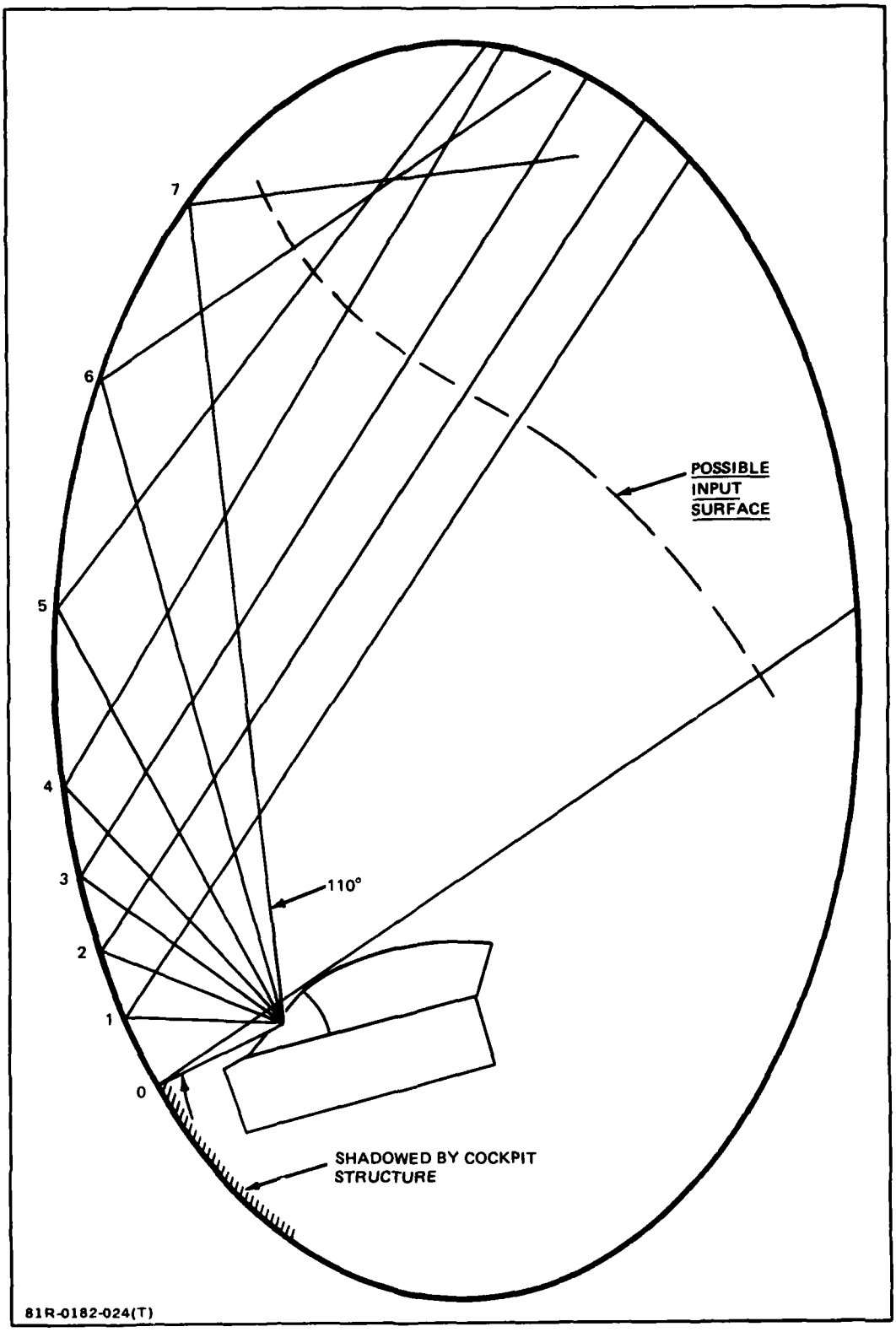

Figure 26 Field of View Limitations

even more limited from the rear seat.

If the input line were rotated about some axis to provide full solid coverage, the problems of shadowing and second reflections would have to be overcome. The view down and to the side would have the cockpit shadow to contend with. In addition, the view over the side would be subject to multiple reflections from two mirror surfaces. In view of the fact that a first-order single-plane solution was not found, the remaining steps in the investigation were not performed.

SECTION IV

EXPERIMENTAL DATA

In order to evaluate the variables identified in the performance predictions, a series of measurements were made on a selected fiber type and an assembly of fibers that was intended to represent a typical wall segment. The measurements, which followed the approved test plan (Appendix C), were:

- Numerical aperture versus fiber length and illumination focal ratio
- Spectral attenuation of the selected fiber
- Luminance uniformity from wall test specimen
- Solar simulation capability for the direct-view CSDF and the translucent-wall CSDF
- Spatial light distribution on a translucent surface
- Reflectance of the wall test specimen
- Cross talk in the wall test specimen
- Visual appearance of the wall test specimen

FIBER OPTIC MATERIAL

A literature search provided data on many fibers that could be candidates for use in a CSDF. With few exceptions, the material was developed for the communication industry which concentrated on transmission properties in the near-infrared. Equal performance in the near-infrared is not necessarily equal when blue light must be transmitted over any substantial distance. An illustration of the spectral attenuation of a representative series of Galileo Electro-Optics fibers is shown in Figure 27. This data was predicted from miscellaneous data sheets published by Galileo. It can be seen that Galite 5020 will probably be the best choice on performance at .43 microns. However, at .7 microns Galite 5000

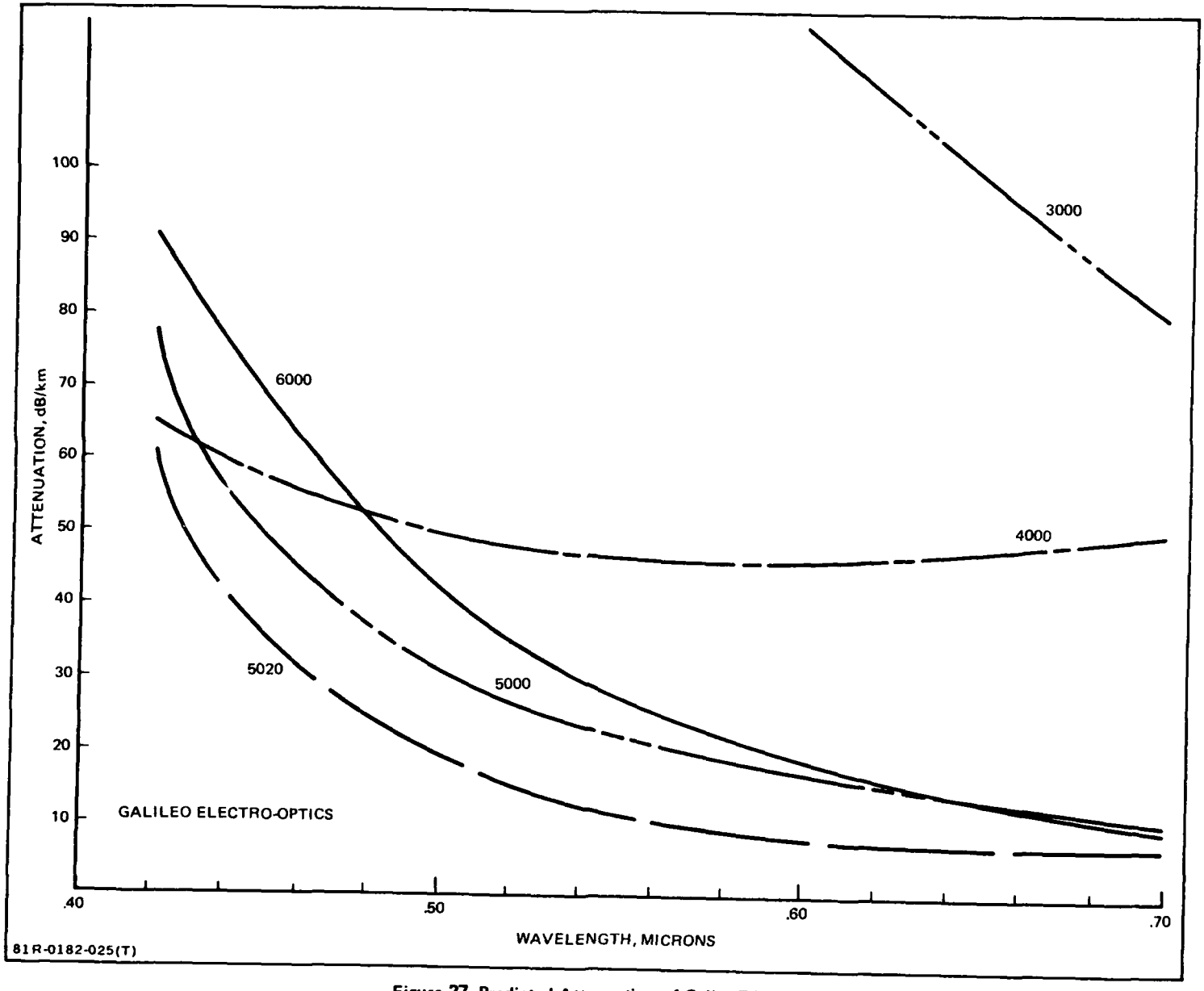

Figure 27 Predicted Attenuation of Galite Fibers

and 6000 are essentially the same. It was decided to procure a 100-meter length of Galite 5020 for tests and also to use 5020 in a fiber optic wall specimen.

FIBER OPTIC WALL SEGMENT

The Statement of Work (SOW) called for a range of test resolutions (0.4, 1.0, 2.0, 5.0 minutes of arc) that was met by constructing one test specimen for viewing at different distances. The distance between fibers was chosen as 1.4 mm which subtends an angle of 0.8 minutes of arc at the 6.1-meter radius of the CSDF. The resulting angular subtense vs viewing distance is shown in Figure 28. The SOW range can be accommodated by viewing the specimen at distances of 1 to 12 meters.

If an attempt was made to have the fibers fill all of the available space on the face of the specimen, they would be 1400 microns in diameter. Whether they would be better classified as fibers or light pipes was not determined because fiber of this diameter is available only in plastic. Since plastic is not suitable, a substitute was employed. Three smaller-diameter fibers were bundled together at each end and placed in the wall specimen as a single-fiber channel. The resulting design for the face of the wall specimen is shown in Figure 29. The relative coupling efficiency of this design is substantially less than the efficiency that could be achieved with large-diameter fibers. However, the actual spacing of fibers was yet to be determined and, if the space between the individual channels were reduced too much, the utility of the specimen to test the translucent-wall CSDF would be compromised.

The fiber specimen has a wall face area of 7.6 x 7.6 cm and a length between input and output faces of one meter. Three individual fibers were cut and assembled with a stainless steel ferrule on each end. After testing for breaks, the ferrules were inserted in a pre-drilled aluminum block by hand, and retained in position with an adhesive. The coherence was maintained by careful monitoring of the assembly procedure. During the assembly, five copper-constantan thermocouples were attached to the back surface of the aluminum block, one in the center and the other four symmetrically located in the quadrants. A photograph of the specimen is shown in Figure 30a, and magnified view of the illuminated fiber is shown in Figure 30b. A wire 25.4 microns in diameter was placed on the block reference purposes.

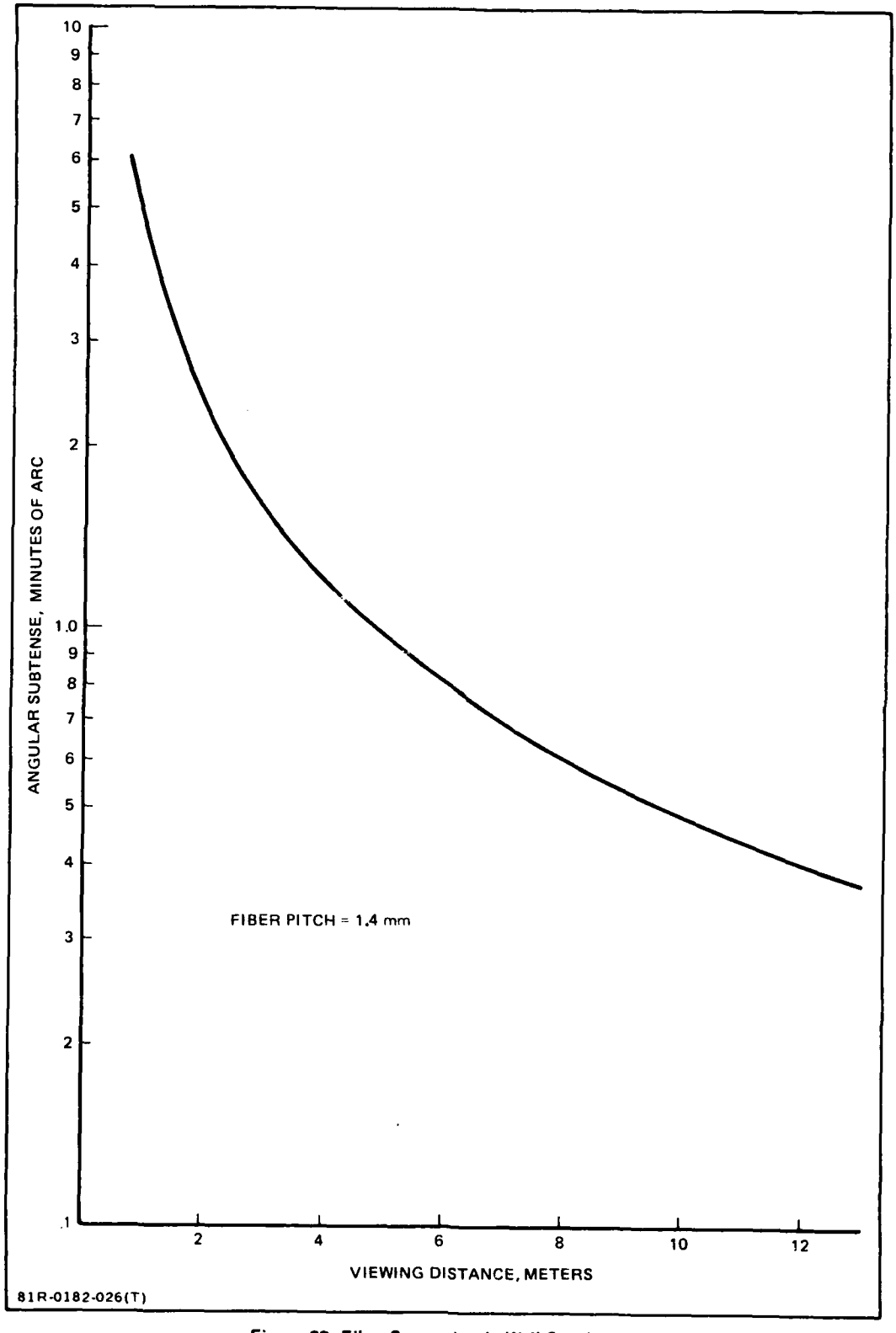

Figure 28 Fiber Separation in Wall Specimen

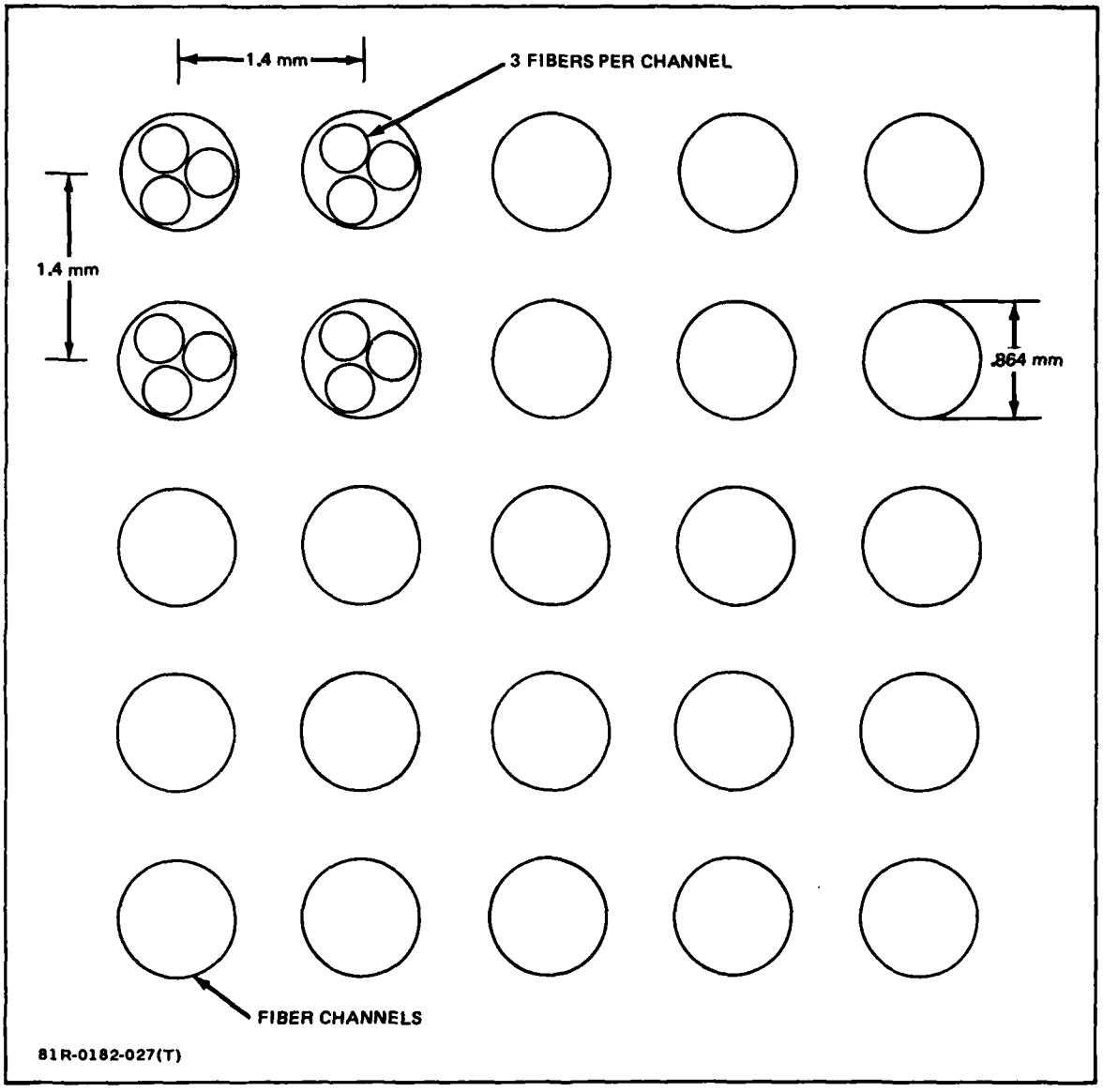

Figure 29 Design for Face of Fiber Optic Wall Specimen

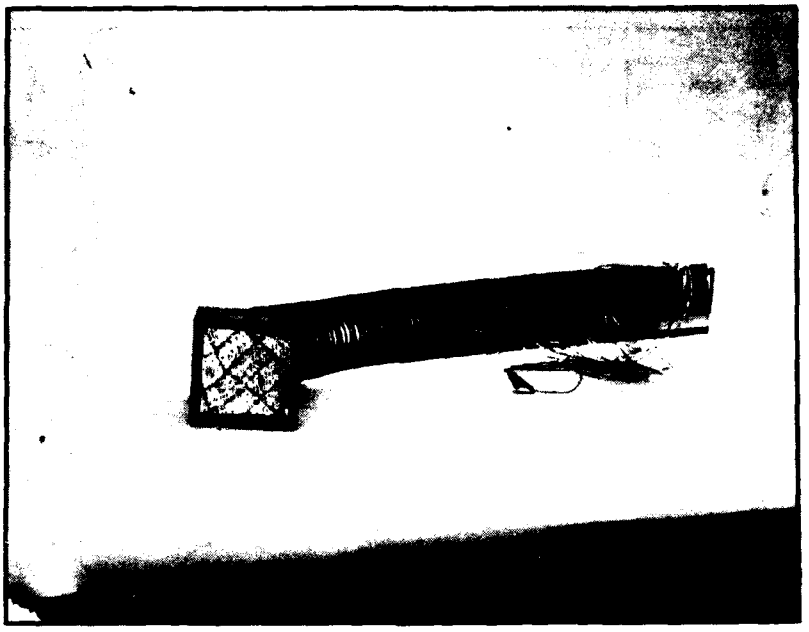

Figure 30a Fiber Optic Specimen Wall Segment

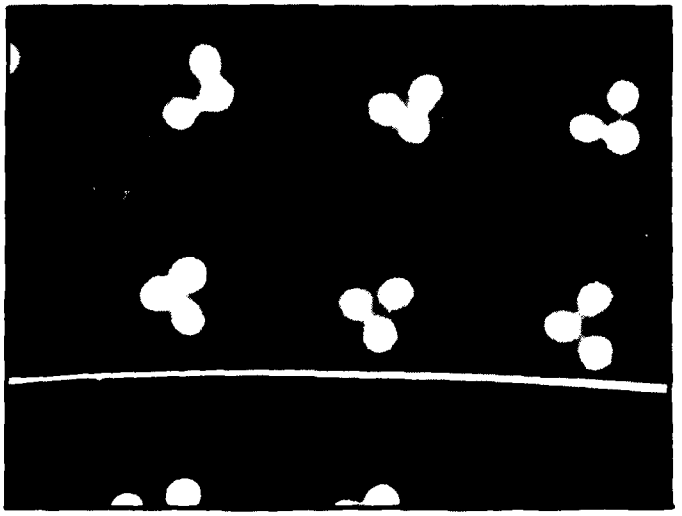

81R—0182-055(T)

Figure 30b Magnified View of Illuminate Fibers with 25.4 - Micron Wire Shown for Comparison

The applicable characteristics of the specimen are:

Core Material	Galite 5020
Core Diameter	125 microns
Refractive Index of Core	1.4797
Diameter of 3-Fiber Bundle	0.864 MM
Open Area Ratio	0.0188

The coupling efficiency is defined as the product of the open area ratio and the input/output face reflectance loss. In the case of the wall specimen, the coupling efficiency is 0.0174.

NUMERICAL APERTURE

The numerical aperture test was performed to determine the NA of the fiber for a 100-meter length. As a control, the NA of 10-meter lengths was also measured. Three illumination NAs were used for each length and scans were taken horizontally and vertically through each emission pattern. The scans are presented in Appendix A as Test #1. The data are summarized in Figure 31 where the relative change in NA is plotted against the input NA. Figure 31 shows that input NAs greater than 0.25 are not sustained by the fiber. It also confirms that the mode structure has the opposite effects on smaller input apertures. This could be interpreted to mean that more-economical high F/NO illumination systems could be used and the fiber would still distribute the light into a larger cone than might be desired. Experimentation showed that this effect cannot be depended upon. When using small NA inputs, the exiting cone was frequently found to have a dark region in the center of the projected image spot. An illustration of this pattern is contained in Figure 32. In the ensuing tests, the illuminating NA was controlled to avoid a possible bias in the results. The definition of NA used in Figure 31 is based essentially on the -20 db point. To be used in the direct-view CSDF, a different point would be chosen to define the NA.

SPECTRAL ATTENUATION

The variation in spectral attenuation in the same glass formula can be as important as the average attenuation at any particular wavelength. A total of 18 fibers were measured by Galileo Electro-Optics using lengths from 43 meters to

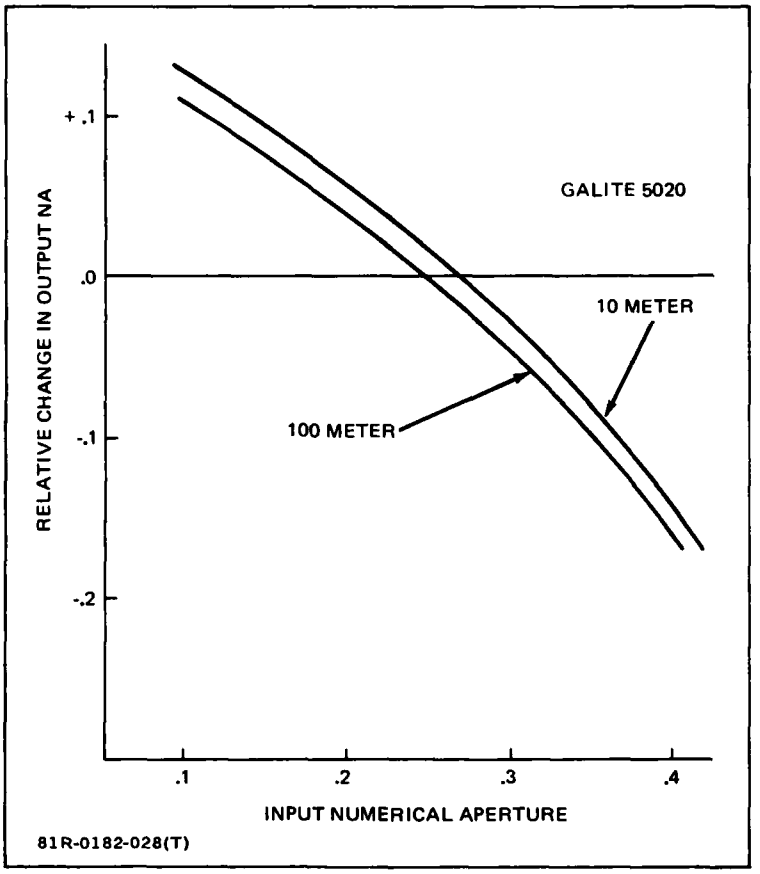

Figure 31 Relative Change of Output NA vs Input NA and Fiber Length

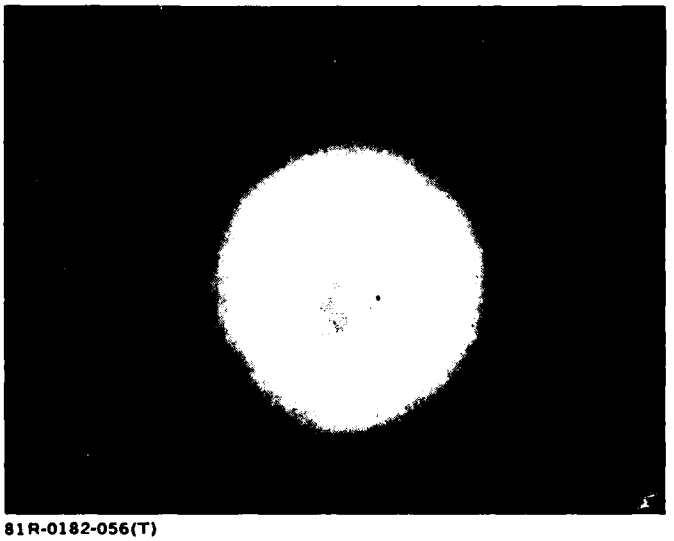

81R-0182-056(T)

Figure 32 Projected Pattern with Dark Center

919 meters. The fiber was drawn over a period of time from September 1979 to June 1980. The sample size, the fiber lengths and the time over which they were produced makes it a truly representative sample of present commercial practice. The attenuation was measured at 8 wavelengths from .4 to .9 microns. The data on each fiber is in Appendix A as Test #2 and a summary of the attenuation measurements is shown in Table 2. Note that the attenuation at communication wavelengths varies from 2.3 to 11.3 db/km while, at the center of the visible spectrum (.55 microns), it varies from 22.5 to 37.7 db/km. The envelope of values is plotted in Figure 33 for comparison with the irreducible losses due to Raleigh scattering.

Assuming that the illuminating source is uniform in the CSDF, the fiber-to-fiber variation in transmission will cause an apparent fiber-to-fiber brightness change. For example, at 0.5 microns, the min/average/max transmissions through 100 meters of fiber is .28/.35/.45 respectively. This will result in a pixel-to-pixel maximum brightness variation of 1.6:1 , which exceeds the conventional definition for a grey shade, i.e. 1.4:1. For a CSDF design using less than 100-meter fibers, the variation will rapidly decrease.

The average curve tracks the Rayleigh scattering limit quite closely. Assuming that material technology could be improved to make Rayleigh scattering the limiting factor, the improvement ratio at 0.50 microns over the average would be 1.6 to 1. This says that the average brightness of the fiber end would be 1.6 times as bright if the fiber was ideal or that the lamp system could provide 62.5 percent of the lumens and still provide the same CSDF brightness. This 1.6 factor increases to 3.2 for blue light.

LUMINANCE UNIFORMITY

Measuring uniformity on a 1-meter test specimen will fail to measure the spectral losses that depend on fiber length, but it will provide a measure of all other effects. To confine the effects to the fiber assembly, the input must be as uniform as possible. A uniform input was achieved by trial and error. Following the calibration procedure of Test #3 in Appendix C, a diffuser was illuminated by the Xenon arc lamp distances ranging from 35 cm to 1 meter from the source, and readings taken on a vertical and horizontal line through its 14.6 cm aperture.

Table 2 Summary of Galite 5020 Attenuation Measurements

DATE	FIBER DRAW LENGTH		WAVELENGTH, MICRONS							
	LONG	SHORT	.4	.45	.50	.55	.60	.65	.70	.90
9/27/79	190 m	2 m	97.4 dB	69.7 dB	40.2 dB	28.3 dB	20.8 dB	17.1 dB	13.8 dB	8.7 dB
11/27/79	200	2	102.6	94.3	54.4	35.9	18.7	12.3	8.1	10.1
11/29/79	210	2	94.7	93.3	54.0	–	24.7	17.6	12.6	6.4
1/10/80	150	2	128.7	72.6	40.5	26.3	19.2	14.9	11.7	7.5
1/16/80	238	2	93.9	90.0	50.8	32.9	23.5	17.0	12.9	7.6
3/31/80	43	2	148.7	77.3	45.7	–	27.8	23.5	21.4	–
3/31/80	171	2	114.5	90.2	50.7	–	23.7	18.4	14.6	6.0
2/31/80	193	2	102.	87.3	48.6	–	21.6	16.6	13.6	–
4/03/80	195	2	103.4	82.8	45.7	–	21.3	15.8	12.1	6.0
4/09/80	80	2	136.6	76.6	45.9	31.1	22.6	18.5	15.4	9.8
4/30/80	919	2	–	–	34.8	26.7	21.8	16.1	12.5	6.6
5/02/80	216	2	134.8 dB	88.2	50.8	34.4	25.8	19.7	15.7	9.1
5/07/80	496	2	–	–	39.0	24.2	17.4	12.5	9.3	4.3
5/12/80	236	2	–	73.8	40.9	25.8	18.1	13.0	9.6	3.8
5/16/80	554	2	–	–	36.4	22.5	15.2	10.2	7.0	2.3
5/21/80	291	2	–	89.8	55.3	37.7	29.2	22.8	18.4	11.3
6/09/80	200	2	–	83.1	48.6	32.6	27.6	17.7	13.6	7.1
6/11/80	198 m	2 m	–	77.7 dB	45.9 dB	30.9 dB	23.2 dB	18.0 dB	14.5 dB	8.4 dB

81R-0182-29(T)

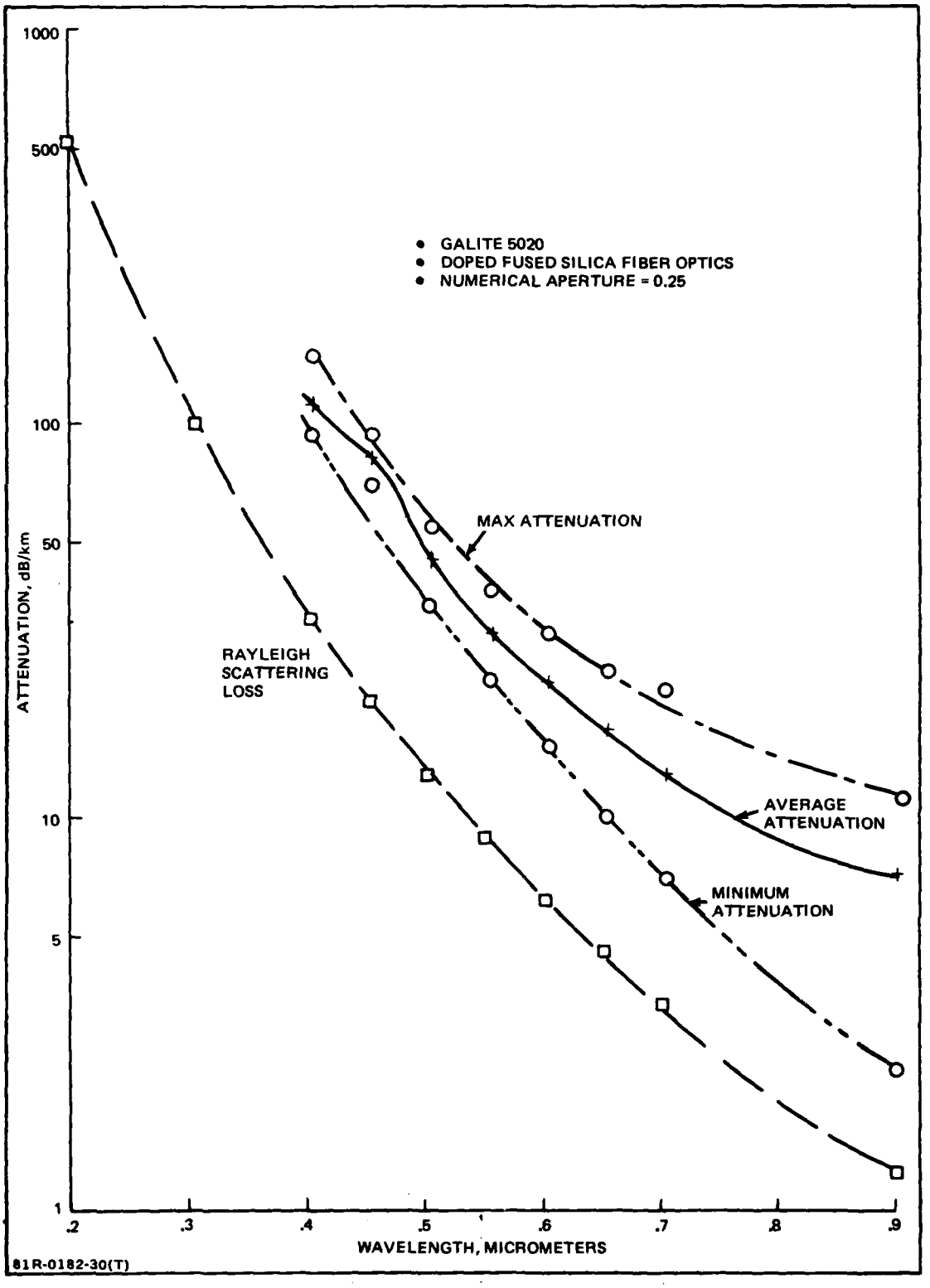

Figure 33 Measured Spectral Attenuation Boundaries

The most-uniform luminance of the diffuser aperture was found at 57.8 cm. The maximum variation of luminance in the aperture was 8.3% with respect to the average. This distance was used for all subsequent tests that used a uniform input. The setup is illustrated in Figure 34.

The emerging flux pattern of the 1-meter fibers was compared to the pattern measured by Galileo Electro Optics on the 100-meter fiber, the NA of which was 0.25. Flux distribution was measured to ±25 degrees and normalized to the intensity normal to the block. Moving the input diffuse surface provided a range of input NA from .58 to .14. The emerging pattern had a confirmed NA of 0.25 when the input NA was 0.20 (at a diffuser to input face distance of 35.6 cm). This distance was used for all other situations requiring a uniform input. The data is contained in Appendix A, Figure A-3a.

The luminance uniformity was read from ±30 degrees in nine regions on the test specimen. In all cases, the photometer was measuring the brightness of an output block surface area that contained 24 fibers. The data, normalized to the brightness normal to the block, is contained in Appendix A, Figure A-3b. Figures 35a and b illustrate the angular coverage where uniform illumination can be expected for the direct view CSDF. Two cases track the calibration curve closely and two show an angular bias. The angular coverage at the 50-percent point is essentially equal for all cases. The loss of coverage due to the bias is one degree. In the direct-view CSDF, the illumianted circle at the cockpit is 2.15 meters in diameter for the "calibrated output" and 2.04 meters for the biased case. To allow for the demonstrated bias at any position in the CSDF, the 2.15-meter diameter should be reduced to 1.93 meters or the design NA increased proportionately.

The data sheets in the Appendix and Figure 35 were normalized for convenient comparison of the radiation pattern. The raw data was measured in foot-lamberts. The mean readings and the standard deviation are contained in Table 3 as a measure of the relative brightness that can be expected in different locations near the center of the CSDF when a uniform brightness is intended.

The measured data indicates that from any cockpit position (±1.3 meters), a wall intended to be uniformly illuminated will have a possible contrast variation of as much as 1.31:1. This is close to the contrast ratio generally accepted to represent a shade of gray in television systems, 1.41:1. In this respect, the wall

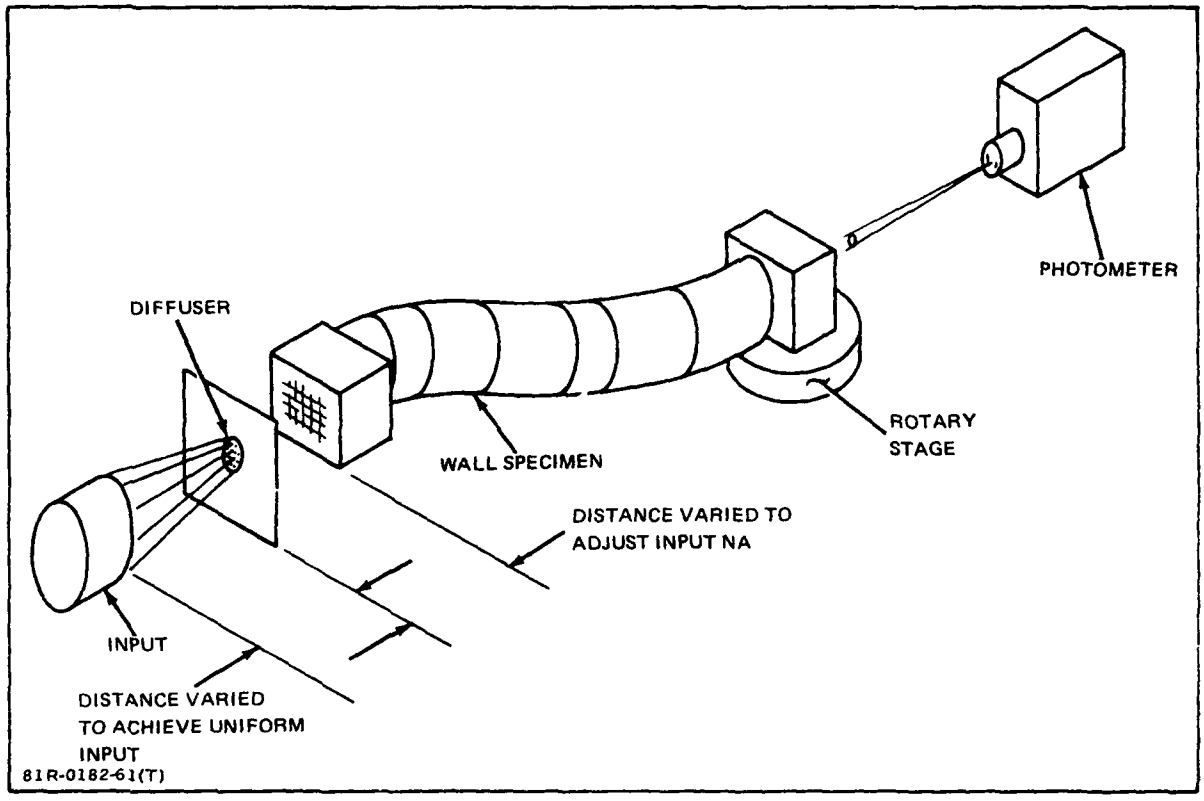

Fig. 34 Setup to Achieve Desired NA and Measure Luminance Uniformity

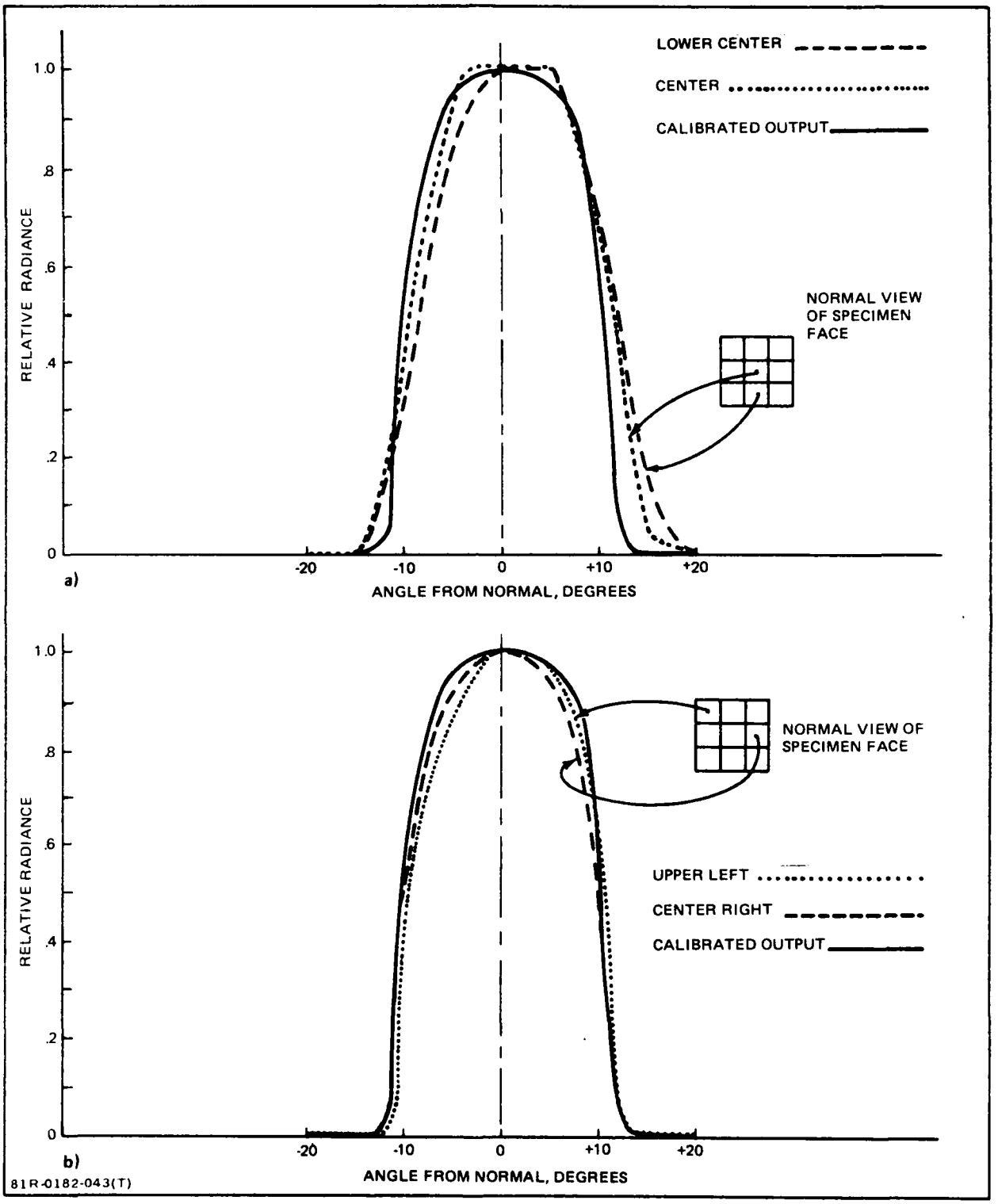

Figure 35 Relative Radiance Pattern from Selected Areas of the Test Specimen

luminance would probably be marginally uniform for a direct view CSDF, especially away from the center of the CSDF. No attempt was made to control uniformity in the assembly of the wall specimen because it is considered impossible to control in a production CSDF.

The data indicates that construction of a direct view CSDF with machine controlled tolerances would probably be marginal in terms of brightness uniformity.

Table 3 also illustrates the apparent changes in mean luminance with viewing position. For the fiber used in the test, the mean luminance that could be expected 1.3 meters from the CSDF radius is half the value seen from the center. This change is not constant in all directions. For example, if 2 observers in a tandem cockpit were 2.6 meters from one another, they would see a mean luminance close to the 1241 Foot-Lambert value if they were viewing a point ahead of the "aircraft" with their lines of sight as close together as possible. If they viewed a portion of the wall directly overhead or to their flanks, they would both be displaced from the CSDF radius and the lower luminance values for $\pm$1.3. meters would apply. Since these variations are predictable functions of the geometry, it is theoretically possible to compensate for them by varying the inputs.

Table 3 Relative Brightness of Wall Specimen vs. Lateral Distance from Center of CSDC

LATERAL DISTANCE, METERS	MEAN LUMINANCE, FOOT LAMBERTS	1-σ FOOT LAMBERTS	POSSIBLE 3-σ CONTRAST RATIO
-1.3	489	51.0	1.31:1
-.53	1083	71.2	1.20:1
0	1241	38.1	1.09:1
+.53	1196	54.8	1.14:1
+1.3	756	73.5	1.29:1

81R-0182-031(T)

The luminance uniformity measured from a translucent screen placed near the output surface of the wall specimen is contained in Appendix A, Figure A-3c. A plot of the data is shown in Figure 36, compared to the angular distribution of flux from the fiber. Looking at a single resolution spot, the change in brightness for different cockpit locations is inconsequential compared to the direct new case.

SOLAR SIMULATION CAPABILITY

The solar simulation capability and lamp requirements were measured at reduced projection distances to avoid extrapolation from small illumination values. They were measured a number of times while changing the uniformity and size of the input pattern in order to assess the possible changes in the illumination pattern.

The physical setup used for the solar simulation measurements is shown in Figure 37. The input was from a solar simulator using a 1000-watt Xenon arc lamp. The simulator produced a 87-mm diameter beam of light which was focused to provide an illuminated spot up to 45 solar constants. External optics and

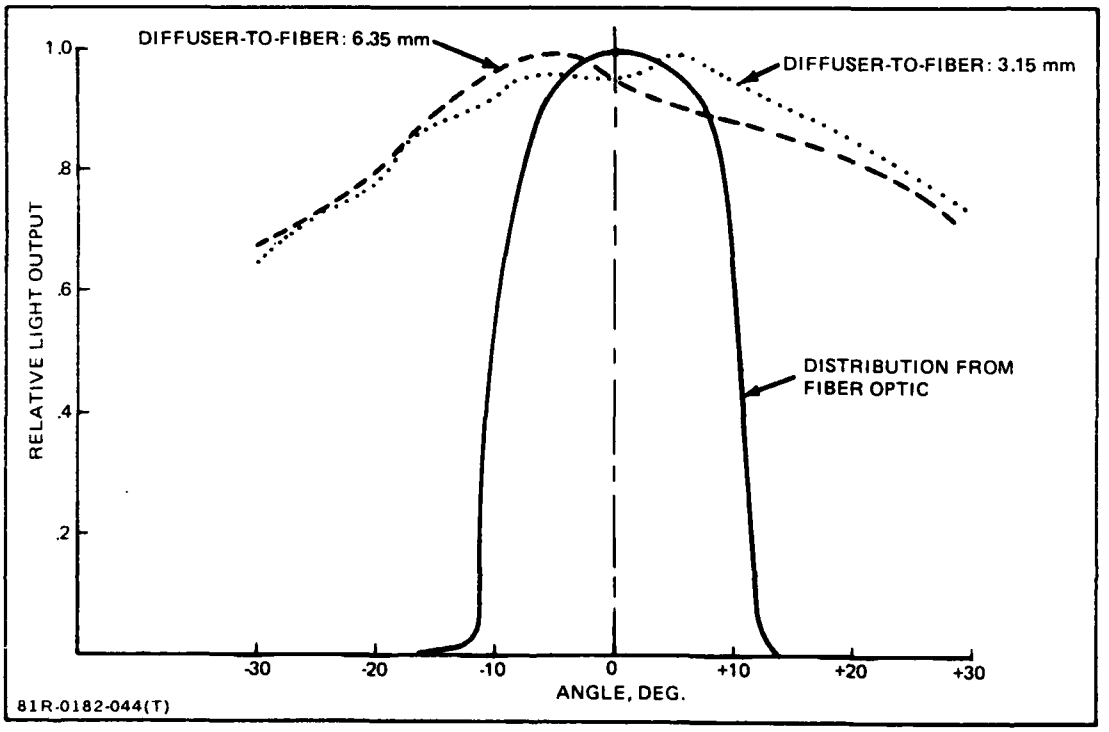

Figure 36 Angular Luminance from Translucent-Screen Diffuser

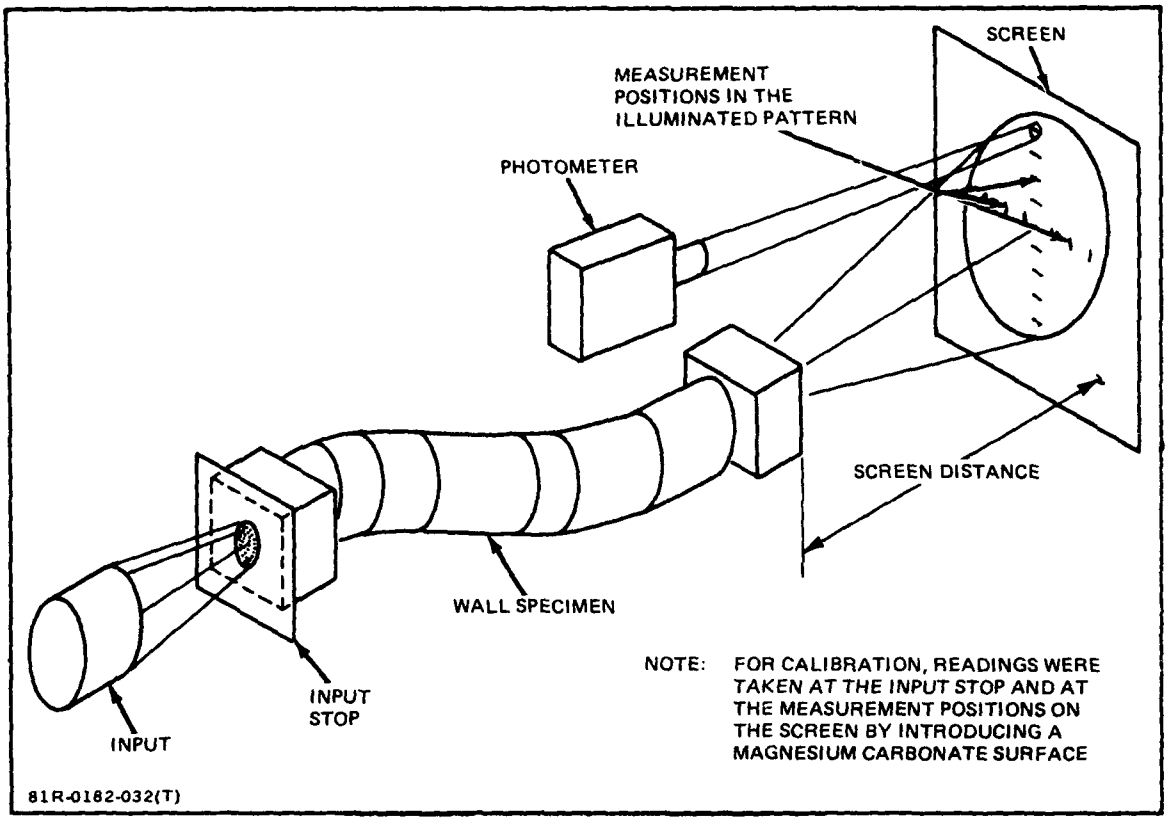

Figure 37 Solar Simulation Measurement Setup

stops were used to modify the intensity, size and uniformity of the input.

To facilitate data extrapolation, the illumination levels were measured on the input face of the specimen, the screen, and with a magnesium carbonate surface at both locations. Since a fresh magnesium carbonate surface is essentially Lambertian with a reflectivity of 0.98, it permits an accurate determination of surface reflectivities and illumination levels. After the screen and input surface reflectivities were characterized, the measurements were not repeated with the magnesium carbonate surface.

A uniformly illuminated input of 3.8×10^4 foot-lamberts was measured on a magnesium carbonate surface. It was permitted to fall on the input face of the test specimen through a 1-inch diameter stop. At a distance of 1.50 meters from the output face, the illumination pattern was measured at 10-cm intervals along the horizontal and vertical axes. The measurements were also made from the magnesium carbonate surface at the projection distance. The data sheet is contained in Figure A-4a in Appendix A.

Since all fibers act as parallel channels, there should not be any differences in the illumination patterns produced by a uniform or a non-uniform solar input. To test this (Test 4B), a non-uniform solar input was delivered to the test specimen. In the 1-inch diameter stage, the illumination varied from 1×10^5 foot lamberts at the center to 5×10^4 at the edge. The arc lamp was delivering flux more efficiently in this case than when a uniform input was used. The peak illumination at the screen increased from 2.40 foot candles for the uniform case to 3.78 foot candles. In addition, the fall-off of illumination with angle from the optical axis was found to be reduced. The relative illumination along the screen is shown in Figure 38 and the data sheet is presented in Appendix A, Figure A-4b. The input NA was apparently greater for the non-uniform input.

A translucent screen was placed 1/4 inch from the output face of the test specimen and Test 4B repeated. The input condition was unchanged from Test 4B except that the screen was placed 1.0 meter from the output face. The data is recorded as Test 4C, Figure A-4c in Appendix A.

A more non-uniform input was set up (Test 4D), where the arc was focused to a 1/4 inch diameter within the 1-inch stop. The arc's image was illuminated with 4.52×10^5 foot candles and the remainder of the 1-inch stop had scatter and

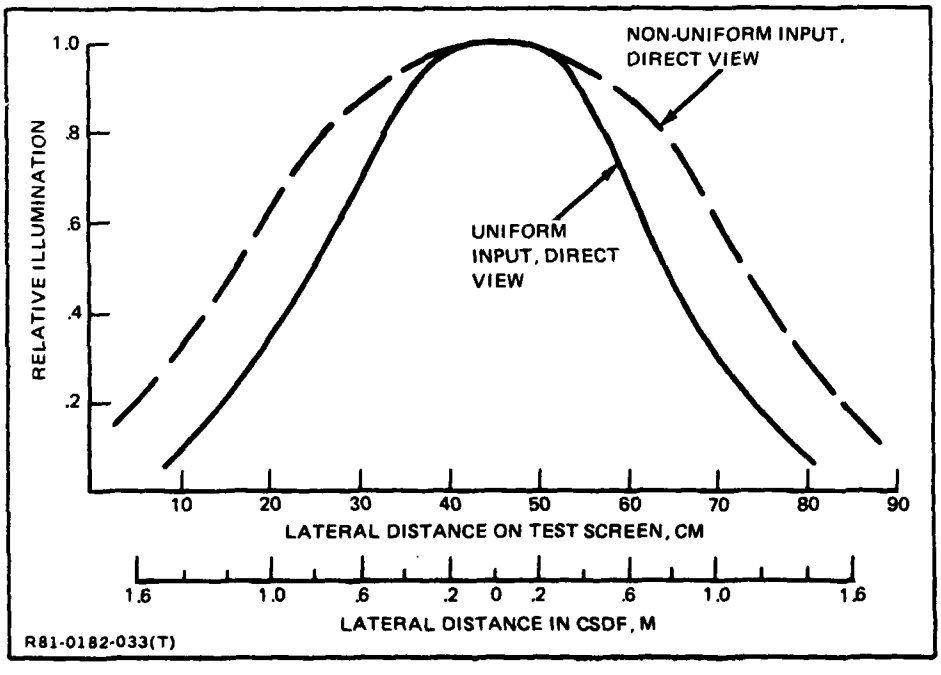

Figure 38 Comparison of Illumination Pattern vs Solar Input Uniformity, Direct-View CSDF

spill-over. The resulting screen illumination was not as high as in Test 4B, where the setup intentionally produced the highest screen illumination. The data is presented in Figure A-4d in Appendix A.

The illumination values for Tests 4A through 4D are consolidated in Table 4. The data was converted to foot candles of illumination at 1.5 meters from the output face.

Both non-uniform cases produced a broader emission pattern than the uniform input. This was attributed to a larger numerical aperture on the nonuniform inputs, the short length of fiber in the test specimen, and the relative distribution of flux in the arc assembly. The net effect of this combination was to change the apparent fiber NA. If a detail design of this concept is undertaken, the relationship between illuminator geometry and fiber numerical aperture must be carefully controlled.

Table 4 Illumination on Screen at 1.5 Meters

	POSITION IN ILLUMINATION PATTERN, cm								
TEST AND INPUT	10	20	30	40	50	60	70	80	90
4A, 38K Uniform	.21	.75	1.64	2.37	2.41	1.70	.73	.20	
4B, 50–100K	.88	2.23	3.22	3.69	3.78	3.54	2.78	1.41	.46
4C, 50–100K w/ Translucent Screen	.18	.26	.38	.48	.51	.44	.33	.23	.19
4D, 452K	.48	1.22	1.92	2.69	3.33	3.31	2.77	1.93	.97
NOTE: ALL VALUES IN CANDLES FT^{-2}									
81R-0182-034(T)									

Solar Simulation with a Translucent Screen

An estimate of the total lumens required in a full-sized CSDF may be made by extrapolating the measured data. Assuming that the desired illumination is 11,520 candles ft^{-2} (12.4 candles cm^{-2}), the lumens delivered by the arc lamp used in the test (L) must be increased by the factor X_1, where:

$$W_T = X_1 L \tag{37}$$

and

$$X_1 = \frac{11,520}{.51} \left(\frac{6.1}{1.5}\right)^2 \left(\frac{.0188}{P_i}\right) \frac{K_1}{1.06} = 6,625 \frac{K_1}{P_i} \tag{38}$$

The P_i and the K_1 values for the test specimen are 0.0188 and 1.06 respectively.

A calibration run on the arc lamp output is shown in Appendix A as Test 4E, Figure A-4e. The area weighted average illumination produced by the arc lamp was 29,774 candles ft^{-2} or 650 lumens. (L) The projected lumen requirement is therefore:

$$W_T = 4.3 \times 10^6 \frac{K_1}{P_i} \quad \text{lumens} \tag{39}$$

The expected value of K_1 can be taken from Figure 21 and P_i from Figure 17. Assuming a 100-meter fiber length ($K_1 = 6.8$) and packing efficiency (P_i) of 0.5, the required lumens are:

$$W_T = 4.3 \times 10^6 \frac{(6.8)}{(0.5)} = 5.8 \times 10^7 \quad \text{lumens} \tag{40}$$

The experimental results were compared with the mathematical model (Equation 12). Using 0.04 for the value of ρ_3, yields:

$$\frac{1.508 \times 10^7}{T_w G_w} \left(\frac{K_1}{P_i}\right) = 4.3 \times 10^6 \left(\frac{K_1}{P_i}\right) \tag{41}$$

Consequently, the experimental data agrees with the predicted value if the transmission-gain product ($T_w G_w$) of the translucent screen is 3.5. This is a reasonable value for an extrapolation of this magnitude. The screen that was used has a measured gain of 2.5.

Solar Simulation with a Direct-View CSDF

A similar comparison made for the direct-view CSDF provides a value for X_1 of:

$$X_1 = \frac{11,520}{3.78}\left(\frac{6.1}{1.5}\right)^2\left(\frac{.0188}{P_i}\right)\left(\frac{K_1}{1.06}\right) = 894\left(\frac{K_1}{P_i}\right) \tag{42}$$

The projected total lumen requirement is, therefore:

$$W_T = 5.811 \times 10^5 \frac{K_1}{P_i} \quad \text{lumens} \tag{43}$$

Comparing this value with Equation 25:

$$\frac{1.448 \times 10^7 K_1 \tan^2(\sin^{-1} NA)}{P_i K_2} = 5.811 \times 10^5 \frac{K_1}{P_i} \tag{44}$$

This requires that:

$$\frac{\tan^2(\sin^{-1} NA)}{K_2} = 4.013 \times 10^{-2} \tag{45}$$

On-axis ($K_2 = 2.0$) the angle whose sine is the numerical aperture should be 15.8 degrees (NA - .273). This agrees reasonably with the measured value for the test specimen (.257).

MODULATION ON THE TRANSLUCENT SCREEN

If a translucent screen is used between the exit face of the fiber optics and the observer, there is a penalty in achieving the desired brightness. This is a tradeoff for a substantial saving in the number of fibers in the CSDF. A

translucent screen is expected to provide uniform brightness where it is desired, and variable resolution without the granularity that is expected when the fibers are viewed directly.

The effect of screen spacing on the ultimate image quality was measured at three distances. The setup for this set of tests is illustrated in Figure 39. A square wave resolution mask was introduced at the input stop and a horizontal scan was made reading the screen luminance along a row of fiber projections. The resolution mask consisted of 4-millimeter opaque bars and transparent spaces. The readings were made from the center of the test specimen horizontally along a line of fiber channels. A similar series was made over different portions of the output face at a single screen distance to establish the essential uniformity of the specimen.

The readings are plotted in Figure 40 for spacings of 1/8, 1/4, and 3/8 inches. The best modulation occurs at 1/8 inch. However, there is evidence of aliasing affects on the bright bars. At 1/4-inch, the modulation is almost as good and the aliasing effects have disappeared. At 3/8 inch, there is a noticeable loss of modulation which can be expected to reduce contrast and "resolution". For this particular numerical aperture, the 1/4-inch spacing is preferred. The data sheets are presented in Figure A-5a, A-5b and A-5c, Appendix A.

The ability to produce a uniform luminance (flat field in TV terminology) was tested with the screen 1/4 inch from the specimen output face with a uniform illumination on the input face. The photometer readings were made at 500-micrometer intervals along the apparent center of a line of fiber channels. Fifty readings were made which covered approximately one inch and traversed 18 fiber channels.

The data sheet is identified as Test 5A, Figure A-5d in Appendix A. A smoothed plot of the trace is presented in Figure 41. The average luminance was 0.507 ft.-Lamberts. The 1-σ deviation was determined to be 0.045 ft. candles.

The center-to-center spacing of the fiber channels is shown in the figures. Exact location of fibers can not be identified from the trace. However, general areas where the luminance varies from the average are clearly seen. The points marked A and B could be 2-fiber channels with 3-fiber channels between them.

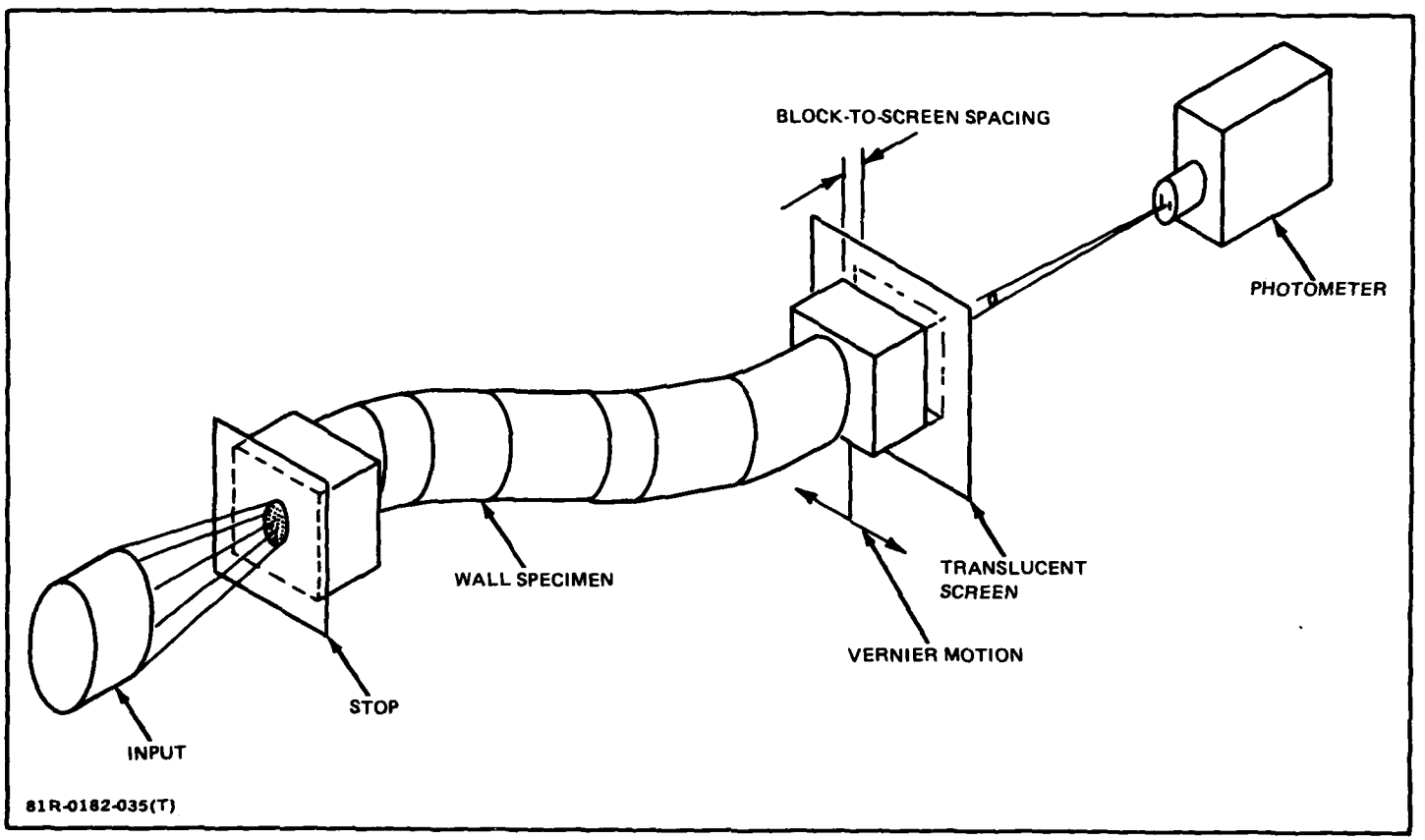

Figure 39 Measurement Setup Using Translucent Screen

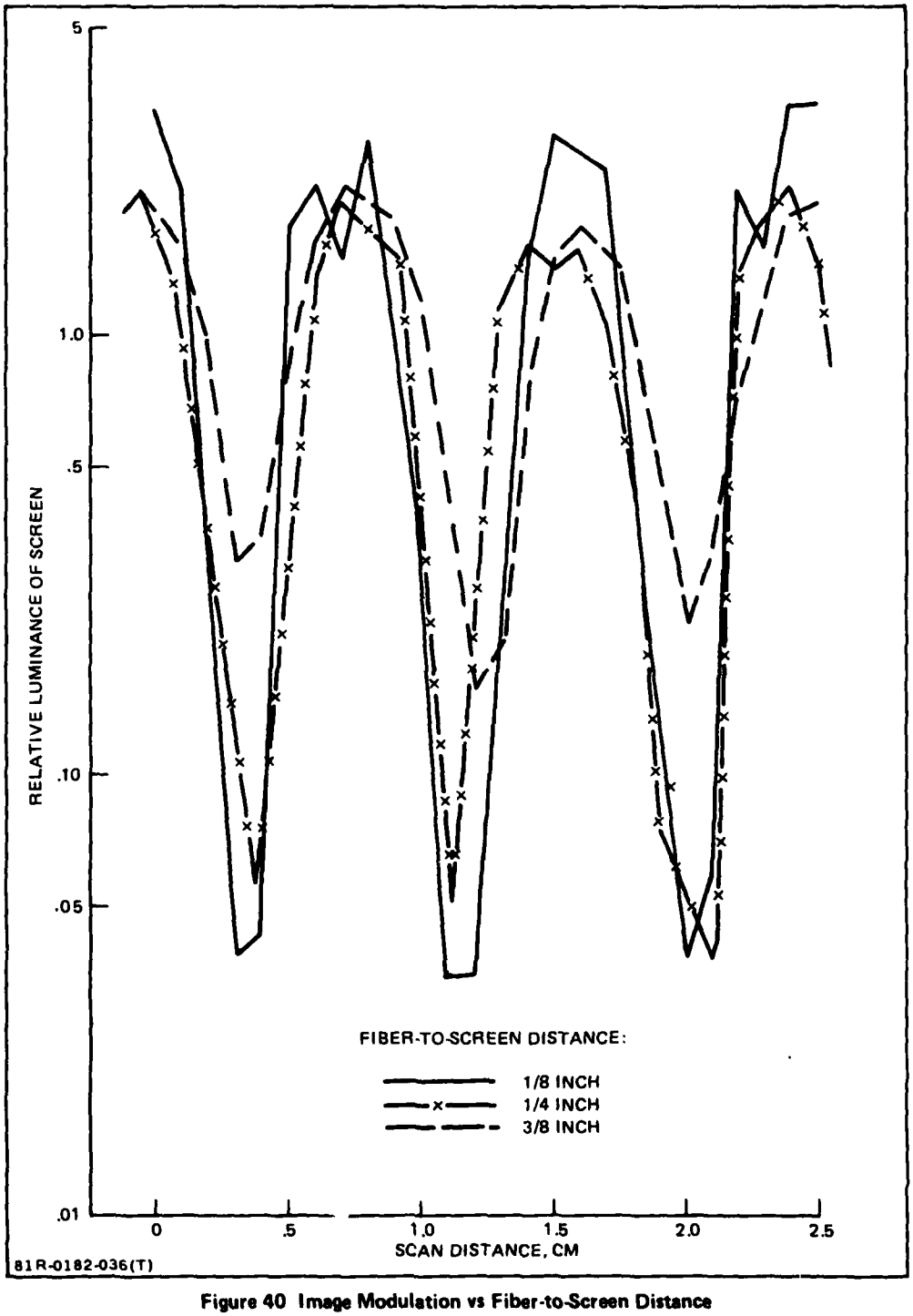

Figure 40 Image Modulation vs Fiber-to-Screen Distance

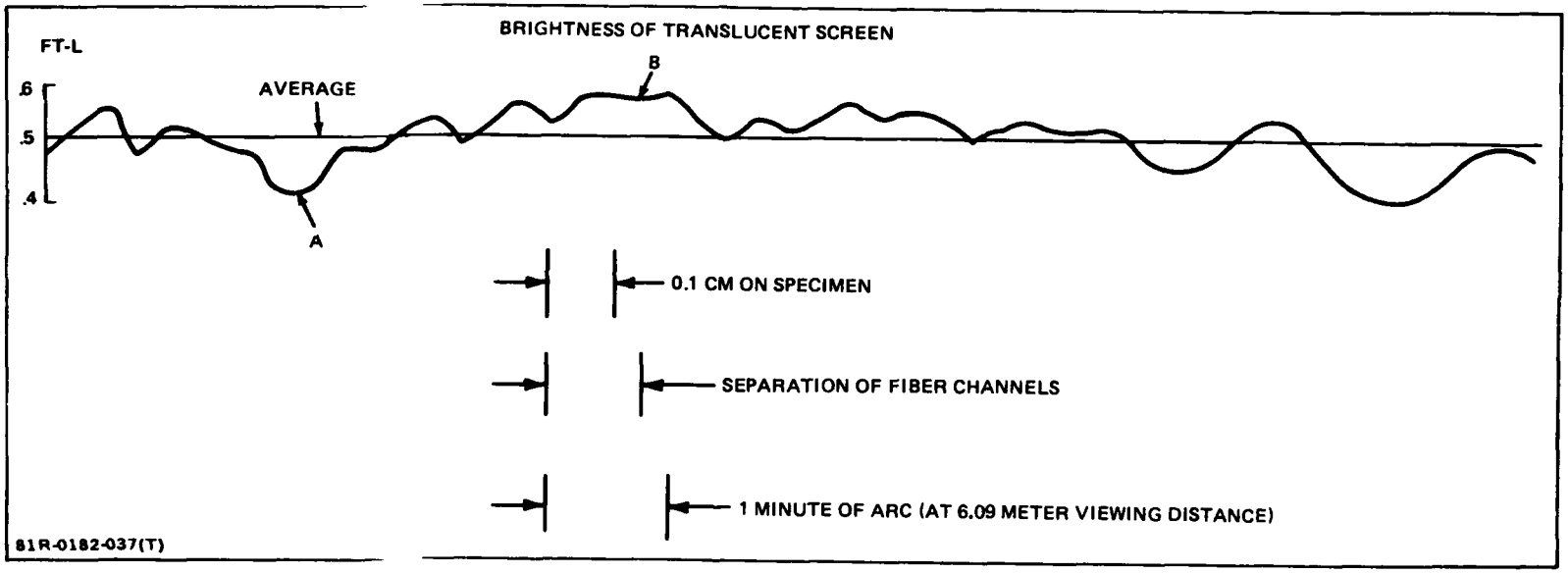

Figure 41 Trace of Output Luminance with Uniform Input

The ratio of maximum to minimum luminance is 1.39:1. The field is marginally flat since one gray shade is accepted as equal to $\sqrt{2}$:1. Figure 42 illustrates the appearance of the screen for fiber-to-screen spacings of 1/8 and 1/4 inch.

SURFACE REFLECTION

When the test plan was drafted, it was assumed that the diffuse and specular reflections would be measured separately. Subsequently, it was found to be extremely difficult to separate the two cases and the utility of the separate data was questionable. The surface reflectivity is an important parameter in the possible loss of contrast due to the unwanted reflection of stray light in the direct-view CSDF. However, the observer's line of sight to the wall is always close to the normal and the stray light sources could be at a wider range of angles. As a result, a single series of measurements was made in which the photometer was kept normal to the surface of the test specimen and the illuminating source was moved $\pm$60 degrees at 10-degree intervals. Readings at the normal were averaged from readings taken at 5 degrees on opposing sides of the photometer. The instant field of the photometer was set for 20 minutes of arc and, at the test distance from the block (two meters), it covered approximately 50 output channels. Readings were also made at the normal with the lambertian surface substituted for the test specimen.

The illumination values were corrected for the cosine factor and the measured reflectivity is recorded in Figure A-6, Appendix A. A plot of the reflectivity of the test specimen relative to the lambertian surface is shown in Figure 43. A reflection gain can be seen for light arriving on the test specimen close to the normal. This will be important for sunlight reflected from cockpit structure. There will be a contrast loss caused by this reflected light. The brightness of the contrast-reducing component will be the reflection coefficient from Figure 42 multiplied by the effective brightness-solid angle product of the illuminated structure.

Fabrication cost precluded the possibility of providing the test specimen with all the features a CSDF would contain. The metallic face of the specimen would have a black matte finish in a CSDF to reduce the reflection coefficient and enhance visual contrast. The black finish would be essentially the same as the

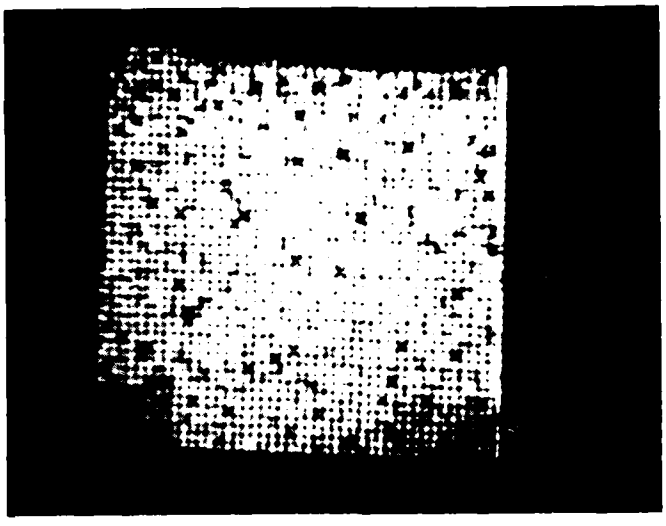

a) 1/8-INCH BETWEEN FIBERS AND SCREEN

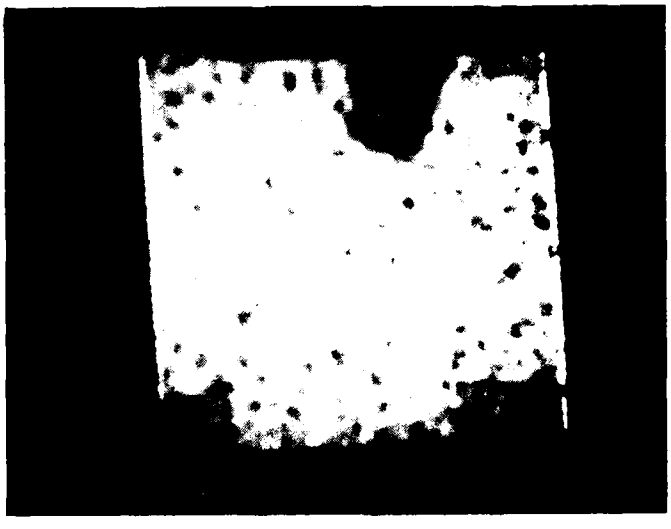

b) 1/4-INCH BETWEEN FIBERS AND SCREEN

81R-0182-057(T)

Figure 42 Appearance of Translucent Screen with Uniform Input

black mask used in color television tubes to enhance contrast. The relative shape of the reflection curve would be essentially unchanged but the absolute values would be reduced if a black matte surface were used.

CROSSTALK BETWEEN CHANNELS

The crosstalk measurement used a mask on the input surface to restrict illumination to one channel. The photometer was used to measure the luminances of other channels that were illuminated. The test was performed but no measurable crosstalk was found.

TEMPERATURE RISE

Five thermocouples were embedded in the test specimen to monitor the temperature rise at high illumination levels. The thermocouples were used to determine the stagnation temperature for long-term illumination of test specimen. The data were taken with 7.4×10^4 ft-candles of illumination on a 1-inch diameter. The center of the illuminated area was positioned over the thermocouple in the center of the block. The data from the test are presented in Table 5.

When the specimen was rotated end for end, the thermocouples were one meter from the input face. The maximum temperature rise was consistently 4.°F.

An analysis of the results to permit an extrapolation to the requirements of an operating CSDF was not performed. The physical differences between the input face of the test specimen and an operational CSDF are considered too great. The relative factors that contribute to the difference are:

Test Specimen	Operational CSDF
• Input face essentially metallic	• Input face essentially glass
• Absorption high and almost entirely on input face	• Absorption low and non-linear through length of fibers
• Transverse conductivity through metallic face is high	• Transverse conductivity through glass fibers relatively low
• Radiation occurs from both surfaces of the metallic face	• Radiation essentially from one surface

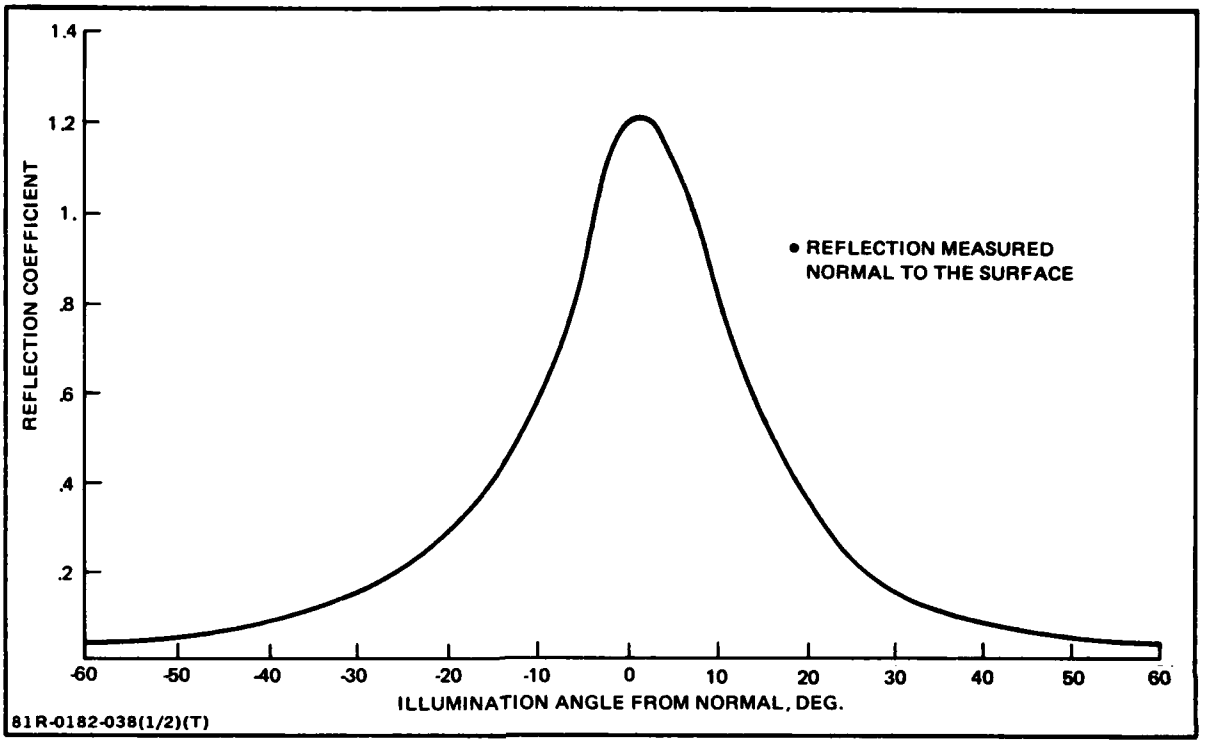

Figure 43 Relative Reflection Coefficient from Test Specimen

Table 5 Temperature Rise on Illuminated Test Specimen

Test	Temperature, °F					
	0 MIN	15 MIN	30 MIN	45 MIN	60 MIN	–
1	75°F	98°F	106°F	109°F	110°F	114°F @ 120 MIn
2	73	87	96	102	108	117 @ 180 Min
3	75	99	107	109	112	117 @ 120 Min
4	75°F	88°F	98°F	101°F	106°F	116°F @ 180 Min

81R-0182-038(2/2)(T)

VISUAL APPEARANCE OF TERRAIN IMAGES

The size of the test specimen would subtend 42 minutes of arc when viewed from 6.1 meters. Its small size would certainly make any subjective image evaluations even more difficult. Therefore, an attempt was made to simulate a large surface, the properties of which were comparable to the test specimen, by use of a photographic contact print. This was done by placing the negative material in contact with the exit face and illuminating the other end of the specimen with uniform diffused light. From the negative, 144 positive transparencies were made. A mosaic of the positive transparencies was fabricated that measured 76 by 76 cm. In fabricating the mosaic, some irregularities were unavoidable. They were considered acceptable, however, because some fabrication variations can be expected in any large fiber optic assembly. Figure 44 is a reproduction of the negative made from the block and a portion of the mosaic.

The 76- by 76-cm positive transparency was backed by a translucent surface. A continuous-tone aerial photograph was back-projected on the screen. The test specimen was placed alongside the mosaic and a portion of the same image with the same scale was projected on its input surface. A second projector and transparency was used for this image to match the image scales. The resulting images in both the mosaic and the specimen looked remarkably similar. An example of the images is presented in Figure 45.

The effect of fiber channel spacing and viewing distance is illustrated in Figure 46a through 46d. A photograph of the aerial image on the mosaic was printed at a series of scales. If each photograph is viewed from a distance of 60 cm, the image will reproduce the appearance of the fiber spacing indicated.

ESTIMATED CSDF COST

An estimate cost for a CSDF should include at least:

- Capital investment for automated fiber drawing towers and fiber handling facilities to fabricate a CSDF module subassembly
- Cost to produce the fiber
- Transportation costs
- CSDF support structure costs

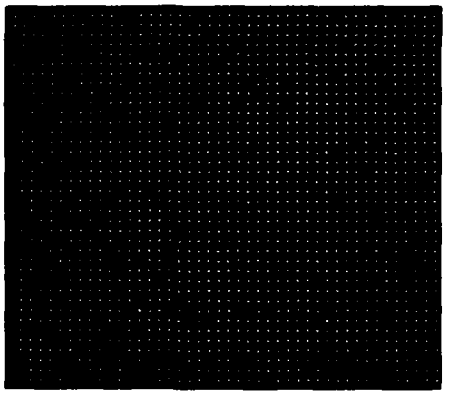

Figure 44 Contact Print of Test Specimen Output

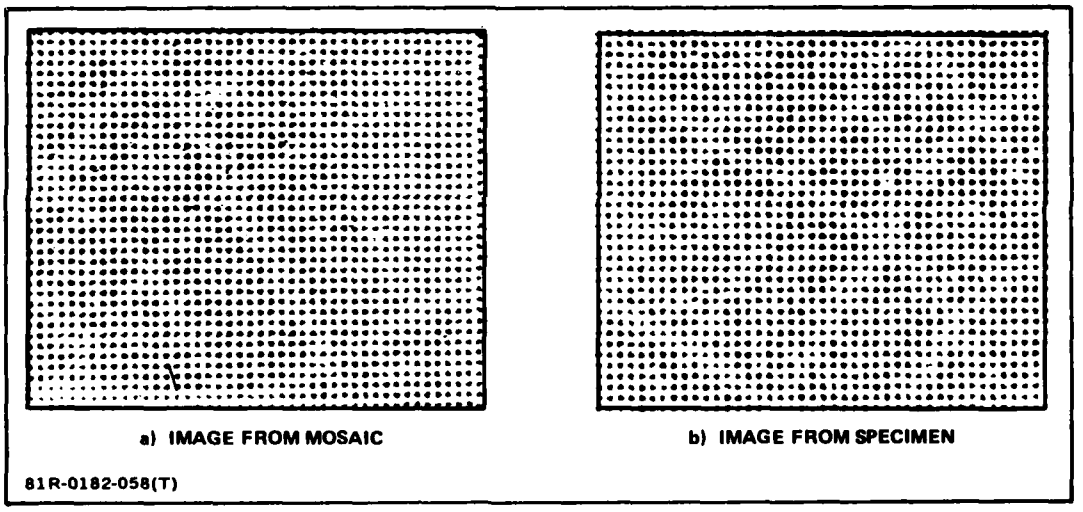

Figure 45 Comparison of Terrain Images

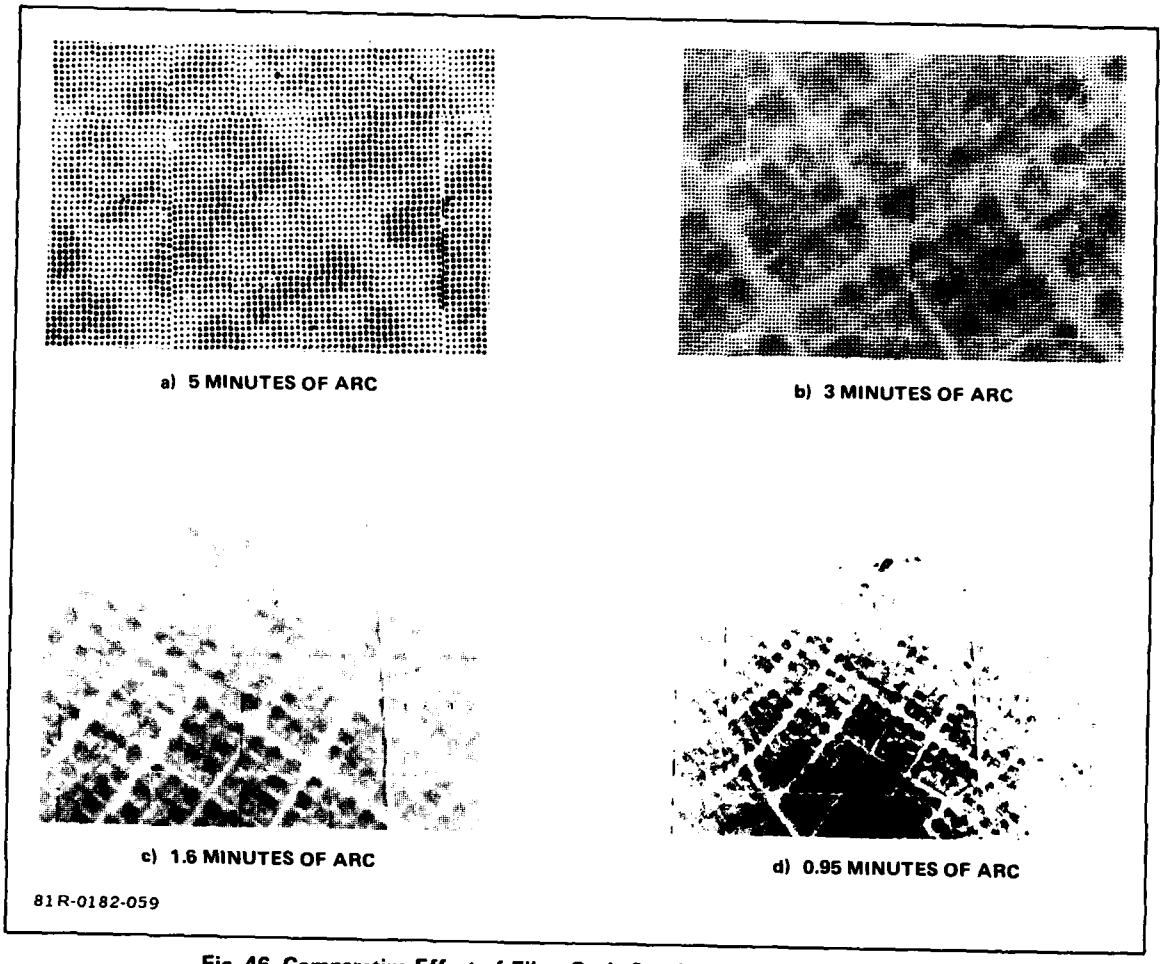

Fig. 46 Comparative Effect of Fiber Optic Spacing Viewed from 60 cm

- CSDF assembly costs
- Scene generation system costs
- Controlling computer system costs
- Software detail design costs
- Interest on the costs of the above.

A reasonable approach to this question is to estimate the cost of the basic building block and to use multipliers for the supporting costs where possible. Consequently, the cost of the fiber is the first consideration.

The possibility of using different resolutions in specific areas of the CSDF

has already been established. However, the specific resolutions and the extent of the area where they will be required is presently undetermined. Consequently, the fiber cost estimate was developed for one steradian of CSDF, with the resolution, fiber length, and cost per unit length being variable.

Assume a rectangular fiber arrangement with the area allocated to each fiber designated as a^2. For one steradian, the wall area is equal to the square of the CSDF radius (R^2). Therefore, the number of fibers per steradian is:

$$\text{Number of fibers/ster} = \frac{R^2}{a^2} \tag{46}$$

If each pixel (fiber) subtends an angle α, then:

$$\tan \alpha = \frac{a}{R} \tag{47}$$

Combining Equations 46 and 47 yields the number of fibers per steradian:

$$\text{Number of fiber/ster} = 1/\tan^2 \alpha \tag{48}$$

If the required fiber length is (L) meters and the production cost is U dollars per meter, the cost, $(\$)_{fiber}$ is:

$$(\$)_{fiber} = \frac{L\,U}{\tan^2 \alpha} \tag{49}$$

This relationship is plotted in Figure 47 for pixel subtenses of 0.5 to 5 minutes of arc and a length of 100 meters.

The need for major capital investment can be estimated from the length of fiber needed. For a one minute of arc subtense, a total of 11,818 kilometers of fiber is required, for each steradian, per meter of length between input and exit face. If the final design could be kept to 50 meters, then 591,000 kilometers would be needed. If a drawing tower produced 20 meters of fiber per minute, 24 hours per day, for 365 days a total of 10, 512 kilometers would be produced. This production would have to be repeated 57 times to satisfy the requirements for one steradian with a 50 meter length. Allowing for contingencies, scrap, down time, etc., approximately 100 drawing towers and the supporting glass preparation and

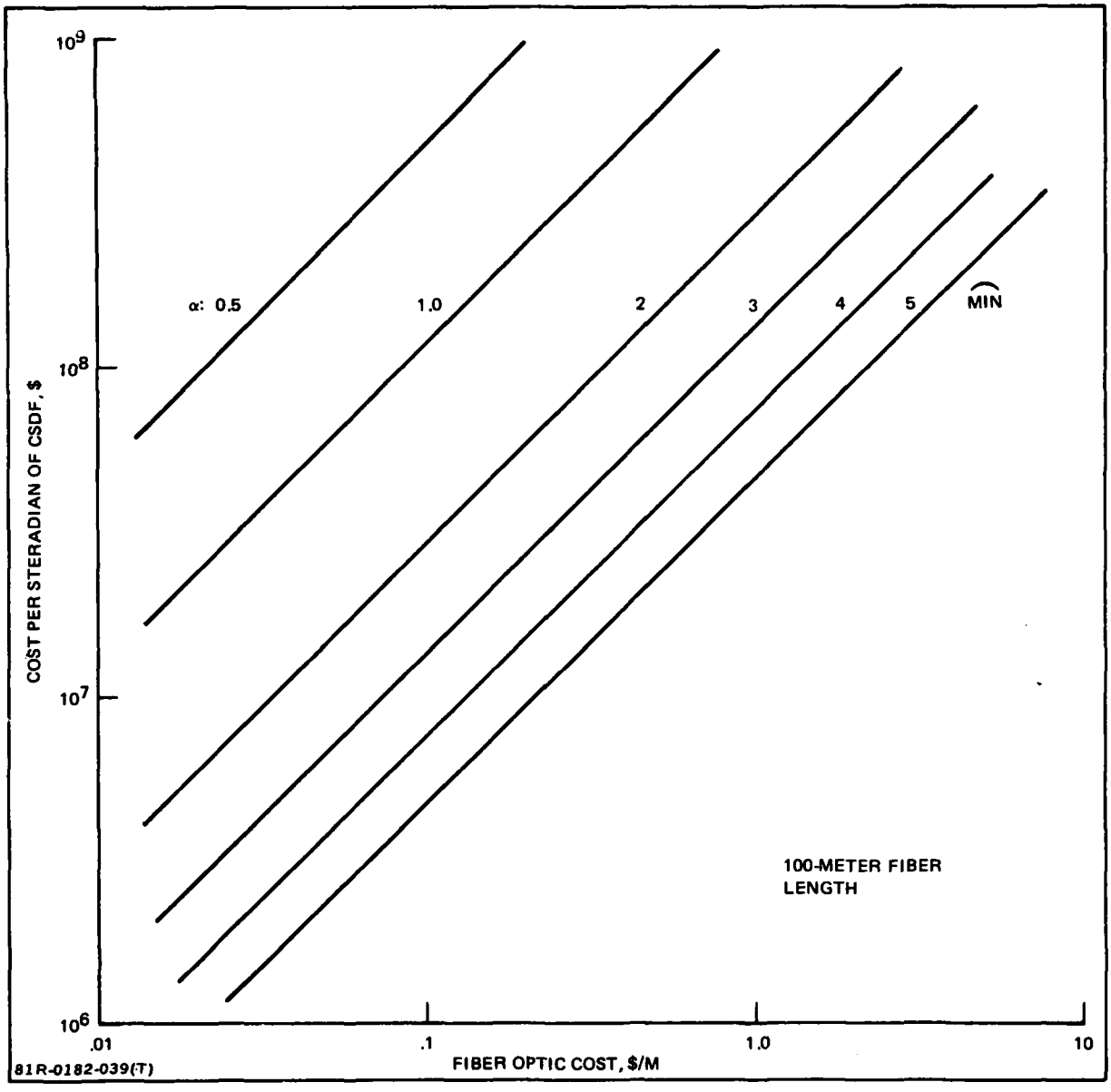

Figure 47 Estimated Cost of Fiber per Steradian of Translucent-Wall CSDF

handling equipment would be required to draw the fiber in one year. There may be as many as seven steradians required in the CSDF.

For a reduced image quality of three minutes of arc, the fiber could be drawn by seven towers in one year at 100 percent efficiency. A figure of 11 towers would probably be needed to account for maintenance, downtime, etc. The fiber drawing equipment cost is proposed as the number of towers ($\#T_W$) multiplied by the cost of the towers and supporting facilities ($\$T_W$). The cost of the towers and material handling equipment is estimated at $600,000 apiece.

In Figure 47, the cost per meter is shown between one cent per meter and one dollar per meter. Communication cable cost is presently near one dollar per meter but specialized equipment, continuous running, reduced overhead, elimination of a plastic sheathing etc. could reduce the cost to 10 cents a meter in 1980 dollars. It is not expected to be less than this figure because the glass quality must remain high. The cost for fiber is represented by $FO.

Transportation costs ($TR) are assumed to be a fraction of the cost of production of the fibers. A value of four percent is assumed for $TR.

CSDF support structure cost ($SS), scene generation cost ($SG), computer and controlling software costs ($CSW) are one-time capital costs. The support structure cost is estimated to be 2 million dollars, exclusive of the building housing the CSDF. No estimate was made for the scene generator or the computer.

CSDF assembly costs (AY) include the assembly provisions at the drawing plant, inspection before and after shipping, and installation into the CSDF supporting structure. It is estimated that the automated assembly cost will be 75 percent of the cost of drawing the fiber.

Detail design of the CSDF system ($DD) to encompass all of the above automation, handling, etc. exclusive of the scene generation and computer is estimated to be $8 million.

Interest cost was not included.

The estimated CSDF cost equation is:

$$\text{CSDF Cost} = (\#TW)(\$TW) + (\$SS) + (\$DD) + (\$SG) + (\$CSW) + \$FO\,(1+TR+AY)$$

SECTION V

BASELINE CSDF

PHYSICAL DESCRIPTION

The present state of the art of large-dome simulators may be used as a point of departure for defining a future CSDF. There are several possible ways to provide background and target imagery. However, a video projection system will be used to represent the present state of the art. Without characterizing any particular system, a representative set of parameters would be:

- Each TV line pair subtends approximately five minutes of arc
- Average brightness of a color scene is eight candles m^{-2}
- Projection covers one steradian.

To improve the resolution and brightness, the projection scale can be reduced at the cost of using more projectors. It is obviously not possible to improve both the resolution and the brightness of TV systems to anything even closely resembling the fiber optic CSDF design goals.

A baseline CSDF can be estimated by using fiber optics to increase the simulated brightness without increasing the apparent resolution. To do this, the spacing between fibers would be such that they would always be individually seen and a translucent-wall CSDF would have to be used. The major CSDF characteristics are summarized in Table 6, assuming a relatively high-gain screen is used.

The size of the image input surface is rather small and the spacing between the CSDF dome and the input would not require 100 meter fibers. An estimated length of 40 meters is used instead. Therefore, the spectral correction factor K_l is 2.1.

The number of 30-kw Xenon lamps estimated for sun and sky simulation assumes that all of the lumens produced by each lamp are collected and redirected

Table 6 Characteristics of Baseline CSDFs (per Steradian)

ANGULAR SPACING BETWEEN FIBERS	5 MINUTES OF ARC		3 MINUTES OF ARC		1 MINUTE OF ARC	
Number of Fibers per Steradian	472,725		1,313,000		11,818,000	
Fiber Core Diameter, Micrometers	220		220		220	
Fiber Core/Clad Diameter Ratio	0.8		0.8		0.8	
Fiber Arrangement	Rectangular		Rectangular		Rectangular	
Input Packing Factor P_i	0.5		0.5		0.5	
Area of Image Input Surface per Steradian, sq meter	0.0357		0.100		0.900	
Fiber Length, meters	40		40		60	
Spectral Correction Factor (K_1)	2.1		2.1		3.0	
Simulated Solar Illumination, lumens m^{-2}	1.24×10^5		1.24×10^5		1.24×10^5	
Simulated Sky Luminance, candles m^{-2}	3×10^4		3×10^4		3×10^4	
Cost of Fiber Per Steradian at $0.10 per meter	$1,891,000		$5,252,000		$70,908,000	
Screen Transmission - Gain Product ($T_W G_W$)	10.0	5.0	10.0	5.0	10.0	5.0
Lumens Required For Solar Simulation	6.3×10^6	12.7×10^6	6.3×10^6	12.7×10^6	9.1×10^6	18.0×10^6
30 KW Xenon Sources Required w/ 100% Efficiency for Solar Simulation	4.0	8.0	4.0	8.0	6.0	12.0
Lumens Required for Sky Simulation per Steradian w/100% Efficiency	1.53×10^6	3.1×10^6	1.53×10^6	3.1×10^6	2.20×10^6	4.4×10^6
30 KW Xenon Sources Required per Steradian of Sky w/100% Efficiency	1.0	2.0	1.0	2.0	2.0	3.0
Input Solar Image Subtense						
1/2° Solar Simulation, Watts cm^{-2}	1.24×10^6	2.5×10^6	4.47×10^5	9.03×10^5	7.19×10^4	1.47×10^5
1° Solar Simulation, Watts cm^{-2}	3.11×10^5	6.27×10^5	1.17×10^5	2.26×10^5	1.79×10^4	3.57×10^4
2° Solar Simulation, Watts cm^{-2}	7.8×10^4	1.57×10^5	2.83×10^4	5.64×10^4	4.49×10^3	8.94×10^3

81R-0182-45(T)

to the input image surface. The illumination system would not be 100% efficient and the number of lamps actually needed would be increased accordingly. However, at least seven 30-kw lamp units would be required for sky simulation in seven steradians and four for solar simulation.

The baseline CSDF could provide full brightness but the resolution would be physically unchanged. The increased brightness would make the image quality less acceptable than in the state of the art TV projection system because the observer's visual acuity and contrast sensitivity are better with the higher scene brightness.

If just the improved visual acuity is compensated for, the angular subtense between fibers would be three minutes of arc. This configuration is described as Baseline CSDF #2 in Table 6. Many of the parameters are unchanged because the size of the input surface is still small enough to permit a 40-meter fiber length, retaining the spectral correction factor of 2.1. As long as the input packing factor is unchanged, the number of lamp units is also unchanged. The larger number of fibers in Baseline #2 requires a larger input solar image with correspondingly lower flux densities.

Baseline CSDF #3 is detailed in Table 6 to illustrate the requirements for full brightness with image quality close to matching the pilot's visual acuity. The image input surface is substantially larger and a longer fiber length was assumed to accomodate the larger bundles and larger input system. The minimum number of 30-kw Xenon lamps was increased accordingly. As a consequence of the larger input surface, the flux density for solar simulation decreased. All three cases in Table 6 provide full brightness but the cost to provide good image quality is substantial.

The feasibility of the fiber optic CSDF concept is critically dependent on two factors: the length of fiber run from the CSDF to the input surface, and the cost-per-meter of the fiber. As the length of fiber is decreased, it reduces the illumination requirement by relaxing the spectral correction factor (K_1) and directly reduces the fiber cost. It also opens the possibility of using a less costly glass composition for the fiber because the spectral correction factor is no longer so dominant. The estimated fiber optic length for each of the baseline configurations is illustrated in Figure 48.

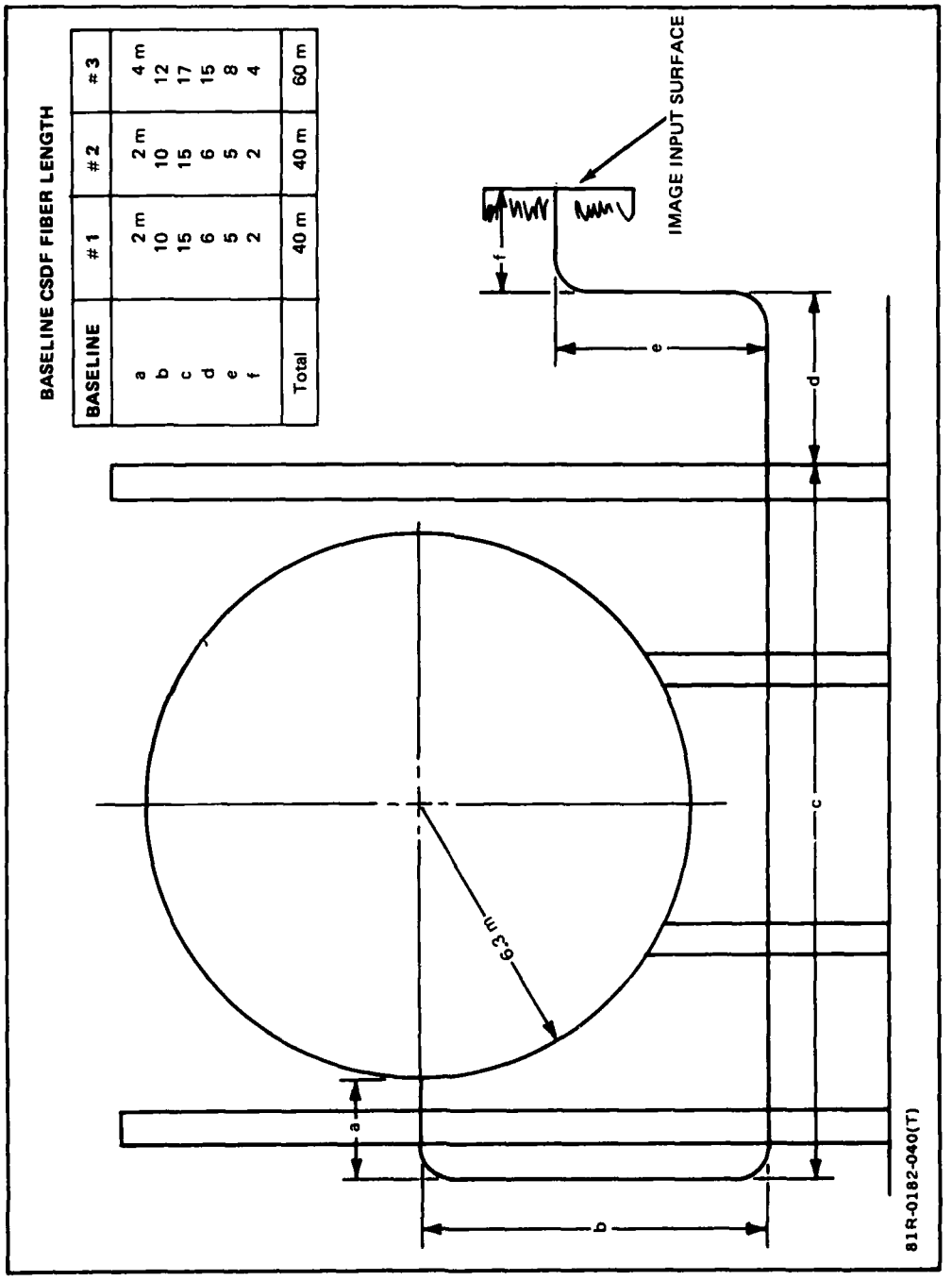

BASELINE	# 1	# 2	# 3
a	2 m	2 m	4 m
b	10	10	12
c	15	15	17
d	6	6	15
e	5	5	8
f	2	2	4
Total	40 m	40 m	60 m

Figure 48 **Estimated Fiber Optic Lengths**

ESTIMATED COST OF BASELINE SYSTEMS

The estimated cost for the three baseline systems was developed using the following groundrules:

- The fiber is drawn and assembled for seven steradians of CSDF in five years
- The cost of fiber optics is $0.10 per meter
- The cost of the building housing the CSDF, the input scene generator, and the computer control is not included.

The cost was estimated for the three baseline configurations and plotted in Figure 49.

AD-A106 117 GRUMMAN AEROSPACE CORP BETHPAGE NY F/G 13/1
STUDY OF FIBER OPTICS TO ENHANCE AN ENVIRONMENTAL LIGHTING LABO--ETC(U)
AUG 81 J CONNELLY F33615-79-C-3629
UNCLASSIFIED AFWAL-TR-81-3098 NL

2 OF 2
AD A
106117

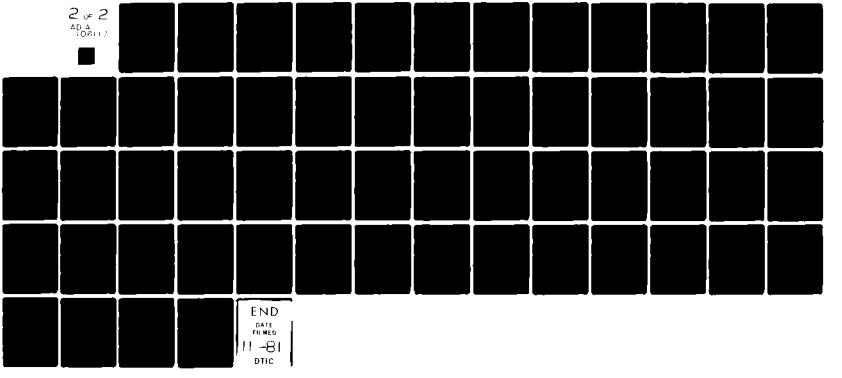

END
DATE FILMED
11-81
DTIC

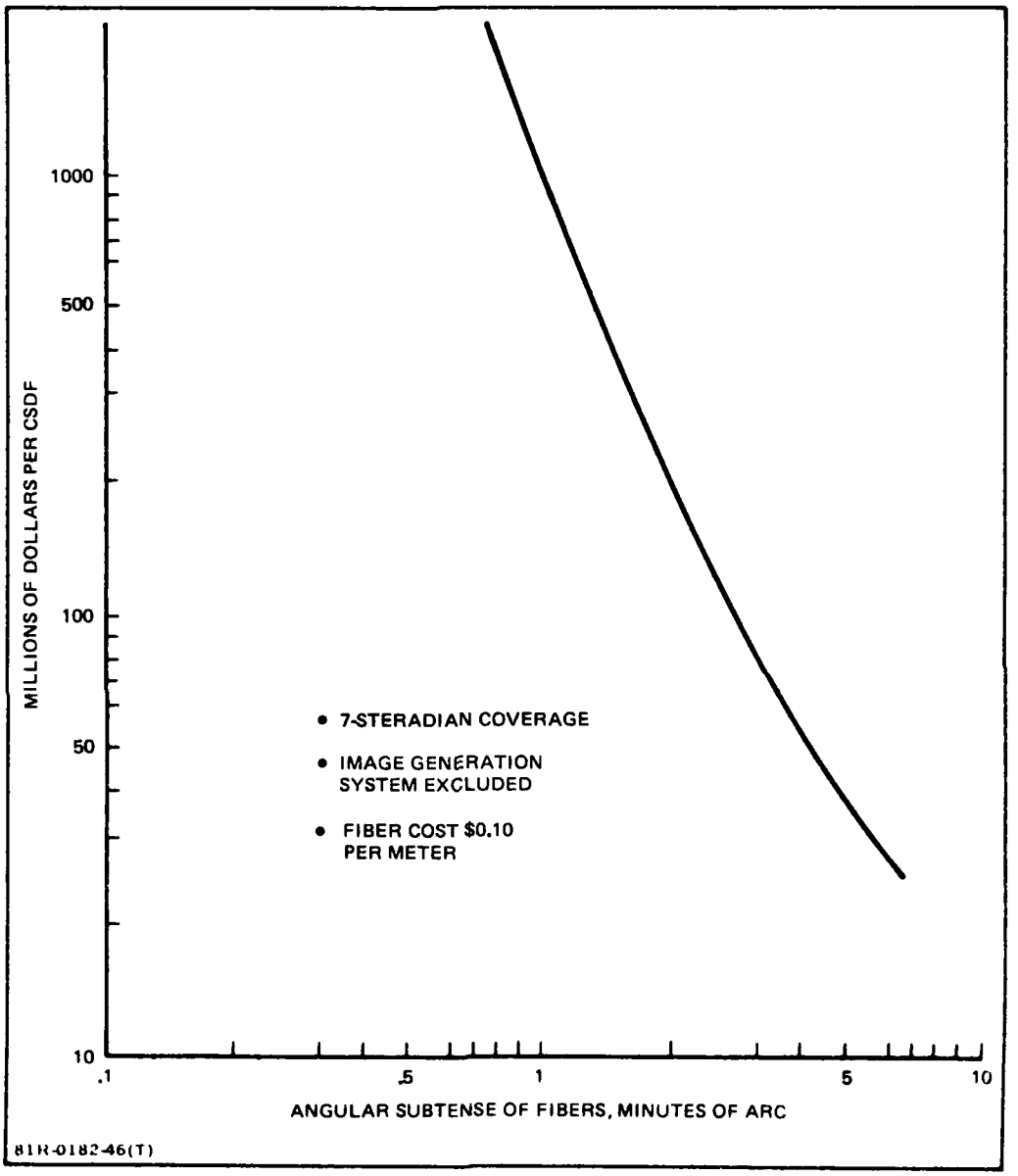

Figure 49 Estimated Cost of CSDF vs Optical Image Quality

APPENDIX A

TEST DATA

Appendix A presents the data sheets prepared by Galileo Electro-Optics and Grumman Aerospace Corporation. The description of the test setup and procedures is contained in the test plan which is reprinted in this report as Appendix C.

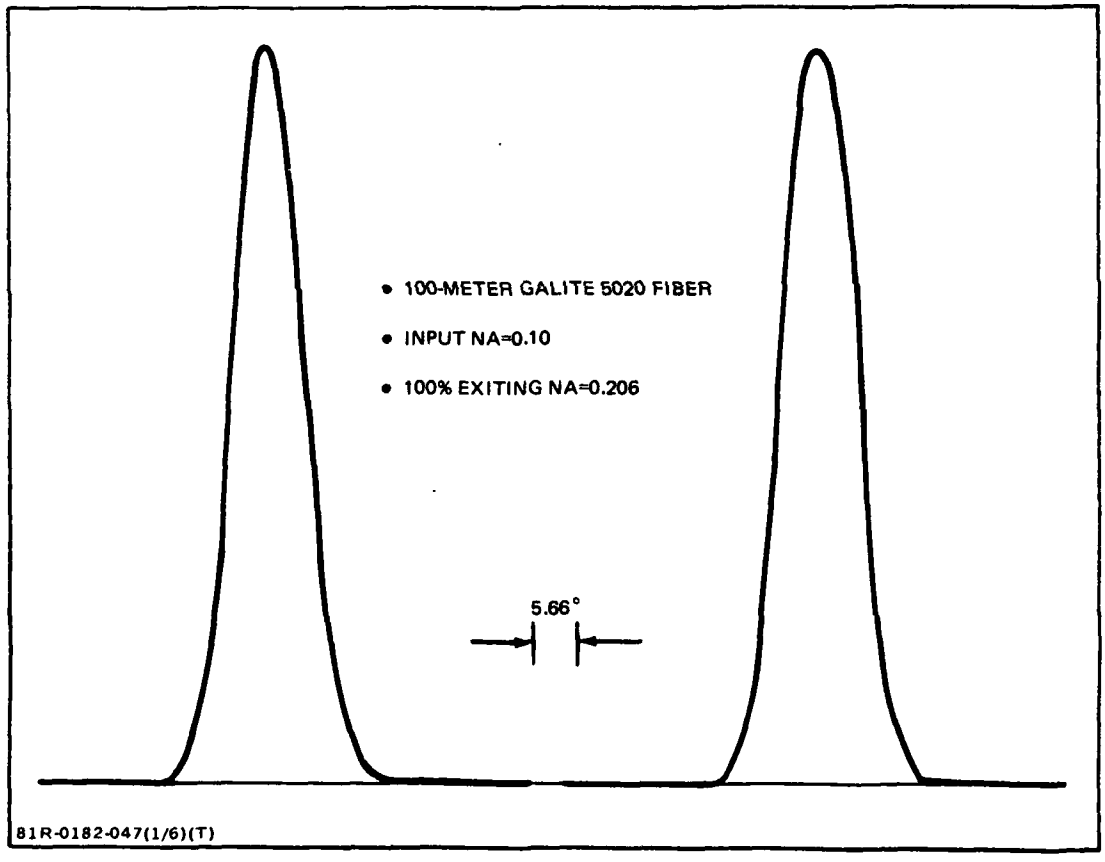

Figure A-1a Test 1, Orthogonal Output Scan, 100-m Fiber, Input NA=0.10

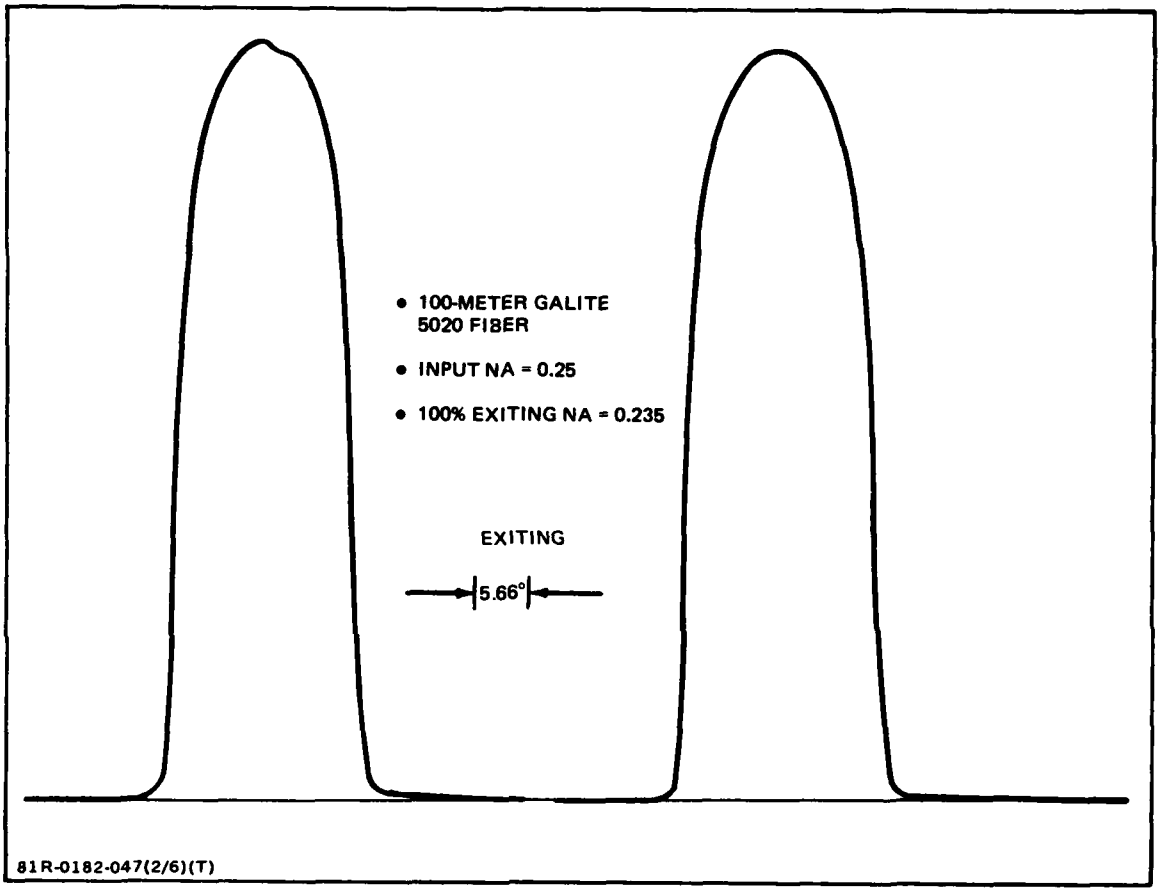

Figure A-1b Test 1, Orthogonal Output Scan, 100-m Fiber, Input NA=0.25

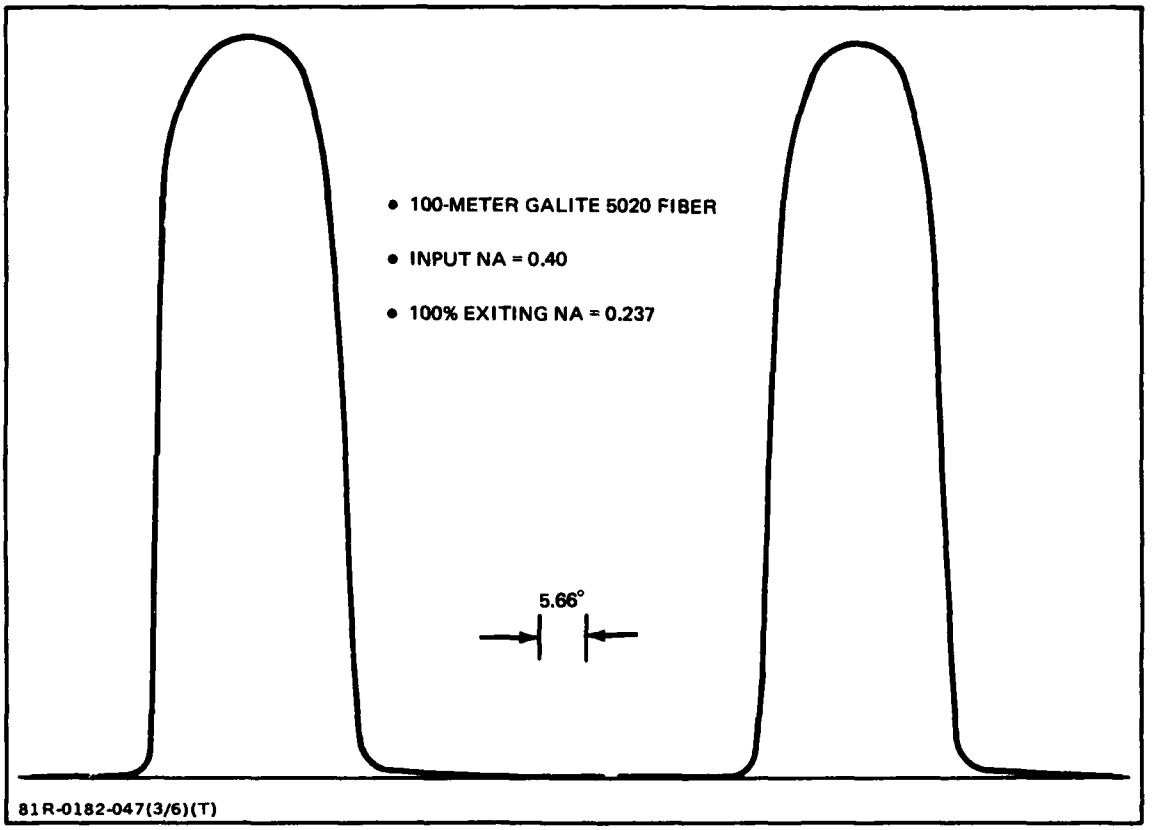

Figure A-1c Test 1, Orthogonal Output Scan, 100-m Fiber, Input NA=0.40

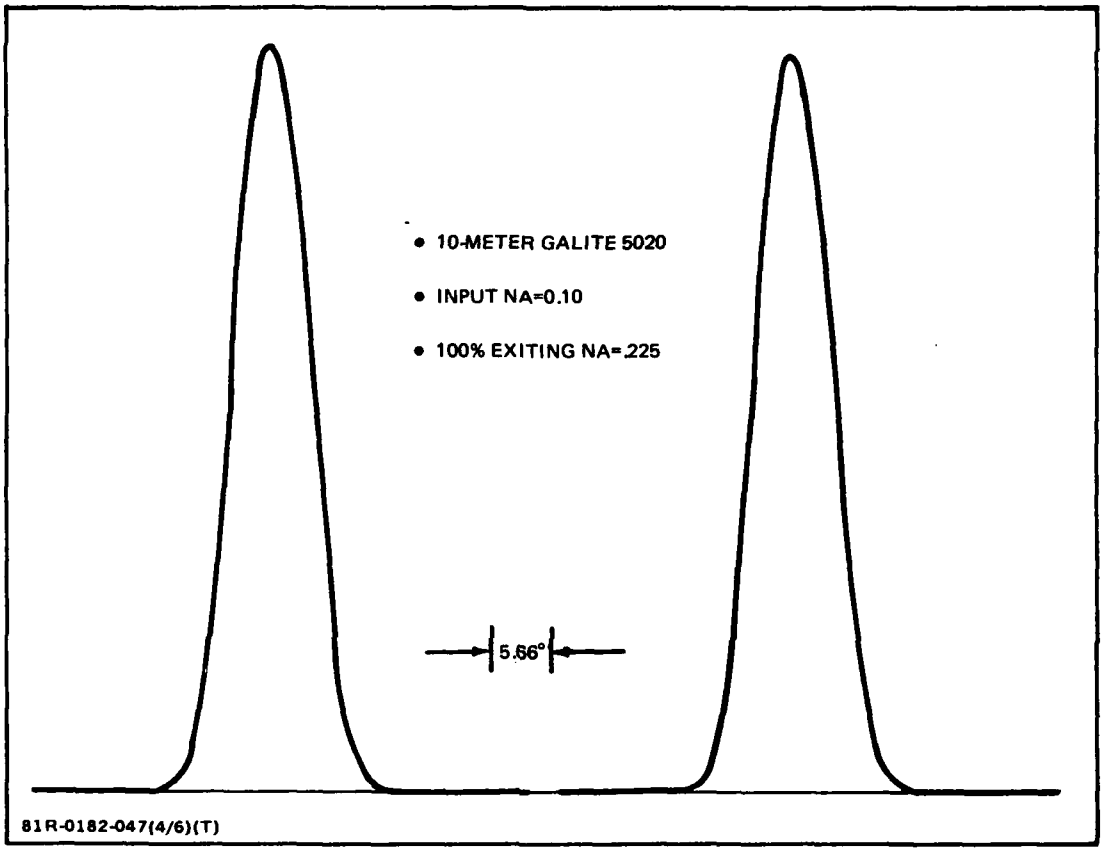

Figure A-1d Test 1, Orthogonal Output Scan, 10-m Fiber, Input NA=0.10

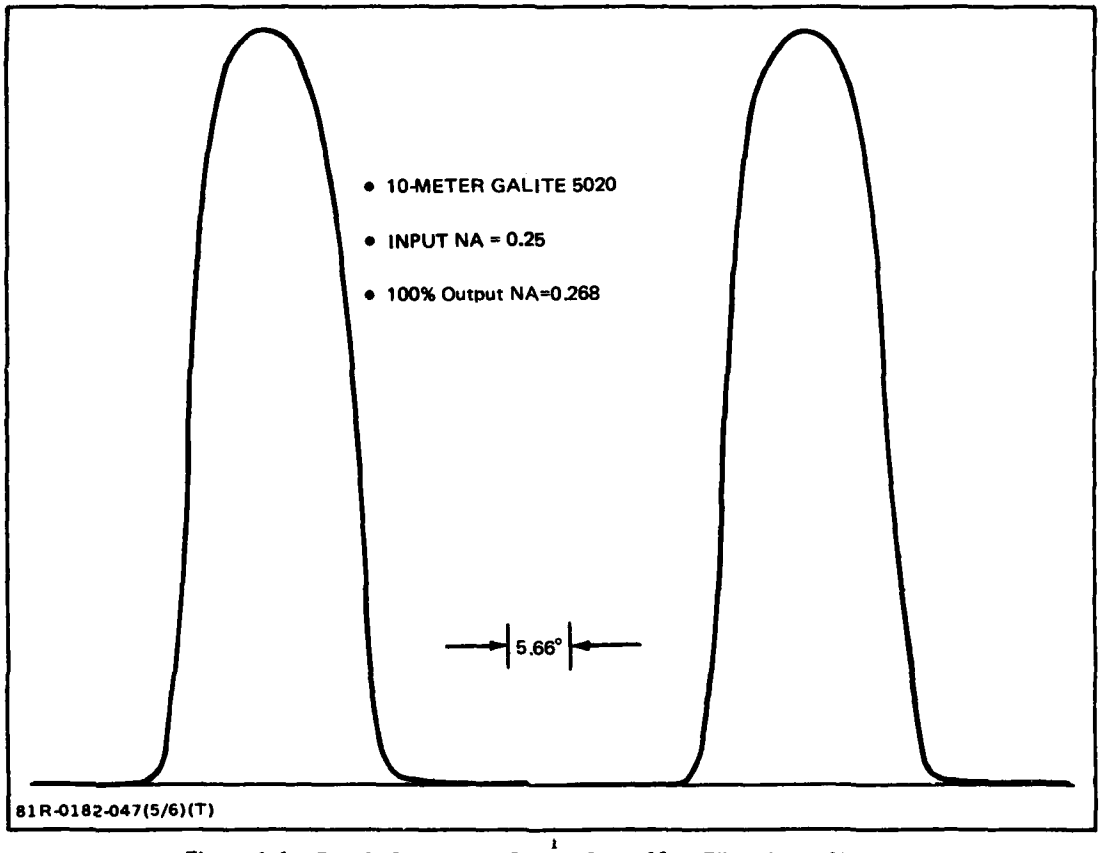

Figure A-1e Test 1, Orthogonal Output Scan, 10-m Fiber, Input NA=0.25

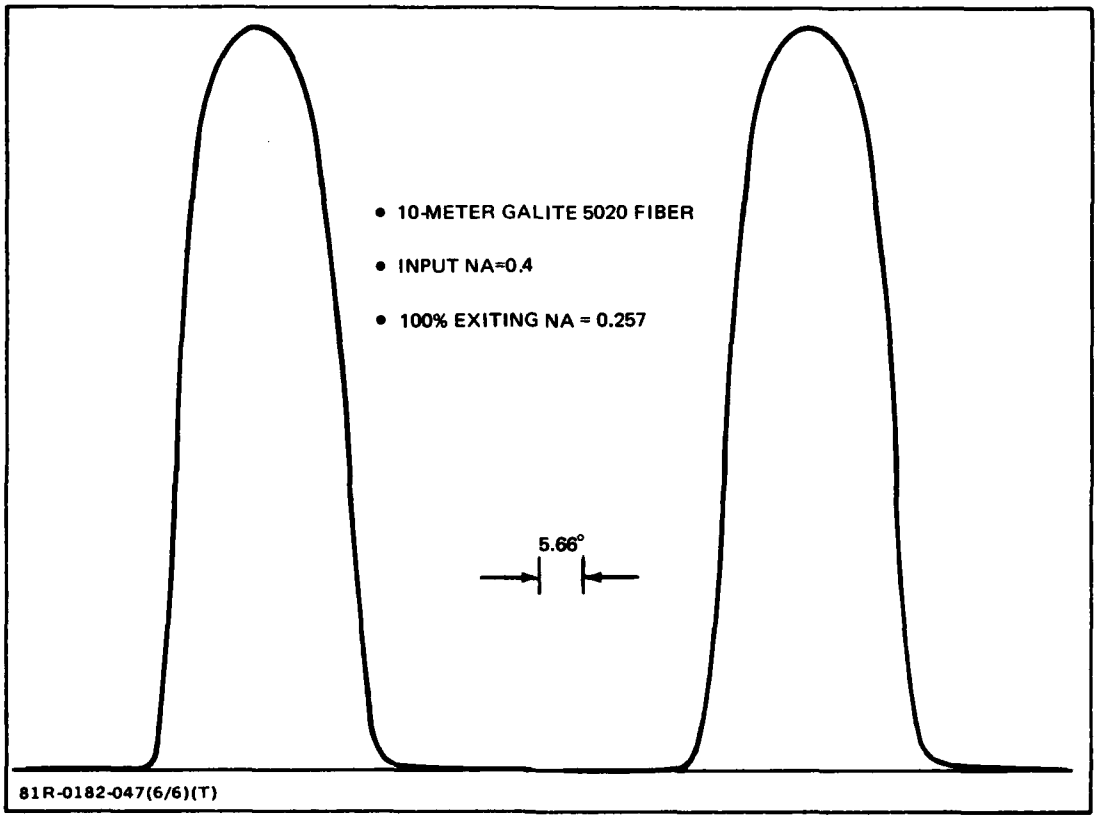

Figure A-1f Test 1, Orthogonal Output Scan, 10-m Fiber, Input NA=0.40

OPTICAL CHARACTERIZATION DATA

FIBER I.D. # 6-11-80 ABS

DRAW DATE _____

SAMPLE LENGTH (L_1) 198m

SHORT LENGTH (L_2) 2m

TEST DATE 6-24-80

TESTED BY LB

LAUNCH N.A. 0.25

FIBER GEOMETRY

c/c Ratio _____

F.O.D. _____

OVERALL O.D. _____

COATING CONCENTRICITY _____

NUMERICAL APERTURE

Type _____ 100% _____ 90% _____

Sample Length _____

Reading _____

SPECTRAL ATTENUATION

λ	SAMPLE LENGTH		SHORT LENGTH		$db/km = \frac{10 \log \frac{P_2}{P_1}}{L_1 - L_2}$
	V_1	SENSITIVITY$_1$	V_2	SENSITIVITY$_2$	
4000	–	–	–	–	–
4500	.745	2.5×10^{-6}	.620	10×10^{-5}	77.7
5000	.860	25×10^{-6}	.683	25×10^{-5}	45.9
6000	.825	250×10^{-6}	.589	100×10^{-5}	23.2
6500	.344	100×10^{-5}	.776	100×10^{-5}	18.0
7000	.317	100×10^{-5}	.611	100×10^{-5}	14.5
9000	.644	100×10^{-5}	.941	100×10^{-5}	8.4
5500	.510	25×10^{-5}	.514	100×10^{-5}	30.9

NOTE: $P_1 = (V_1)$ (SENSITIVITY$_1$), $P_2 = (V_2)$ (SENSITIVITY$_2$)

81R-0182-048(1/18)(T)

Figure A-2a Test 2, Fiber Optical Data

OPTICAL CHARACTERIZATION DATA

FIBER I.D. # 6-09-80 ABS

TEST DATE 6-24-80

DRAW DATE _____

TESTED BY LB

SAMPLE LENGTH (L_1) 200m

SHORT LENGTH (L_2) 2m

LAUNCH N.A. 0.25

FIBER GEOMETRY

c/c Ratio _____

F.O.D. _____

OVERALL O.D. _____

COATING CONCENTRICITY _____

NUMERICAL APERTURE

Type _____ 100% _____ 90% _____

Sample Length _____ _____

Reading _____

SPECTRAL ATTENUATION

λ	SAMPLE LENGTH		SHORT LENGTH		db/km = $\frac{10 \log \frac{P_2}{P_1}}{L_1 - L_2}$
	V_1	SENSITIVITY$_1$	V_2	SENSITIVITY$_2$	
4000	–	–	.789	2.5×10^{-5}	–
4500	.483	25×10^{-7}	.534	10×10^{-5}	83.1
5000	.678	250×10^{-7}	.623	25×10^{-5}	48.6
6000	.728	250×10^{-6}	.535	100×10^{-5}	23.6
6500	.312	100×10^{-5}	.700	100×10^{-5}	17.7
7000	.299	100×10^{-5}	.557	100×10^{-5}	13.6
9000	.638	100×10^{-5}	.883	100×10^{-5}	7.1
5500	.435	25×10^{-5}	.480	100×10^{-5}	32.6

NOTE: $P_1 = (V_1)$ (SENSITIVITY$_1$), $P_2 = (V_2)$(SENSITIVITY$_2$)

81R-0182-048(2/18)(T)

Figure A-2b Test 2, Fiber Optical Data

OPTICAL CHARACTERIZATION DATA

FIBER I.D. # 5-21-80 ABS

DRAW DATE

SAMPLE LENGTH (L_1) 291m

SHORT LENGTH (L_2) 2m

TEST DATE 6-17-80

TESTED BY HW

LAUNCH N.A. 0.25

FIBER GEOMETRY

c/c Ratio

F.O.D.

OVERALL O.D.

COATING CONCENTRICITY

NUMERICAL APERTURE

Type ____ 100% ____ 90% ____

Sample Length

Reading

SPECTRAL ATTENUATION

λ	SAMPLE LENGTH		SHORT LENGTH		$db/km = \frac{10 \log \frac{P_2}{P_1}}{L_1 - L_2}$
	V_1	SENSITIVITY$_1$	V_2	SENSITIVITY$_2$	
4000	–	–			
4500	.225	2.5×10^{-7}	.221	10×10^{-5}	89.8
5000	.777	25×10^{-7}	.772	10×10^{-5}	55.3
6000	.432	100×10^{-6}	.301	100×10^{-5}	29.2
6500	.888	100×10^{-6}	.405	100×10^{-5}	22.8
7000	.968	100×10^{-6}	.330	100×10^{-5}	18.4
9000	.265	100×10^{-5}	.564	100×10^{-5}	11.3
5500	.224	10×10^{-5}	.275	100×10^{-5}	37.7

NOTE: $P_1 = (V_1)$ (SENSITIVITY$_1$), $P_2 = (V_2)$ (SENSITIVITY$_2$)

81R-0182-048(3/18)(T)

Figure A-2c Test 2, Fiber Optical Data

OPTICAL CHARACTERIZATION DATA

FIBER I.D. # 5-16-80 ABS

TEST DATE 6-12-80

DRAW DATE _____

TESTED BY LB

SAMPLE LENGTH (L_1) 554m

SHORT LENGTH (L_2) 2m

LAUNCH N.A. 0.25

FIBER GEOMETRY

c/c Ratio _____

F.O.D. _____

OVERALL O.D. _____

COATING CONCENTRICITY _____

NUMERICAL APERTURE

Type _____ 100% _____ 90% _____

Sample Length _____

Reading _____

SPECTRAL ATTENUATION

λ	SAMPLE LENGTH		SHORT LENGTH		db/km = $\frac{10 \log \frac{P_2}{P_1}}{L_1 - L_2}$
	V_1	SENSITIVITY$_1$	V_2	SENSITIVITY$_2$	
4000	–	–			
4500	–	–			
5000	.587	10×10^{-7}	.608	10×10^{-5}	36.4
6000	.324	100×10^{-6}	.900	25×10^{-5}	15.2
6500	.806	100×10^{-6}	.295	100×10^{-5}	10.2
7000	.996	100×10^{-6}	.244	100×10^{-5}	7.0
9000	.308	100×10^{-5}	.413	100×10^{-5}	2.3
5500	.473	2.5×10^{-5}	.832	25×10^{-5}	22.5

NOTE: $P_1 = (V_1)$ (SENSITIVITY$_1$), $P_2 = (V_2)$ (SENSITIVITY$_2$)

81R-0182-048(4/18)

Figure A-2d Test 2, Fiber Optical Data

OPTICAL CHARACTERIZATION DATA

FIBER I.D. # 5-12-80 ABS

TEST DATE 6-25-80

DRAW DATE _____

TESTED BY LB

SAMPLE LENGTH (L_1) 236m

SHORT LENGTH (L_2) 2m

LAUNCH N.A. 0.25

FIBER GEOMETRY

c/c Ratio _____

F.O.D. _____

OVERALL O.D. _____

COATING CONCENTRICITY _____

NUMERICAL APERTURE

Type _____ 100% _____ 90% _____

Sample Length _____

Reading _____

SPECTRAL ATTENUATION

λ	SAMPLE LENGTH V_1	SAMPLE LENGTH SENSITIVITY$_1$	SHORT LENGTH V_2	SHORT LENGTH SENSITIVITY$_2$	db/km = $\frac{10 \log \frac{P_2}{P_1}}{L_1 - L_2}$
4000	–	–			
4500	.333	2.5×10^{-6}	.443	10×10^{-5}	73.8
5000	.549	25×10^{-6}	.498	25×10^{-5}	40.9
6000	.662	250×10^{-6}	.439	100×00^{-5}	18.1
6500	.289	100×10^{-5}	.584	100×10^{-5}	13.0
7000	.276	100×10^{-5}	.462	100×10^{-5}	9.6
9000	.592	100×10^{-5}	.726	100×10^{-5}	3.8
5500	.385	25×10^{-5}	.387	100×10^{-5}	25.8

NOTE: $P_1 = (V_1)$ (SENSITIVITY$_1$), $P_2 = (V_2)$ (SENSITIVITY$_2$)

81R-0182-048(5/18)(T)

Figure A-2e Test 2, Fiber Optical Data

OPTICAL CHARACTERIZATION DATA

FIBER I.D. # 5-07-80 ABS

TEST DATE 6-24-80

DRAW DATE _____

TESTED BY HW

SAMPLE LENGTH (L_1) 496m

SHORT LENGTH (L_2) 2m

LAUNCH N.A. 0.25

FIBER GEOMETRY

c/c Ratio _____

F.O.D. _____

OVERALL O.D. _____

COATING CONCENTRICITY _____

NUMERICAL APERTURE

Type _____ 100% _____ 90% _____

Sample Length _____

Reading _____

SPECTRAL ATTENUATION

	SAMPLE LENGTH		SHORT LENGTH		
λ	V_1	SENSITIVITY$_1$	V_2	SENSITIVITY$_2$	db/km = $\frac{10 \log \frac{P_2}{P_1}}{L_1 - L_2}$
4000	–		–		
4500	–		–		
5000	.156	1×10^{-5}	.527	25×10^{-5}	39.0
6000	.619	10×10^{-5}	.447	100×10^{-5}	17.4
6500	.569	25×10^{-5}	.590	100×10^{-5}	12.5
7000	.639	25×10^{-5}	.461	100×10^{-5}	9.3
9000	.449	100×10^{-5}	.729	100×10^{-5}	4.3
5500	.262	10×10^{-5}	.410	100×10^{-5}	24.2

NOTE: $P_1 = (V_1)$ (SENSITIVITY$_1$), $P_2 = (V_2)$ (SENSITIVITY$_2$)

81R-0182-048(6/18)(T)

Figure A-2f Test 2, Fiber Optical Data

OPTICAL CHARACTERIZATION DATA

FIBER I.D. # 5-02-80 ABS

TEST DATE 6-12-80

DRAW DATE

TESTED BY LB

SAMPLE LENGTH (L_1) 216m

SHORT LENGTH (L_2) 2m

LAUNCH N.A. 0.25

FIBER GEOMETRY

c/c Ratio

F.O.D.

OVERALL O.D.

COATING CONCENTRICITY

NUMERICAL APERTURE

Type ____ 100% ____ 90% ____

Sample Length

Reading

SPECTRAL ATTENUATION

λ	SAMPLE LENGTH V_1	SAMPLE LENGTH SENSITIVITY$_1$	SHORT LENGTH V_2	SHORT LENGTH SENSITIVITY$_2$	db/km = $\frac{10 \log \frac{P_2}{P_1}}{L_1 - L_2}$
4000	.016	1×10^{-6}	.491	25×10^{-6}	134.8
4500	.443	1×10^{-6}	.339	100×10^{-6}	88.2
5000	.800	1×10^{-5}	.999	100×10^{-6}	50.8
6000	.401	25×10^{-5}	.357	100×10^{-5}	25.8
6500	.700	25×10^{-5}	.463	100×10^{-5}	19.7
7000	.695	25×10^{-5}	.377	100×10^{-5}	15.7
9000	.405	100×10^{-5}	.633	100×10^{-5}	9.1
5500	.580	10×10^{-5}	.316	100×10^{-5}	34.4

NOTE: $P_1 = (V_1)$ (SENSITIVITY$_1$), $P_2 = (V_2)$ (SENSITIVITY$_2$)

81R-0182-048(7/18)(T)

Figure A-2g Test 2, Fiber Optical Data

OPTICAL CHARACTERIZATION DATA

FIBER I.D. # 4-30-80 ABS

TEST DATE 6-17-80

DRAW DATE

TESTED BY HW

SAMPLE LENGTH (L_1) 919m

SHORT LENGTH (L_2) 2m

LAUNCH N.A. 0.25

FIBER GEOMETRY

c/c Ratio

F.O.D.

OVERALL O.D.

COATING CONCENTRICITY

NUMERICAL APERTURE

Type 100% 90%

Sample Length

Reading

SPECTRAL ATTENUATION

λ	SAMPLE LENGTH		SHORT LENGTH		db/km = $\frac{10 \log \frac{P_2}{P_1}}{L_1 - L_2}$
	V_1	SENSITIVITY$_1$	V_2	SENSITIVITY$_2$	
4000	–	–			
4500	–	–			
5000	.219	2.5×10^{-7}	.343	250×10^{-6}	34.8
6000	.328	100×10^{-7}	.325	100×10^{-5}	21.8
6500	.577	250×10^{-7}	.437	100×10^{-5}	16.1
7000	.255	100×10^{-6}	.359	100×10^{-5}	12.5
9000	.601	250×10^{-6}	.606	100×10^{-5}	6.6
5500	.996	1×10^{-6}	.282	100×10^{-5}	26.7

NOTE: $P_1 = (V_1)$ (SENSITIVITY$_1$), $P_2 = (V_2)$ (SENSITIVITY$_2$)

81R-0182-048(8/18)(T)

Figure A-2h Test 2, Fiber Optical Data

OPTICAL CHARACTERIZATION DATA

FIBER I.D. # 4-09-80 ABS — TEST DATE 5-13-80

DRAW DATE _____ — TESTED BY LB

SAMPLE LENGTH (L_1) 80m

SHORT LENGTH (L_2) 2m — LAUNCH N.A. 0.25

FIBER GEOMETRY

c/c Ratio _____

F.O.D. _____

OVERALL O.D. _____

COATING CONCENTRICITY _____

NUMERICAL APERTURE

Type _____ 100% _____ 90% _____

Sample Length _____

Reading _____

SPECTRAL ATTENUATION

λ	SAMPLE LENGTH V_1	SAMPLE LENGTH SENSITIVITY$_1$	SHORT LENGTH V_2	SHORT LENGTH SENSITIVITY$_2$	db/km = $\frac{10 \log \frac{P_2}{P_1}}{L_1 - L_2}$
4000	.129	1×10^{-5}	.150	10×10^{-5}	136.6
4500	.424	2.5×10^{-5}	.420	10×10^{-5}	76.6
5000	.557	10×10^{-5}	.508	25×10^{-5}	45.9
6000	.291	100×10^{-5}	.445	100×10^{-5}	23.6
6500	.412	100×10^{-5}	.574	100×10^{-5}	18.5
7000	.352	100×10^{-5}	.464	100×10^{-5}	15.4
9000	.614	100×10^{-5}	.732	100×10^{-5}	9.8
5500	.234	100×10^{-5}	.409	100×10^{-5}	31.1

NOTE: $P_1 = (V_1)$ (SENSITIVITY$_1$), $P_2 = (V_2)$ (SENSITIVITY$_2$)

81R-0182-048(9/18)(T)

Figure A-2i Test 2, Fiber Optical Data

OPTICAL CHARACTERIZATION DATA

FIBER I.D. # 4-03-80 ABS

TEST DATE 5-13-80

DRAW DATE

TESTED BY LD

SAMPLE LENGTH (L_1) 195m

SHORT LENGTH (L_2) 2.0m

LAUNCH N.A. 0.25

FIBER GEOMETRY

c/c Ratio

F.O.D.

OVERALL O.D.

COATING CONCENTRICITY

NUMERICAL APERTURE

Type ____ 100% ____ 90% ____

Sample Length

Reading

SPECTRAL ATTENUATION

λ	SAMPLE LENGTH V_1	SAMPLE LENGTH SENSITIVITY$_1$	SHORT LENGTH V_2	SHORT LENGTH SENSITIVITY$_2$	db/km = $\frac{10 \log \frac{P_2}{P_1}}{L_1 - L_2}$
4000	.120	1×10^{-6}	.119	10×10^{-5}	103.4
4500	.834	1×10^{-6}	.331	10×10^{-5}	82.8
5000	.505	25×10^{-6}	.966	10×10^{-5}	45.7
5500	.515	250×10^{-6}	.332	100×10^{-5}	21.3
6000	.849	250×10^{-6}	.429	100×10^{-5}	15.8
7000	.801	250×10^{-6}	.344	100×10^{-5}	12.1
9000					6.0

NOTE: $P_1 = (V_1)$ (SENSITIVITY$_1$), $P_2 = (V_2)$ (SENSITIVITY$_2$)

81R-0182-048(10/18)(T)

Figure A-2j Test 2, Fiber Optical Data

OPTICAL CHARACTERIZATION DATA

FIBER I.D. # 3-31-80 ABS

DRAW DATE

SAMPLE LENGTH (L_1) 173m

SHORT LENGTH (L_2) 2m

TEST DATE 5-13-80

TESTED BY HH

LAUNCH N.A. 0.25

FIBER GEOMETRY

c/c Ratio

F.O.D.

OVERALL O.D.

COATING CONCENTRICITY

NUMERICAL APERTURE

Type ____ 100% ____ 90% ____

Sample Length

Reading

SPECTRAL ATTENUATION

λ	SAMPLE LENGTH V_1	SAMPLE LENGTH SENSITIVITY$_1$	SHORT LENGTH V_2	SHORT LENGTH SENSITIVITY$_2$	db/km = $\frac{10 \log \frac{P_2}{P_1}}{L_1 - L_2}$
4000	.190	1×10^{-6}	.106	10×10^{-5}	102.
4500	.482	2.5×10^{-6}	.150	25×10^{-5}	87.3
5000	.703	25×10^{-6}	.119	100×10^{-5}	48.6
6000	.700	250×10^{-6}	.410	100×10^{-5}	21.6
6500	.281	100×10^{-5}	.541	100×10^{-5}	16.6
7000	.256	100×10^{-5}	.438	100×10^{-5}	13.6

NOTE: $P_1 = (V_1)$ (SENSITIVITY$_1$), $P_2 = (V_2)$ (SENSITIVITY$_2$)

81R-0182-048(11/18)(T)

Figure A-2k Test 2, Fiber Optical Data

OPTICAL CHARACTERIZATION DATA

FIBER I.D. # 3-31-80 ABS

DRAW DATE

SAMPLE LENGTH (L_1) 171m

SHORT LENGTH (L_2) 2m

TEST DATE 5-13-80

TESTED BY LB

LAUNCH N.A. 0.25

FIBER GEOMETRY

c/c Ratio

F.O.D.

OVERALL O.D.

COATING CONCENTRICITY

NUMERICAL APERTURE

Type ____ 100% ____ 90% ____

Sample Length

Reading

SPECTRAL ATTENUATION

λ	SAMPLE LENGTH V_1	SAMPLE LENGTH SENSITIVITY$_1$	SHORT LENGTH V_2	SHORT LENGTH SENSITIVITY$_2$	db/km = $\frac{10 \log \frac{P_2}{P_1}}{L_1 - L_2}$
4000	.140	1×10^{-6}	.483	25×10^{-6}	114.5
4500	.981	1×10^{-6}	.328	100×10^{-6}	90.2
5000	.553	25×10^{-6}	.994	100×10^{-6}	50.7
6000	.565	250×10^{-6}	.356	100×10^{-5}	23.7
6500	.945	250×10^{-6}	.483	100×10^{-5}	18.4
7000	.912	250×10^{-6}	.402	100×10^{-5}	14.6
9000					6.0

NOTE: $P_1 = (V_1)$ (SENSITIVITY$_1$), $P_2 = (V_2)$ (SENSITIVITY$_2$)

81R-0182-048(12/18)(T)

Figure A-2l Test 2, Fiber Optical Data

OPTICAL CHARACTERIZATION DATA

FIBER I.D. # 3-31-80 ABS

TEST DATE 5-13-80

DRAW DATE

TESTED BY LB

SAMPLE LENGTH (L_1) 43m

SHORT LENGTH (L_2) 2m

LAUNCH N.A. 0.25

FIBER GEOMETRY

c/c Ratio

F.O.D.

OVERALL O.D.

COATING CONCENTRICITY

NUMERICAL APERTURE

Type ___ 100% ___ 90% ___

Sample Length

Reading

SPECTRAL ATTENUATION

λ	SAMPLE LENGTH		SHORT LENGTH		$db/km = \frac{10 \log \frac{P_2}{P_1}}{L_1 - L_2}$
	V_1	SENSITIVITY$_1$	V_2	SENSITIVITY$_2$	
4000	.383	10×10^{-6}	.156	10×10^{-5}	148.7
4500	.200	100×10^{-6}	.415	10×10^{-5}	77.3
5000	.324	250×10^{-6}	.499	25×10^{-5}	45.7
6000	.343	100×10^{-5}	.446	100×10^{-5}	27.8
6500	.404	100×10^{-5}	.579	100×10^{-5}	23.5
7000	.380	100×10^{-5}	.465	100×10^{-5}	21.4

NOTE: $P_1 = (V_1)$ (SENSITIVITY$_1$), $P_2 = (V_2)$ (SENSITIVITY$_2$)

81R-0182-048(13/18)(T)

Figure A-2m Test 2, Fiber Optical Data

OPTICAL CHARACTERIZATION DATA

FIBER I.D. # 1-16-80 ABS

DRAW DATE

SAMPLE LENGTH (L_1) 238m

SHORT LENGTH (L_2) 2m

TEST DATE 5-13-80

TESTED BY LB

LAUNCH N.A. 0.25

FIBER GEOMETRY

c/c Ratio

F.O.D.

OVERALL O.D.

COATING CONCENTRICITY

NUMERICAL APERTURE

Type ____ 100% ____ 90% ____

Sample Length

Reading

SPECTRAL ATTENUATION

λ	SAMPLE LENGTH V_1	SAMPLE LENGTH SENSITIVITY$_1$	SHORT LENGTH V_2	SHORT LENGTH SENSITIVITY$_2$	db/km = $\frac{10 \log \frac{P_2}{P_1}}{L_1 \cdot L_2}$
4000	.095	1×10^{-6}	.156	10×10^{-5}	93.9
4500	.302	1×10^{-6}	.402	10×10^{-5}	90.0
5000	.797	10×10^{-6}	.505	25×10^{-5}	50.8
6000	.489	250×10^{-6}	.438	100×10^{-5}	23.5
6500	.887	250×10^{-6}	.559	100×10^{-5}	17.0
7000	.885	250×10^{-6}	.446	100×10^{-5}	12.9
9000	.196	250×10^{-5}	.296	250×10^{-5}	7.6
5500	.263	25×10^{-5}	.393	100×10^{-5}	32.9

NOTE: $P_1 = (V_1)$ (SENSITIVITY$_1$), $P_2 = (V_2)$ (SENSITIVITY$_2$)

81R-0182-048(14/18)(T)

Figure A-2n Test 2, Fiber Optical Data

OPTICAL CHARACTERIZATION DATA

FIBER I.D. # 1-10-80 ABS

DRAW DATE _____

SAMPLE LENGTH (L_1) 150m

SHORT LENGTH (L_2) 2m

TEST DATE 5-13-80

TESTED BY LB

LAUNCH N.A. 0.25

FIBER GEOMETRY

c/c Ratio _____

F.O.D. _____

OVERALL O.D. _____

COATING CONCENTRICITY _____

NUMERICAL APERTURE

Type _____ 100% _____ 90% _____

Sample Length _____

Reading _____

SPECTRAL ATTENUATION

λ	SAMPLE LENGTH V_1	SAMPLE LENGTH SENSITIVITY$_1$	SHORT LENGTH V_2	SHORT LENGTH SENSITIVITY$_2$	$db/km = \frac{10 \log \frac{P_2}{P_1}}{L_1 - L_2}$
4000	.167	1×10^{-6}	.536	2.5×10^{-5}	128.7
4500	.300	10×10^{-6}	.356	10×10^{-5}	72.6
5000	.279	100×10^{-6}	.444	25×10^{-5}	40.5
6000	.813	250×10^{-6}	.392	100×10^{-5}	19.2
6500	.121	250×10^{-5}	.503	100×10^{-5}	14.9
7000	.108	250×10^{-5}	.403	100×10^{-5}	11.7
9000	.204	250×10^{-5}	.658	100×10^{-5}	7.5
5500	.144	100×10^{-5}	.353	100×10^{-5}	26.3

NOTE: $P_1 = (V_1)(\text{SENSITIVITY}_1)$, $P_2 = (V_2)(\text{SENSITIVITY}_2)$

81R-0182-048(15/18)(T)

Figure A-2o Test 2, Fiber Optical Data

OPTICAL CHARACTERIZATION DATA

FIBER I.D. # 11-29-79 ABS

TEST DATE 5-13-80

DRAW DATE _____

TESTED BY LB

SAMPLE LENGTH (L_1) 210m

SHORT LENGTH (L_2) 2m

LAUNCH N.A. 0.25

FIBER GEOMETRY

c/c Ratio _____

F.O.D. _____

OVERALL O.D. _____

COATING CONCENTRICITY _____

NUMERICAL APERTURE

Type _____ 100% _____ 90% _____

Sample Length _____

Reading _____

SPECTRAL ATTENUATION

λ	SAMPLE LENGTH		SHORT LENGTH		$\text{db/km} = \frac{10 \log \frac{P_2}{P_1}}{L_1 - L_2}$
	V_1	SENSITIVITY_1	V_2	SENSITIVITY_2	
4000	.179	1×10^{-6}	.167	10×10^{-5}	94.7
4500	.516	1×10^{-6}	.451	10×10^{-5}	93.3
5000	.402	25×10^{-6}	.524	25×10^{-5}	54.0
6000	.564	250×10^{-6}	.461	100×10^{-5}	24.7
6500	.255	100×10^{-5}	.592	100×10^{-5}	17.6
7000	.261	100×10^{-5}	.478	100×10^{-5}	12.6
9000	.559	100×10^{-5}	.761	100×10^{-5}	6.4

NOTE: $P_1 = (V_1)$ (SENSITIVITY_1), $P_2 = (V_2)$ (SENSITIVITY_2)

81R-0182-048(16/18)(T)

Figure A-2p Test 2, Fiber Optical Data

OPTICAL CHARACTERIZATION DATA

FIBER I.D. # 11-27-79 ABS

DRAW DATE

SAMPLE LENGTH (L_1) 200m

SHORT LENGTH (L_2) 2m

TEST DATE 5-13-80

TESTED BY LB

LAUNCH N.A. 0.25

FIBER GEOMETRY

c/c Ratio

F.O.D.

OVERALL O.D.

COATING CONCENTRICITY

NUMERICAL APERTURE

Type ____ 100% ____ 90% ____

Sample Length

Reading

SPECTRAL ATTENUATION

λ	SAMPLE LENGTH V_1	SAMPLE LENGTH SENSITIVITY$_1$	SHORT LENGTH V_2	SHORT LENGTH SENSITIVITY$_2$	db/km = $\frac{10 \log \frac{P_2}{P_1}}{L_1 - L_2}$
4000	.129	1×10^{-6}	.139	10×10^{-5}	102.6
4500	.504		.370		94.2
5000	.954	10×10^{-6}	.455	25×10^{-5}	54.4
6000	.478	250×10^{-6}	.280	100×10^{-5}	18.7
6050	.821	$250 + 10^{-6}$	.359	100×10^{-5}	12.3
7000	.799	250×10^{-6}	.289		8.1
9000	.166	250×10^{-5}	.263	250×10^{-5}	10.1
5500	.278	25×10^{-5}	.143	250×10^{-5}	35.9

NOTE: $P_1 = (V_1)$ (SENSITIVITY$_1$), $P_2 = (V_2)$ (SENSITIVITY$_2$)

81R-0182-048(17/18)(T)

Figure A-2q Test 2, Fiber Optical Data

OPTICAL CHARACTERIZATION DATA

FIBER I.D. # 9-27-79 ABS

DRAW DATE

SAMPLE LENGTH (L_1) 190m

SHORT LENGTH (L_2) 2m

TEST DATE 5-13-80

TESTED BY LB

LAUNCH N.A. 0.25

FIBER GEOMETRY

c/c Ratio

F.O.D.

OVERALL O.D.

COATING CONCENTRICITY

NUMERICAL APERTURE

Type ____ 100% ____ 90% ____

Sample Length

Reading

SPECTRAL ATTENUATION

λ	SAMPLE LENGTH V_1	SAMPLE LENGTH SENSITIVITY$_1$	SHORT LENGTH V_2	SHORT LENGTH SENSITIVITY$_2$	db/km = $\frac{10 \log \frac{P_2}{P_1}}{L_1 - L_2}$
4000	.113	1×10^{-6}	.767	10×10^{-6}	97.4
4500	.447	2.5×10^{-6}	.913	2.5×10^{-6}	69.7
5000	.454	2.5×10^{-6}	.648	100×10^{-6}	40.2
6000	.942	100×10^{-6}	.926	250×10^{-6}	20.8
6500	.577	250×10^{-6}	.121	250×10^{-5}	17.1
7000	.561		.102	250×10^{-5}	13.8
9000	.112	250×10^{-5}	.163	250×10^{-5}	8.7
5500	.254	25×10^{-5}	.217	100×10^{-5}	28.3

NOTE: $P_1 = (V_1)$ (SENSITIVITY$_1$), $P_2 = (V_2)$ (SENSITIVITY$_2$)

81R-0182-48(18/18)(T)

Figure A-2r Test 2, Fiber Optical Data

ANGULAR ORIENTATION	DISTANCE, DIFFUSE APERTURE TO INPUT FACE								
	10 cm	14 cm	17.8 cm	22.9 cm	28 cm	35.6 cm	40.6 cm	45.7 cm	50.8 cm
−30°						.000028	.000027	.000023	.000024
−25°	.025	.023	.017	.000094	.000083	.000041	.000037	.000031	.000031
−20°	.063	.063	.059	.038	.023	.000077	.000062	.00005	.000048
−15°	.56	.488	.541	.581	.491	.079	.029	.00016	.00013
−10°	.933	.936	.924	.973	.903	.761	.585	.351	.236
− 5°	.984	.993	.981	.994	.983	.975	.966	.949	.899
0°	1	1	1	1	1	1	1	1	1
+ 5°	.969	.969	.954	.99	.929	.983	.966	.96	.901
+10°	.873	.884	.861	.871	.710	.815	.540	.403	.207
+15°	.121	.137	.118	.084	.046	.102	.025	.024	.00012
+20°	.034	.035	.025	.00013	.000092	.000085	.000057	.000054	.000045
+25°						.000043	.000037	.000035	.000031
+30°						.00003	.000027	.000023	.000025
INPUT NA 81R0182-049(T)	.58	.46	.38	.30	.25	.20	.18	.16	.14

Figure A-3a Test 3, Exit Flux Distribution vs Input Numerical Aperture

ANGULAR ORIENTATION	TEST LOCATION								
	UPPER LEFT	LOWER LEFT	CENTER LEFT	TOP CENTER	CENTER CENTER	LOWER CENTER	LOWER RIGHT	CENTER RIGHT	TOP RIGHT
−30°	.000027	.000026	.000028	.000030	.000024	.000024	.000025	.000028	.000021
−25°	.000043	.000035	.000042	.000044	.000034	.000027	.000035	.000032	.000029
−20°	.000080	.000064	.000073	.000069	.000054	.000040	.000058	.000045	.000480
−15°	.00043	.00018	.00031	.00025	.00014	.00012	.00024	.00018	.00041
−10°	.418	.405	.364	.402	.414	.312	.387	.441	.399
− 5°	.849	.917	.861	.925	.935	.824	.810	.907	.811
0°	1	1	1	1	1	1	1	1	1
+ 5°	.959	.996	.908	1.008	1	1.001	.958	.928	.920
+10°	.573	.629	.681	.613	.694	.688	.524	.526	.561
+15°	.00099	.00100	.00092	.0012	.072	.177	.177	.00065	.0013
+20°	.00014	.00007	.00010	.000083	.000087	.000016	.000071	.000067	.000069
+25°	.000076	.000039	.000051	.000040	.000046	.000079	.000036	.00004	.00004
+30°	.000047	.000027	.000034	.000029	.000032	.000035	.000027	.000027	.000032

NOTE: MEASURED FROM 24 CHANNELS
81R-082-050(T)

Figure A-3b Test 3, Luminance Uniformity Read Directly from Face of Test Specimen

ANGULAR ORIENTATION	SCREEN-TO-OUTPUT BLOCK DISTANCE	
	3.18 mm SEPARATION	6.35 mm SEPARATION
−30°	.640	.670
−25°	.719	.725
−20°	.777	.798
−15°	.877	.893
−10°	.928	.969
− 5°	.956	1.00
0°	.950	.958
+ 5°	1.00	.906
+10°	.945	.884
+15°	.900	.855
+20°	.858	.811
+25°	.792	.765
+30°	.723	.691
81R-0182-051(T)		

Figure A-3c Test 3, Luminance Uniformity Read Directly from Translucent Screen

TEST = 4A

DATE: Sept. 24, 1980

1. Size of solar disk on Lambertian Surface Diam. 1 inch
2. Intensity on the Lambertian Surface 38000 FL homogeneous input measured from $MgCo_3$ surface
3. Intensity over the projected pattern.

POSITION ON THE PATTERN	INTENSITY F.L. HORIZONTAL	INTENSITY F.L. VERTICAL	AT 1.50 METER BLOCK (OUTPUT) TO SCREEN DISTANCE
	LEFT	TOP	
1. 10 cm	.205	.218	*Readings are from Lambertian surface that was moved across the screen*
2. 20 cm	.785	.724	
3. 30 cm	1.62	1.67	
4. 40 cm	2.50	2.25	
5. 50 cm	2.57	2.25	
6. 60 cm	1.95	1.44	
7. 70 cm	.776	.689	
8. 80 cm	.21	.18	
	RIGHT	BOTTOM	

4. Intensity on the Lambertian Surface at the screen position. F.L. See above
5. Intensity of same location on the screen. F.L. .98 FL at position 5

81R-0182-052(1/5)(T)

Figure A-4a Test 4A, Solar Simulation Capability

TEST = 4B DATE:

1. Size of solar disk on Lambertian Surface Diam. 1 inch
2. Intensity on the Lambertian Surface 50K to 100K F.L. at center
3. Intensity over the projected pattern. _____

POSITION ON THE PATTERN	INTENSITY F.L. HORIZONTAL	INTENSITY F.L. VERTICAL	
	LEFT	TOP	
1. 10 cm	.251	.605	Readings off the screen 1.5 meters from the output surface
2. 20 cm	.87	1.29	
3. 30 cm	1.36	1.76	
4. 40 cm	1.73	1.84	
5. 50 cm	1.85	1.81	
6. 60 cm	1.82	1.61	
7. 70 cm	1.54	1.15	
8. 80 cm	.901	.46	
90 cm	.225		
	RIGHT	BOTTOM	

4. Intensity on the Lambertian Surface at the screen position. F.L. 3.78 at point 5
5. Intensity of same location on the screen. F.L. 1.81

81R-0182-052(2/5)(T)

Figure A-4b Test 4B, Solar Simulation Capability

TEST = 4C DATE:

1. Size of solar disk on Lambertian Surface Diam. 1" no aperture.
2. Intensity on the Lambertian Surface 50K to 100K F.L.
3. Intensity over the projected pattern. _____

POSITION ON THE PATTERN	INTENSITY F.L. HORIZONTAL	INTENSITY F.L. VERTICAL	AT ONE METER
	LEFT	TOP	
1. 10 cm	.251	.306	With Projection Screen at one meter and translucent wall 1/4 inch
2. 20 cm	.367	.442	from fiber output.
3. 30 cm	.531	.643	
4. 40 cm	.726	.768	
5. 50 cm	.795	.775	
6. 60 cm	.719	.636	
7. 70 cm	.569	.459	
8. 80 cm	.402	.309	
90 cm	.287	.	
	RIGHT	BOTTOM	

4. Intensity on the Lambertian Surface at the screen position. F.L. 1.13* at position 5
5. Intensity of same location on the screen. F.L. .775

* 5.56 F.L. without translucent screen

81R-0182-052(3/5)(T)

Figure A-4c Test 4C, Solar Simulation Capability

TEST #4D

DATE: Sept. 25, 1980

1. Size of solar disk on Lambertian Surface Diam. 1" (Focused arc) 1/4"

2. Intensity on the Lambertian Surface 452000 FL

3. Intensity over the projected pattern. _____

POSITION ON THE PATTERN	INTENSITY F.L. HORIZONTAL	INTENSITY F.L. VERTICAL	
	LEFT	TOP	
1. 10 cm	.203	.490	Readings off the screen at 1.5 meters
2. 20 cm	.550	.796	
3. 30 cm	.840	1.05	
4. 40 cm	1.24	1.36	
5. 50 cm	1.48	1.37	
6. 50 cm	1.45	1.11	
7. 70 cm	1.25	.807	
8. 80 cm	.84	.47	
90 cm	.36		
	RIGHT	BOTTOM	

4. Intensity on the Lambertian Surface at the screen position. F.L. 3.12 at position 5

5. Intensity of same location on the screen. F.L. 1.36

81R-0182-052(4/5)(T)

Figure A-4d Test 4D, Solar Simulation Capability

TEST # 4E DATE:

1. Size of solar disk on Lambertian Surface Diam. 2"
2. Intensity on the Lambertian Surface See below
3. Intensity over the projected pattern. _____

POSITION ON THE PATTERN	INTENSITY F.L. HORIZONTAL	INTENSITY F.L. VERTICAL	
	LEFT	TOP	
1. 10 cm	33.8K	41.8K	
2. 20 cm	30.1K	29.6K	
3. 30 cm	27.5K	26.2K	
4. 40 cm	26.9K	28.2K	
CENTER	25.7K	27.3K	
5. 50 cm	26.0K	27.0K	
6. 60 cm	26.3K	19.1K	
7. 70 cm	32.3K	28.4K	
8. 80 cm	4.12K	19.7K	
	RIGHT	BOTTOM	

4. Intensity on the Lambertian Surface at the screen position. F.L._____
5. Intensity of same location on the screen. F.L._____
   a) Lens/Lamp distance 8 1/2"
   b) Lens/Block distance 5"
   c) Illumination Diameter on the lens 4 1/4"

81R-0182-052(5/5)(T)

Figure A-4e Test 4E, Solar Simulation Capability

TRANSLUSCENT SURFACE TEST DATA SPATIAL SCAN UNIFORM ILLUMINATION	
DISPLACEMENT, MM	INTENSITY BRIGHTNESS, F.L.
0	3.22
1	2.10
2	.249
3	.039
4	.043
5	1.79
6	2.15
7	1.46
8	2.75
9	1.17
10	.315
11	.035
12	.035
13	.206
14	1.49
15	2.89
16	2.59
17	2.38
18	.451
19	.129
20	.038
21	.059
22	2.11
23	1.59
24	3.35
81R-0182-053(1/4)(T) 25	3.36

Figure A-5a Test 5, Spatial Distribution with 1/8-inch Block-to-Screen Distance, Measured Center/Center Using 4 mm Square Wave Mask

TRANSLUSCENT SURFACE TEST DATA SPATIAL SCAN UNIFORM ILLUMINATION	
DISPLACEMENT, MM	INTENSITY BRIGHTNESS, F.L.
0	.071
1	.359
2	1.33
3	2.02
4	1.82
5	1.49
6	.468
7	.049
8	.242
9	1.19
10	1.16
11	1.41
12	1.58
13	1.04
14	.351
15	.078
16	.051
17	.375
18	1.00
19	1.79
20	2.11
21	1.47
22	.502
23	.177
24	.046
81R-0182-053(3/4)(T) 25	.384

Figure A-5b Test 5, Spatial Distribution with 1/4" Block-to-Screen Distance, Center/Center Using 4 mm Square Wave Mask

TRANSLUSCENT SURFACE TEST DATA SPATIAL SCAN UNIFORM ILLUMINATION	
DISPLACEMENT, MM	INTENSITY BRIGHTNESS, F.L.
0	1.85
1	1.57
2	.94
3	.305
4	.356
5	.925
6	1.66
7	2.14
8	2.01
9	1.72
10	1.16
11	.469
12	.155
13	.211
14	.756
15	1.45
16	1.73
17	1.52
18	1.06
19	.548
20	.216
21	.312
22	.801
23	1.37
24	1.85
81R-0182-053(4/4)(T) 25	1.95

Figure A-5c Test 5, Spatial Distribution with 3/8" Block-to-Screen Distance, Center/Center Using 4 mm Square Wave Mask

TRANSLUSCENT SURFACE TEST DATA SPATIAL SCAN UNIFORM ILLUMINATION	
DISPLACEMENT, MM	INTENSITY BRIGHTNESS, F.L.
0	.48
.5	.52
1.0	.56
1.5	.48
2.0	.52
2.5	.52
3.0	.49
3.5	.48
4.0	.41
4.5	.42
5.0	.49
5.5	.48
6.0	.52
6.5	.54
7.0	.49
7.5	.53
8.0	.57
8.5	.52
9.0	.57
9.5	.58
10 0	.57
10.5	.58
11.0	.53
11.5	.51
12.0	.54
12.5	.52
13.0	.54
13.5	.57
14.0	.54
14.5	.55
15.0	.54
15.5	.51
16.0	.52
16.5	.54
17.0	.52
17.5	.52
18.0	.52
18.5	.47
19.0	.45
19.5	.46
20.0	.51
20.5	.54
21.0	.53
21.5	.47
22.0	.42
22.5	.41
23.0	.41
23.5	.44
24.0	.50
24.5	.49
81R-0182-053(2/4)(T) 25.0	.47

Figure A-5d Test 5, Spatial Distribution with 1/4" Block-to-Screen Distance, Center/Left and Uniform Input

TEST	PHOTOMETER READING, F.L., 20 MIN APERTURE ILLUMINATION ANGLE, DEG												
	−60	−50	−40	−30	−20	−10	0	+10	+20	+30	+40	+50	+60
FIRST PASS READ HORIZONTALLY	.0041	.0060	.0084	.0133	.0245	.0499	.0726 .0950	.0684	.0338	.0127	.0097	.0057	.0041
SECOND PASS SPECIMEN ROTATED 90°	.0006	.0009	.0013	.0021	.0046	.0147	.0290 .0630	.0210	.0510	.0022	.0012	.0008	.0005
NORMAL READING FROM LAMBERTIAN SURFACE 0.0170 F.L. (AVG)													

81R-0182-054(T)

Figure A-6 Test 6 and 7, Reflectance Data from Dome

APPENDIX B

TEST EQUIPMENT

Glass Lenscreen Polacoat Inc.	LS60G 1/8 Rated Gain - 2.5
Thermometer (Thermocouple)	Fluke 2168A Digital
Photometer	Spectra Pritchard 1980 #A51V29009-1 Calibrated 8/26/80
Beam Focusing Lens	#963174
Slide Projector	Golde #241
Camera Lens	B&J View Camera 8x10 #DP375.22 Kodak Ektar F:6.3 12" #DP376.2
Xenon Lamp Assembly	Schoffel Instrument Corp. Model LH151
Power Supply	Electro Power Pacs Model 354

APPENDIX C

TEST PLAN FOR THE FIBER OPTIC CREW SYSTEM DESIGN STATION TEST ARTICLE

Introduction

This test plan is intended to validate the analysis performed in the CSDS study. To this end it fulfills the technical requirements and intent of the Contract and the Grumman proposal.

A CSDS fiber optic (F-O) dome section is being fabricated in accordance with the CSDS contract.

Tests will be performed on the fabricated dome section and on individual fiber cables as described in the following test procedures.

Purpose

The purpose of the tests listed here is:

(1) To evaluate the properties of F-O fibers applicable to the CSDS.

(2) To validate the analysis data developed for various tasks in the work plan.

Tests to be Performed

The fiber optic characteristics that affect their use in a Crew System Design Facility require seven specific tests performed on individual fibers or the fabricated dome test article, as appropriate. The tests measure spectral losses, numerical aperture, input and output coupling efficiency, fiber optic uniformity, resolution and achievable solar simulation. The tests can be performed in any order with one exception. The numerical aperture of the fibers in the test article must be determined first so that subsequent tests will have proper input illumination. The tests are listed in Table 1.

TABLE C-1

TESTS TO BE PERFORMED

Test #1	Numerical Aperture
Test #2	Spectral Attenuation
Test #3	Luminance Uniformity from Dome Section Test Article
Test #4	Solar Simulation Capability
Test #5	Spatial Distribution on a Translucent Surface
Test #6	Specular Reflectance
Test #7	Diffuse Reflectance
Test #8	Visual Appearance on The Test Sample

TABLE C-2

TEST EQUIPMENT LIST

1. Spectra Pritchard Photometer and Tripod
2. 1000 Watt Tungsten-Halogen Lamp with Reflector
3. Monochrometer
4. Rotating Disk Light Beam Chopper
5. Lock-in Analyzer/Amplifier
6. Sapphire F-O Scribing Knife
7. Optical Table and Mounting Fixtures
8. Solar Simulator Lamp
9. Collimating Telescope
10. Small mirror
11. Lambertian Reflecting Surface

TEST #1 NUMERICAL APERTURE

Purpose

The purpose of the test is to validate published data for the numerical aperture of the 100 meter optical fibers. This data will be used to assure proper input illumination for subsequent tests and extrapolations.

Test Technique

The test will be performed by sweeping the output radiation pattern of each fiber across a point detector. A rotating front surface mirror having its rotating axis thru the plane of the front surface is used. The mirror intercepts the radiation pattern and reflects it thru a pinhole aperture where a sensor detects the time varying light signal.

Test Arrangement

The test equipment and test samples will be mounted on an optical bench. The input and output ends of the 100 meter fiber are mounted to separate stationary fixtures on the optical bench. A lamp is arranged to illuminate the input end of the fiber directly. The distance between the input end and the lamp is not important other than coupling enough light for measurement at the output. A rotating mirror is located at the fiber output end on the fiber axis close enough to intercept the full radiation pattern of the fiber. The mirror drive and detector output is connected to an X-Y recorder to trace a plot of the output with respect to the fiber discrete radiation angles from -30° to $+30^{\circ}$. The fiber is then rotated by 90° around the fiber axis so that the orthogonal plane of the radiation pattern is scanned over the pin-hole aperture.

Test Procedure

1. Fasten the input and output ends of a 100 meter fiber to the holders provided on the numerical aperture test fixture. Check the vertical pointing alignment to assure that the center of the pattern will be measured.

2. Operate the equipment to get a plot of the radiation pattern.

3. Rotate the output fiber holding fixture 90° and plot the crossed field radiation pattern.

4. Repeat the test using the remaining 19 fibers.

TEST #2 SPECTRAL ATTENUATION MEASUREMENTS

Purpose

The purpose of this test is to validate the published data for losses in fibers through the visual range and to determine the variability between a statistical number of fibers manufactured to the same specification.

Test Technique

The test will measure the power emitted from the exit end of a series of long fibers with calibrated power input (by measurement of the output of a short fiber) through the visual range.

The ratio of the short fiber calibrating output and the long fiber output will be the loss factor.

Test Arrangement

The test arrangement will have the individual fibers input and output ends mounted on an optical bench for ease of achieving a firm mount. The monochromator is focused on the fiber input terminal. The convergence of the input illumination should be consistent with the numerical aperture measured on the 100 meter fibers. Output is chopped by a rotating disk to provide modulation detection with a lock in analyzer.

Test Procedure

1. Fasten each end of a 100 meter fiber to separate fixtures on the optical bench. Focus a monochromator on the input face of the fiber.
2. Position a rotating disk light chopper between the detector and fiber to intercept the beam.
3. Arrange a shield between the light source and detector to prevent stray light from entering the measuring device.
4. Connect a lock in analyzer/amplifier to the detector.
5. Measure and record the power output from the amplifier indicator at 20 nanometer intervals from 400 nanometers to 700 nanometers.
6. Scribe the fiber with a sapphire knife one meter from the input end. Do not disturb the input holding fixture and lamp. Pull and break the fiber at the scribe mark.
7. Measure and record the power output from the short fiber on the fiber axis at 20 nanometer intervals of wavelength starting at 400 nanometers and ranging to 700 nanometers.
8. Repeat the above procedure for each fiber being measured.

TEST #3 LUMINANCE UNIFORMITY FROM DOME SECTION TEST ARTICLE

Purpose

The purpose of this test is to validate the luminance pattern of the dome section test sample.

Test Technique

The test technique will be to illuminate the input surface of the Dome section test sample and read the output luminance at a number of individual fiber optic channels. The output block is rotated through angles from -30° to +30° while reading the output from each channel.

The input N.A. must first be calibrated to assure that the correct transmission modes are excited in the short test sample length. Since the short length of the test sample may not perform stripping of unwanted modes, the angular distribution of the input illumination must be calibrated and controlled. The calibration technique will illuminate the input surface of the test sample with a lamp placed at several distances. The output radiation pattern will be measured for each distance. The distance giving the correct output radiation pattern will be selected for all subsequent measurements.

Test Arrangement

A Spectra Pritchard Photometer will be mounted to read the dome section output face which is mounted on a rotating fixture having a horizontal angle scale. The dome section input face will be mounted on a stationary fixture facing an illuminating lamp assembly. A light shield is placed between the lamp and photometer to prevent stray light from reaching the photometer.

Calibration Procedure

1. Assemble the test article output block on an optical rail fixture with an angular scale.
2. Assemble the input block to a solid fixture and position a lamp assembly on an adjustable linear rail to focus illumination on the input block from various distances.
3. Set the lamp a convenient distance from the input block.
4. Position and set the Photometer to read the face of the output block. Use a small external aperture stop on the photometer.

LUMINANCE UNIFORMITY TEST CHART

Angular Orientation	LAMP DISTANCE					
-30°						
-25°						
-20°						
-15°						
-10°						
- 5°						
0°						
+ 5°						
+10°						
+15°						
+20°						
+25°						
+30°						

Figure C-1

TEST #3 LUMINANCE UNIFORMITY FROM DOME SECTION TEST ARTICLE (cont.)

Calibration Procedure (cont.)

5. Read the light output from the Photometer through the range of -30° to +30° orientation of the output test Block. Record the readings in the test chart, and plot on graph paper.

6. Adjust the lamp assembly and repeat step 5 until the output pattern matches the N.A. measured from the 100 meter samples. Record the lamp distance.

Test Procedure - Luminance Pattern Uniformity

1. Set the Dome section output face normal to the photometer and set the illuminating lamp at the distance determined from the calibration data. Record the photometer reading on the face of the test section.

2. Focus the photometer on a selected region on the output surface of the test article. Adjust the angle between the photometer and the test article for a peak photometer reading. Record the Reference angle.

3. Rotate the test article output table through angle from -30° to +30° and record the photometer readings at each angle.

4. Reposition the photometer onto several other regions on the output surface. Repeat the measurements described in (3).

TEST #4 SOLAR SIMULATION CAPABILITY

Purpose

This test is intended to measure the ability of the dome section test article to simulate the sun and illuminate the required cockpit area.

Test Technique

A very bright circular image will be focused on the input face of the dome section test article. The illumination pattern and intensity will be measured from a screen placed to represent a surface at the cockpit in the full sized simulator.

Test Arrangement

The solar simulation lamp will be positioned to place a bright circular image no larger than 1 inch in diameter on the input face of the test article. The output face will be normal to a screen placed between 5 and 20 feet from the output face. The screen distance may be varied to provide convenient illumination levels for measurement. Baffles should be provided to restrict illumination on the screen to that provided by the output face.

Test Procedure

1. Measure and record the distance from the output face to the screen.
2. Place a distance scale horizontally and vertically on the screen.
3. Focus the solar input image on a lambertian surface. Measure and record the surface luminance and the size of the illuminated circle.
4. Replace the lambertian surface with the dome test article input face. Measure and record the surface luminance and the size of the illuminated circle.
5. Measure and record the luminance projected on the screen using the distance scale as a guide. Use sufficient points in X and Y axis to characterize the radiation pattern from the output face.
6. Measure the relative luminance of a point in the illumination pattern off the screen and off the lambertian surface. Record both measurements.

SOLAR SIMULATION MEASUREMENT

1. Size of solar disk on Lambertian Surface Diam._____cm.

2. Intensity on the Lambertian Surface _____

3. Intensity over the projected pattern.

Position on the Pattern	Intensity F.L. on side	Intensity F.L. on side	
1.	F.L. on Hor. Scale	F.L. on Vert Scale	
2.			
3.			
4.			
5.			
6.			
7.			
8.			

4. Intensity on the Lambertian Surface at the screen position.

F.L. _____

5. Intensity of same location on the screen. F.L._____

Figure C-2

TEST #5 SPATIAL DISTRIBUTION ON A TRANSLUCENT SURFACE

Purpose

The purpose of this test is to determine whether the fiber output can be focused onto a simulated inner dome surface which has a translucent characteristic. The data collected will help to determine image characteristics on the inner translucent dome surface.

Test Technique

A lamp assembly will be used to illuminate the input surface of the test sample at the correct distance to achieve a proper output radiation pattern as determined by Test No. 1. The output of the test article will fall on a translucent screen and the illumination pattern will be measured at a series of block to screen distances. The maximum distance will give 50% overlap of the spots.

Test Arrangement

The test section will be mounted on an optical bench with a translucent screen. The distance between the two can be changed for measurements at various spacings. A Spectra Pritchard Photometer will be arranged to scan across the translucent surface. A light source is mounted on the optical bench to illuminate the input surface of the test article using a resolution test pattern and uniform input illumination.

Test Procedure

1. Assemble a fixture with the screen on the test rail 1/4 inch from the output test block. The matte surface of the screen is to be facing towards the Photometer. The plane of the screen must be normal to the Photometer.

2. The output test Block surface should be normal to the photometer (0° setting).

3. Translate the photometer parallel to the face of the Block and screen. Record the distance and photometer output with sufficient number of points to characterize the projected pattern.

4. Translate the screen to a different distance relative to the block and repeat (3).

5. Using input illumination containing a resolution pattern repeat steps (3) and (4).

TRANSLUCENT SURFACE TEST DATA

SPATIAL SCAN

UNIFORM ILLUMINATION

Distance - Screen to Block (mm)	Displacement (X)	Intensity Brightness

Figure C-3

TRANSLUSCENT SURFACE TEST DATA

SPATIAL SCAN

RESOLUTION PATTERN

Distance - Screen to Block (mm)	Displacement (X)	Brightness

Figure C-4

TEST #6 SPECULAR REFLECTANCE

Purpose

The purpose of this test is to determine the reflection characteristics of the dome surface. The data will show the nature of possible multiple reflections of images inside the dome. Reflection of spurious images visible to the crew will tend to distort real images at intended locations.

Test Technique

The test will illuminate the output surface of the dome section with a known illumination level using a collimated light beam. The incident light beam will be set to several incident angles. The reflected light will be measured at reflection angles equal to the incident angle.

Test Arrangement

The test will use a Spectra Pritchard Photometer, the dome section test article (output surface), and collimated light source mounted on an optical table. The photometer will be mounted on a tripod for ease in moving to the reflected angle position. The photometer is positioned by sighting back to the source off a mirror substituted for the test article between changes in incidence angle.

Test Procedure

(1) Align the setup by auto-reflection using a mirror substituted at the output surface of the dome section test article. Record the reference angle at the rotating table. Set the angle of incidence to 60° and locate the photometer at the correct position to intercept the reflected light beam. Record the photometer reading off the mirror and the test article and record them both.

(2) Reset the angle of the rotating table to change the angle of incidence in steps of 10° from -60° to $+60^{\circ}$ recording the Photometer reading at each angle.

REFLECTION TEST DATA

TEST	PHOTOMETER READING ANGLE													
	-60	-50	-40	-30	-20	-10	0	+10	+20	+30	+40	+50	+60	
Specular Refl. First Pass Second Pass	Rotate the Block 90° about the block horizontal axis.													
Diffuse Refl. First Pass Second Pass	Rotate the Block 90° about the block horizontal axis.													

Figure C-5

TEST # 7 DIFFUSE REFLECTANCE

Purpose

The purpose of this test is to determine the diffuse reflection from the output surface of the dome section test article that is most important to a CSDF.

Test Technique

The test will illuminate the output face of the test article with a collimated light beam at several incident angles. The diffusely reflected light will be measured with a Spectra Pritchard Photometer normal to the output face of the test article.

Test Procedure

1. Arrange the test equipment as described in the arrangement for the specular reflection test.

2. Perform alignment of the test setup by auto-reflection using a mirror fastened to the output face of the test article and zero the rotary scale. Set the angle of the rotating table to -5° and set the photometer to the correct height by reading the specular reflection. Record the photometer reading.

3. Set the rotating table to -30°. Move the photometer to a position normal to the face of the output block determined by auto reflection and record the photometer reading.

4. Rotate the rotating table by 10° steps from -60° to +60°. Record the photometer readings at each step moving the photometer normal to the output face of the test article for each reading.

TEST # 8 VISUAL APPEARANCE ON THE TEST SAMPLE

Purpose

The purpose of the test is to evaluate the general appearance of images projected from the output surface of the dome test section. Projected images should be recognizable at a distance equal to the dome radius (viewing distance). The image edges should have resolution characteristics equivalent to real world images. This evaluation will assure that images seen in a completed CSDF will present a realistic simulation of real world images.

Test Technique

The test will be performed by mounting the output block of the test article in a larger surface having a transmission pattern equivalent to the test section, fiber size, and fiber pitch. The input surface of the test section will be illuminated by a lamp. The large surface surrounding the test article is intended to make the test more realistic. The surrounding surface is illuminated from the rear with a second lamp.

Small image cut-outs will be attached to the input surface of the test article and viewed from the proper distance at the output surface to evaluate image characteristics.

Test Arrangement

The test arrangement must be located in an area with an unobstructed viewing distance of 50 feet. The test article is mounted in a cut-out of a shadow mask previously prepared. The shadow mask is supported on a table and illuminated at the back side with a 1000 watt lamp connected to a variac control to adjust the intensity. The lamp is placed five feet from the test assembly. The test sample input block is fastened to a tripod and illuminated with the same lamp as in Test #3 placed at a distance as indicated by the test data of Test #3. Viewing distances should be marked off on the floor at five foot intervals from the front of the test article.

Test Procedure

1. Arrange the test equipment and test article as described in the test arrangement. Assure that there is no light leaking around the edge of the test article when mounted in the cut-out of the shadow mask. Adjust the apparent luminance of the test article to TBD F.L.

TEST # 8 VISUAL APPEARANCE ON THE TEST SAMPLE

Test Procedure (Cont.)

2. Adjust the shadow mask illumination to the same intensity as that of the output surface of the dome test section.

3. Each subject will view the test article and record the distance at which the appearance of the illuminated fibers in the test block output surface is acceptable (blending in).

4. Fasten a small opaque image cut-out of an aircraft silhouette on the input surface of the test sample. View the output surface at several distances and record comments with regard to recognition of the image and resolution of the edges of the image.

5. Introduce line resolution patterns on the input surface of the test article. View the output surface from variable distances and record the distance where they are considered resolved.

6. Repeat the test at TBD F.L. steps.

7. Repeat with TBD subjects.

8. Arrange a translucent screen at the output surface of the test article.

9. Repeat items 3 through 7 for several spacings between the translucent screen and test article.

Comments on Appearance of Test Image

VISUAL APPEARANCE TEST CHART

Brightness F. L.	Dist. Ft. Uniform Ill.	Distance - Feet Resolution #1	Resolution #2	Resolution #3		
Translucent Screen at ____ MM						
B_1 B_2						

Figure C-6


DATE
ILME